ADSORPTION AND FLOW OF WATER IN NEARLY DRY LURGI RETORTED OIL SHALE

Prepared for

Standard Oil Company (Indiana)
AMOCO Research Center
Naperville, Illinois

and

U.S. Environmental Protection Agency
Industrial Environmental Research Lab
Cincinnati, Ohio

Prepared by

Department of Agricultural
and Chemical Engineering
Engineering Research Center
Colorado State University
Fort Collins, Colorado

D. B. McWhorter
G. O. Brown

February, 1985

ACKNOWLEDGEMENTS

This research into the adsorption and flow of water in nearly dry Lurgi retorted oil shale has been funded in part by the Standard Oil Company (Indiana), AMOCO Research Center, Naperville, Illinois. Additional funding was provided by the U.S. Environmental Protection Agency, Industrial Environmental Research Lab, Cincinnati, Ohio. The project officers for AMOCO were Messrs. George Watson and Erik G. Funegard. The Project Officer for EPA was Mr. Edward R. Bates. This paper represents the final report under AMOCO funding, while additional work under EPA funding will be reported at a later date.

TABLE OF CONTENTS

LIST OF TABLES

LIST OF FIGURES

LIST OF SYMBOLS

Symbol	Description
C_s	solute concentration
C_w	concentration of water in solution
D_a	vapor diffusivity in air
D_l	liquid diffusivity
D_s	solute diffusivity
D_{lv}	combined liquid-vapor diffusivity
D_s	solute diffusivity
D_v	vapor diffusivity
F_l	liquid water flux
F_{lv}	combined liquid-vapor water mass flux
F_s	solute mass flux
F_v	vapor water mass flux
g	acceleration of gravity
h_c	capillary water presure head
K	hydraulic conductivity (permeability)
K_r	relative conductivity
K_s	hydraulic conductivity at saturation
M	molecular weight of water
Q	mas influx
q	volume flux of solution
R	rate of penetration of wetting front
R^o	gas constant
RH	relative humidity
T	tortuosity
T^o	temperature

t	time
x	coordinate in horizontal direction
z	coordinate in vertical direction
θ	volumetric solution (water) content
θ_k	volumetric solution content at critical point
ρ_v	water vapor density (mass per volume)
ρ_{vs}	water vapor density at saturation
ϕ	porosity

CHAPTER 1

INTRODUCTION

Research into the movement of water and dissolved constituents in retorted oil shale has been motivated by the adverse impacts that can be anticipated if leachate is generated and left uncontrolled in the large disposal piles that are anticipated. To a large extent, such research is based on the implicit assumption that leachate generation is inevitale. Surprisingly little research has been directed toward the investigation of the circumstances under which leachate producton would not occur and to the degree that such circumstances can be assured in an appropriately engineered and managed disposal operation.

Leachate could potentially result from both internal drainage of moisturizing water and from net infiltration of precipitation below the root zone. The position that the latter source will be, or can be made to be, effectively zero cannot be convincingly defended. It was on this premise that a previous study (Golder Associates, 1983) investigated vapor diffuson as a mechanism by which net infiltration could escape the etorted shale pile without generating liquid leachate.

One conclusion of the above referenced study was that the transport properties of both liquid and vapor at low water contents were of central importance. While it is known that total water transport is dominated by bulk liquid flow at high water contents and gradually becomes dominated by vapor diffusion at low water contents, separation of the two transport mechanisms has proven difficult. This is unfortunate because the relative dominance of vapor and liquid transpot as a function of water content determines the mass flux of salts for a given rate of total water flow. The liquid water content below which liquid water flow is essentially zero is particularly important in the assessment of drainage of waters and

solutes through future disposal piles.

The work presented here has determined four main properties of the Lurgi spent shale. They are: 1) the critical water content above which internal drainage will occur, 2) the volume of infiltration that can be accommodated if permanent storage as a function of placement water content, 3) the rate at which water will drain if the water content is above the critical value, and 4) the rate of penetration of net infiltration though a disposal pile. To achieve the above objectives several tests have been performed. These include tests of the materials, cementing properties, (hydration test, x-ray diffraction and scanning electron microscope), water holding capacity (vapor sorption and pressure plate test) and hydraulic properties (diffusivity and conductivity). The following chapters describe the testing procedures and results along with an illustrative analysis of flow in a disposal pile.

Chapter 2

PHYSICAL PROPERTIES OF LURGI RETORTED SHALE

GENERAL

The material tested in this study was a retorted oil shale produced by a pilot Lurgi plant operated by Gulf Research and Development Co., Gulf Corporation, at Harmarville, Pennsylvania. The material designation was 10/31/83-2100-Run 108.9C. In the Lurgi pilot plant the raw shale was crushed to about -3 mm and retorted to extract the kerogen. It is then combusted or decarbonized to remove residual carbon compounds. The process produces a fine textured, gray colored solid residue, commonly referred to as retorted shale. Rio Blanco (1976, 1977 and 1981) presents details of the Lurgi process and proposed operations while Fox (1983) reviews previous work on the leaching properties of oil shale solid wastes.

Lurgi retorted shale is a chemically active material due to the high process temperatures to which it is exposed. Upon the addition of water the material hydrates, similar to a cement and generates noticeable amounts of ammonia. Similar Lurgi retorted shales have yielded 2 percent of the dry weight (or more) as soluble minerals in column leaching tests (Nazareth, 1984). Thus, several supplemental experiments were carried out to explore the material behavior when initially mixed with water. These supplemental tests were intended to indicate the processes by which water interacts with the Lurgi spent shale.

The following sections describe the various tests that were performed to characterize the material. Also described is the procedure used in sample preparation for the later hydraulic testing.

PARTICLE SIZE AND DENSITY

A particle size analysis of the material was performed by dry sieving. The method used was ASTM D 422. The results of the analysis are shown in Figure 2-1. Thirty-five percent by weight of the material was 0.045 mm or smaller. A large portion of the material, 31 percent, was between 1.0 and 2.0 mm. The largest particle was 5 mm and the median diameter (d_{50}) was 0.5 mm. It was observed that the larger particles were darker in color than the fines. The color difference may be due to different mineralogy or a difference in residual kerogen.

The apparent specific gravity or particle density of the material was determined using the ASTM D 854 method. For unsorted samples an average specific gravity of 2.74 was obtained. Material passing finer than 0.045 mm averaged 2.743 while material larger than 2 mm averaged 2.728. The difference between the fine and coarse samples is not significant.

The water content of the material as received was zero as measured by ASTM D 2217. It is assumed the material was packaged soon after leaving the retort and was not exposed to water or high humidity.

BATCH LEACHING TEST

A 150 gm sample of Lurgi spent shale was added to three liters of distilled water (20:1 water to shale ratio) in a stainless steel container. The mixture was gently stirred by a mechanical mixer to prevent any cementing of separate particles. After 24 hours a one liter water sample for chemical analysis was filtered through a 0.45 micron filter and refrigerated.

The results of the chemical analysis of the leachate water are presented in Table 2-1. The first column shows the ion concentration, while the second lists the soluble mass in mg per gm of material. The

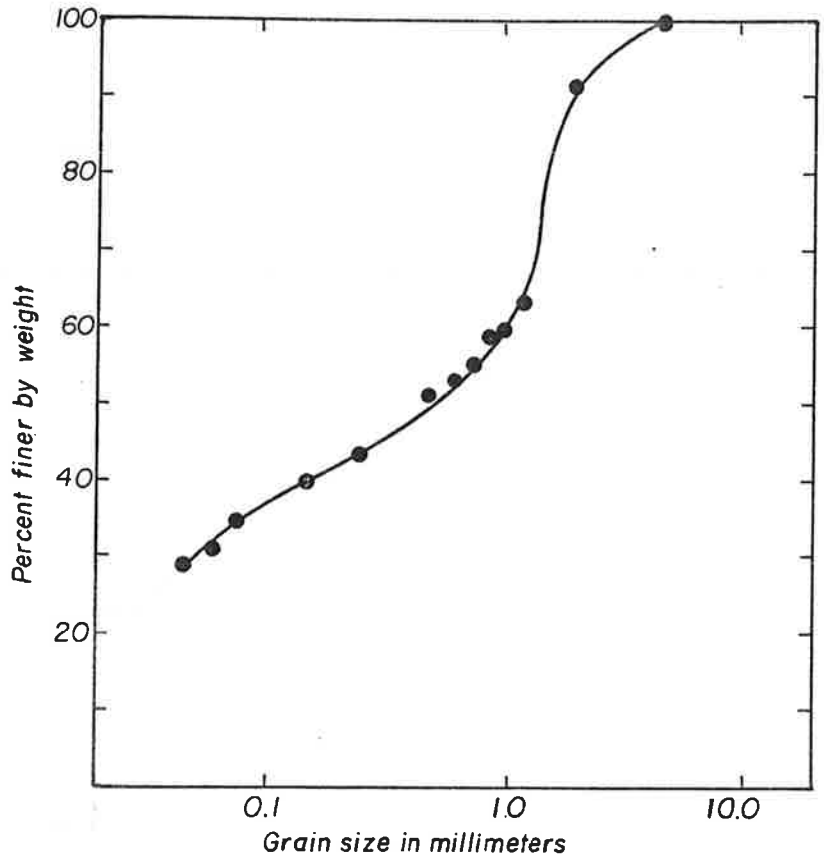

Figure 2-1. Particle size distribution for Lurgi retorted shale.

total soluble mass was 2.18% of the retorted shale. The ions that were determined account for 87 percent of the total dissolved solids. Calcium and sulfate comprise the majority of the material present accounting for 26 percent and 50 percent, respectively. All of the sulfate and most of the calcium could be accounted for by dissolved gypsum comprising 1.5% of the dry solid. Cations beside calcium were present only in small amounts.

It is unlikely that the 20:1 liquid-to-solids ratio was sufficient to relax all solubility constraints. An even larger liquid-to-solids ratio would probably have resulted in a somewhat greater soluble mass.

Table 2-1. Chemical analysis of Lurgi batch leachate.*

Cations	Concentration mg/l	Soluble Mass mg/gm
Calcium	281	5.62
Sodium	22	.44
Magnesium	<1	-
Potassium	2	.04
Anions		
Hydroxide	36	.72
Bicarbonate	0	0
Carbonate	59	1.18
Chloride	9	.18
Sulfate	542	10.84
Nitrate	1	.02
Total Phosphate	.01	-
Total Dissolved Solids	1,090	21.8
pH	11.1	
Conductivity	1700 µmhos/cm	

*20:1 liquid to solids ratio, 24 hr leach.

COMPOSITION OF GAS GENERATED UPON WETTING

It was observed that when the retorted shale was hydrated in a closed container a strong ammonia odor was generated. Gas testing was performed to determine if indeed ammonia was formed, and if any other gases were produced. Since the gases and amounts present were unknown, it was determined that an efficient means of testing would be with a portable sampling pump and specific compound analysis tubes. This type of equipment is normally used to detect and measure airborne pollutants. Equipment, supplies and assistance in completing the tests were provided by the Colorado State University Department of Microbiology and Environmental Health.

Samples were taken from a closed 20 l vessel that contained 4 kg of spent shale which had been wetted to 30 percent water content by weight and allowed to hydrate for 26 days. The atmosphere within the vessel was tested for seven different compounds or groups. The results of this

screening test are presented in Table 2-2. Two compounds were detected, ammonia and a halogen. Ammonia was detected at 90 ppm which is significant, but of no concern for hydraulic testing or health effects. A halogen compound was detected but it is uncertain if it was generated by the shale or was residual chlorine from a solution used to clean the vessel. Five compounds and groups were not detected: sulfur dioxide, nitrous oxide, hydrogen sulfide, mercaptans, and toluene. These negative results indicate that no sulfur or hydrocarbon gases were generated in amounts greater than 1 to 5 ppm.

Cooper and Evans (1983) found that inorganic NH_4^+ substitutes for K^+ in Green River formation oil shale. The NH_4^+ replaces K^+ in feldspar. While some NH_4^+ was lost on retorting, significant amounts over 1000 ppm in most samples remained. It is unknown why the ammonia is released upon wetting or if its release is associated with the cementing processes.

CEMENTING PROPERTIES

Lurgi retorted shale exhibits cementing properties when initially mixed with water. This property has been reported by others (Pilz, 1982, and Marcus, Sangrey and Miller, 1984), although it appears that the cementing properties of the material studied herein is more pronounced than reported for similar retorted shales. When the material tested here is wetted to about 50 percent water content (by weight), a paste is formed. If the paste is allowed to dry it forms a rock-like mass with considerable strength.

Since this study is concerned with liquid and vapor flow at low water contents, and the volumes of water which would drain from disposal piles, it was necessary to explore the cementing properties of the Lurgi retorted shale. The purpose of the tests was to determine the amounts and manner by

Table 2-2. Gas composition screening tests.

Compound	Number of Samples	Analysis*	Comments
Ammonia (NH_4)	2	90 ppm 90 ppm	Test accuracy ± 25%
Sulfur dioxide (SO_2)	1	ND	
Nitrous oxide (NO_2)	1	ND	
Hydrogen sulfide (H_2S)	2	ND	Test would detect most sulfur compounds
Mercaptans	1	ND	Test for common mercury binding carbon compounds
Toluene	1	ND	Test would detect most hydrocarbons
Halogenated Hydrocarbons	2	P	Nonspecific test for halogen group elements. Sample may have been polluted by cleaning agents

*ND - not detected
P - present

which water is held, so that the hydraulic tests could be adjusted to account for these properties.

Properties of Cement

In order to fully understand some of the tests undertaken, it is necessary to have some knowledge of the properties of cements. Cements are produced by the burning of natural materials at high temperatures to produce a clinker, which is then ground to a powder. When water is added, the cement will first form a plastic paste and then "set" or become rigid. Finally, the cement will harden into a rock-like mass.

Cement is mainly composed of calcium carbonate and aluminum silicates. Portland cement is made using two or more materials to provide the proper composition. Many materials can be used to produce cements, including

limestone, clay, chalk, shales, blastfurnace slag and marlstone. The Cambridgeshire (England) marlstone approximates the composition of Portland cement and at one time was used by itself to make a natural cement (Lea, 1970). Modern cements will contain (in various forms and combinations) 60 to 65 percent CaO, 1 to 4 percent MgO, 3 to 6 percent Al_2O_3, 2 to 5 percent Fe_2O_3, 1 to 3 percent SO_3, and 20 to 25 percent SiO_2. When water is added, these materials will hydrate, forming interlocking mineral crystals which provide the cement's strength. Gypsum, $CaSO_4.2H_2O$ is often added to cement to slow its setting.

The chemistry of cement hydration is complex. The minerals formed generally cannot be described accurately. In a simple sense, it can be stated that water and hydroxyl ions are used to combine simple minerals such as SiO_2, CaO, MgO and Al_2O_3 into large plate-like minerals which stack upon one another with water trapped between forming a gel.

Water in cement can be in three different physical states. First, it can be in capillary pores or adsorptive films between particles as in any porous media. Second, it can be incorporated into a water cement gel, and third, it can hydrate various mineral compounds to become part of a mineral crystal matrix. The division of the total water in these three states is a function of the total water content, the sample composition and most importantly, the history of the sample. The most important historical factor is the time between the addition of the water and the measurement.

Initially all added water will be in capillary pores. Within a few minutes some small amount of cement will hydrate and, with additional water, will produce a gel. In the gel, molecular water will be trapped between hydrated cement. It is the formation of the gel which produces a cement "set". Hydration of the remaining cement proceeds slowly.

Complete hydration generally will take one year or longer.

For a completely hydrated cement, the weight of water retained at 105°C will be about 25 percent of the anhydrous material. It should be noted that there is no particular vapor pressure or temperature that can be used to distinguish gel water from water of hydration. At 105°C some water of hydration is lost from the calcium sulphoaluminates and the hexagonal tetracalcium aluminate hydrate, while some gel water may remain.

Hydration at Different Initial Water Contents

The Lurgi retorted shale is expected to be disposed in a moist condition. The amount of water that will be used to moisturize the solids is not known at this time but is expected to be in the range of 10 to 20 percent by weight of dry material. A test was performed to explore the effects on hydration of varying amounts of initial water.

Dry weights were obtained for six samples of approximately 40 gm each. Distilled water was added to each sample in amounts ranging from 2.5 percent to 50 percent of dry weight. The 2.5 percent sample was only wetted in a small area, while the 50 percent sample was a liquid paste. The samples were covered and stored for 15 days at 22° ± 1°C. At the end of this period the samples were oven dried at 105°C. After drying the samples were weighed and their water content determined. All weights were measured to 0.01 gm which provides an accuracy in the water content determination within 0.04 percent by dry weight.

The test results were quite uniform. Figure 2-2 shows that the water retained depends upon the amount of water initially added to the samples. The driest sample retained 1.0 percent of dry weight of water while the wettest samples retained 3.2 percent. As can be seen in the graph there was no difference in retained water between the samples with initially 30

percent and 50 percent water, while the 20 percent initial water sample retained only slightly less. The variation in the amount of water retained may be due to the experimental method. Because it was impossible to uniformly mix the initial water in the drier samples, it is felt that those samples may not be representative of the actual process. In all subsequent experiments, the sample material was hydrated at a water content of 30 percent by weight to insure complete hydration in a reasonable time.

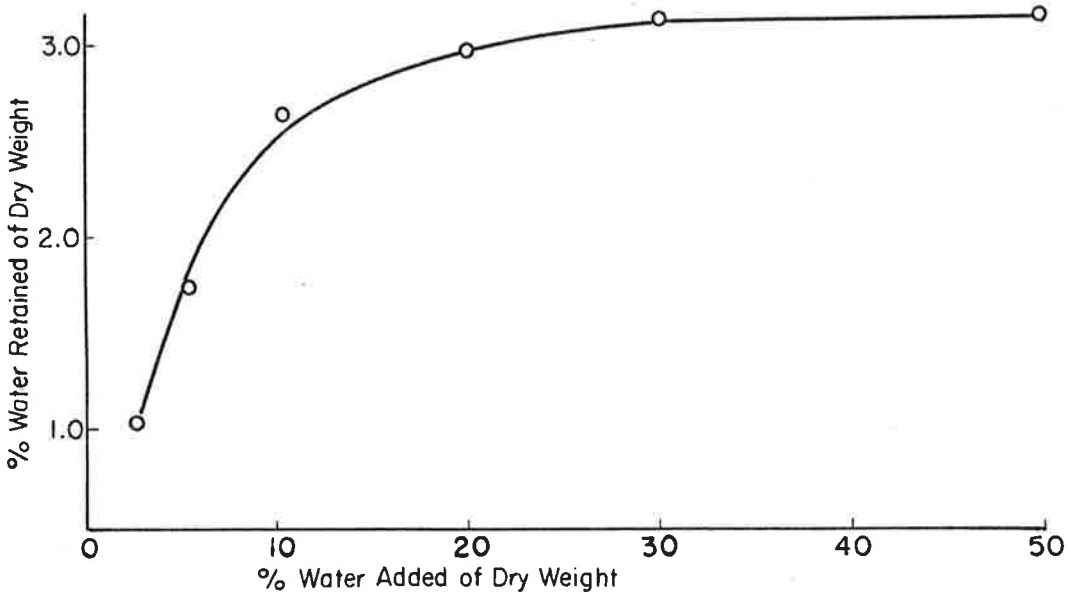

Figure 2-2. Water hydrated at varying initial water contents by weight.

Curing Time

A curing time test was performed to determine the time required for the cementing processes to occur. Since mineral hydration is a surface reaction it may take long time periods for a sample to fully hydrate. As noted previously, hydration in a normal cement will proceed for a year or more.

Samples of approximately 40 gm each were wetted to 30 percent water

content and stored at 22° ± 1°C at 100 percent relative humidity. At 1, 2, 5, 28, 55, and 89 days duplicate samples were removed, oven dried at 105°C and the amount of water retained calculated. Figure 2-3 present the results of the test. After 28 days the amount of water retained is relatively constant at 3.6 percent. Marcus et al. (1984) have shown that mineral changes are still occuring up to 100 days but these data indicate that the effects of such changes on total water hydration must be less than 0.1 percent by dry weight.

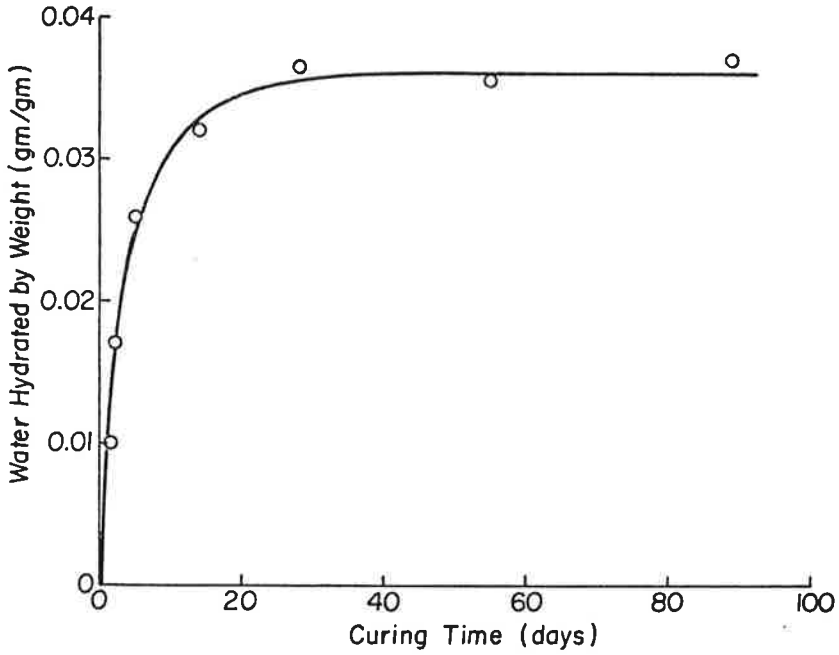

Figure 2-3. Water hydrated as a function of time.

Variable Drying Tests

Central to this study is the ability of the Lurgi retorted shale to hold water in cement gels and in hydrated minerals. High temperature and low humidity drying was conducted in an effort to determine the amount and phase in which water is held.

While there is no absolute temperature or humidity which distinguishes water held in the different phases (Lea, 1970), rough divisions can be made. At 105°C all free water and most gel water is assumed to be removed, while at 550°C all gel water and some water of hydration is assumed to be removed. The free water can be further divided into capillary water and adsorbed water. Many times the difference between these two states is not considered and adsorbed water is lumped with capillary water. True capillary water is held mainly by capillary forces between material grains, while adsorbed water is held in thin films by electro-static charges on the mineral surface (Kemper, 1960). In drier materials, most water present is contained in adsorptive films while at higher water contents most water is present in capillary pores. Water in adsorptive films is considered to be less mobile than water in capillary pores. Again, there is no absolute division between these states but it can be reasoned that no capillary water can exist below 45 to 65 percent relative humidity.

Samples of the material were weighed, wetted with distilled water to 30 percent by weight, stored at 100 percent relative humidity and allowed to hydrate for 28 days. At the end of the curing period, two samples were dried for 24 hours at temperatures of 105°, 330° and 550°C in succession. Two additional samples were dried at 22 ± 1°C with a relative humidity of approximately 32 percent for 28 days. After drying, the samples were weighed and their water contents determined. The sample average results are presented in Table 2-3.

At 32 percent R.H. hydrated, gel and adsorbed water comprise 7.12 percent of the unhydrated dry weight. From adsorbtion tests presented in the next section, it is shown that the adsorbed water accounts for about 3.0 percent, leaving 4.1 percent for the hydrated and gel water. At 105°C

Table 2-3. Drying of hydrated Lurgi material under different conditions.

Drying Condition	% of Unhydrated Dry Weight	% H_2O Content
32% R H	107.12	7.12
105°C	103.66	3.66
330°C	101.50	1.05*
550°C	95.75	--*

*Water contents questionable due to possible volatile minerals.

the material retained 3.7 percent water. At this temperature, a small amount of hydrated water may be lost but most loss is gel water. Thus, gel water is believed to comprise about 0.4-0.5 percent.

At 330°C the material retained 1.05 percent water, while at 550°C the samples lost 4.25 percent of their unhydrated weight. The cause of the weight loss is unknown but may be due to loss of hydrated water already present in the samples or by the breakdown of a mineral which releases a gas. It has already been noted that ammonia is generated during hydration. X-ray mineral analysis described in the next section found no difference between 110°C and 550°C heated samples. Thus, it is speculated the weight loss is from organic compounds. This weight loss places the weights obtained at the two higher temperature in question. Thus, it was not possible to further quantify the state of the hydrated water.

X-Ray Diffraction Analysis

In an attempt to determine the reactions in the cementing process a mineral analysis was performed. X-ray crystal diffraction was performed on raw and 28 day hydrated samples using a General Electric XRD-6 X-ray Diffraction machine by personnel of the Earth Resources Department, CSU. Samples were ground to a fine powder, mixed with an acetone medium, then mounted on glass slides for diffraction analysis. For each sample, an

oven-dried (105°C) and a heat treated (550°C for 1 hour) specimen were examined. Analysis proceeded, for each slide, on the XRD-6 using a copper source at 1000 counts per second with an initial goniometer setting of 3° and chart recorded at 5° (2θ) per inch to 65° (2θ).

Mineral identification consisted of keying maximum diffraction peaks on the chart to corresponding degrees 2θ and d-spacings of crystal lattices, measured in angstroms. Patterns for the retort samples were searched in the J.C.P.D.S. Mineral Powder Diffraction Search Manual (Joint Committee on Powder Diffraction Standards - 1974).

Figure 2-4 shows the XRD diffraction pattern for the raw and hydrated 110°C samples. No significant difference was found between 110°C and 550°C samples. Table 2-4 lists the minerals identified, their relative abundance and any significant changes in occurrence after hydration. Only calcite and hinsdalite showed an increase upon hydration.

Scanning Electron Microscope

Hydrated and raw samples were examined using a scanning electron microscope (SEM) by personnel of the Department of Anatomy, Colorado State University using a Hitachi HHS-2R. X-ray elemental spectrum analysis was also performed on selected particles. A beryllium window was used on the detector such that sodium and lighter elements could not be detected. Figures 2-5 and 2-6 show comparable views at 800 magnification of raw and hydrated material, respectfully. The only observable difference in the materials is a slight reduction in small particles with hydration. It appears that the particles are simply stuck together by hydration but not modified otherwise. Full picture elemental analysis on these two views indicate similar composition. Elements detected in order of abundance were calcium, silicon, aluminum, magnesium and potassium. Phosphorus is

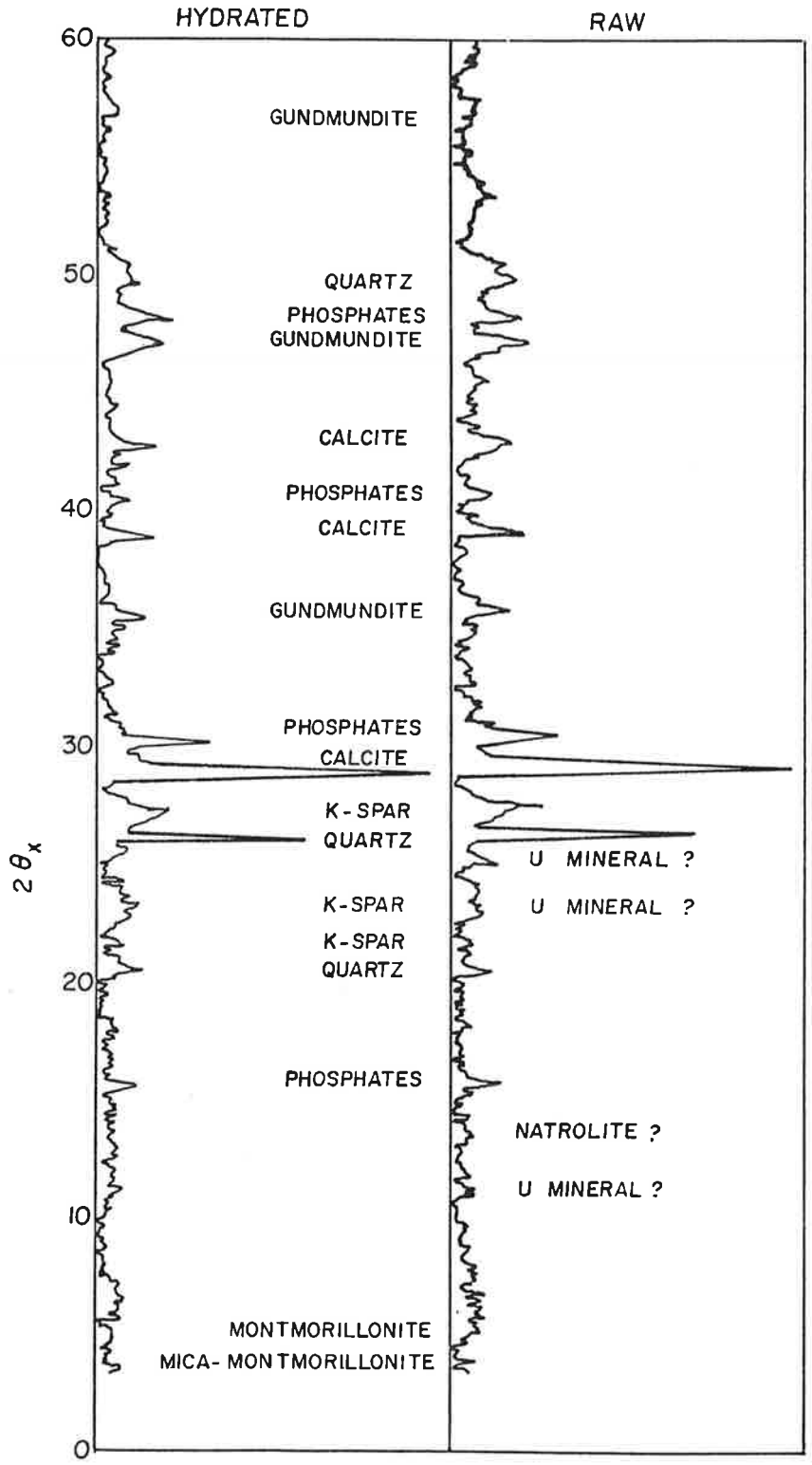

Figure 2-4. X-Ray Diffraction Patterns.

Table 2-4. Minerals detected by X-ray crystal diffraction.

Mineral	Composition	Sample Raw	Sample Hydrated
Quartz	SiO_2	M	M
Calcite	$CaCO_3$	M	M+
K-Feldspar	$KAlSi_3O_8$	M	M
Montmorillonite	$(Al,Mg)_8(Si_4O_{10})_3(OH).12\ H_2O$	T	T
Mica-Montmorillonite (mixed-layer clay)	Not Given	T	T
Phosphate Minerals			
Hinsdalite	$(Pb,Sr)Al_3PO_4SO_4(OH)_6$	M	M+
Goyazite	$SrAl_3(PO_4)_2(OH)_5.H_2O$	T	T
Crandallite	$Ca\text{-}Sr\text{-}Pb\text{-}Al\text{-}PO_4OH.H_2O$	*	*
Natrolite	$Na_2Al_2Si_3O_{10}.2H_2O$	*	
Beta-uranophane	$Ca(UO_2)_2(SiO_3)_2(OH)_2.5H_2O$	T	
Carnotite	$K_2(UO_2)_2(VO_4)_2.1\text{-}3H_2O$	*	
Gundmundite	FeSbS	T	T

M Mineral present in amounts greater than 8 percent by weight.

T Mineral present in amounts less than 6 percent by weight.

\+ Mineral with relative increase after hydration.

*May or may not be present due to incomplete identification or presence in trace amounts.

difficult to detect in small amounts due to the large amount of silicon. Figures 2-7 and 2-8 show the two typical large particles in the hydrated material. Figure 2-7 shows a large smooth relatively pure quartz particle which contains some aluminum while Figure 2-8 shows a large rough particle which contains calcium, silicon and magnesium. At higher magnification in Figure 2-9 the small particle in the center was found to contain relatively large amounts of potassium and is probably a potassium feldspar.

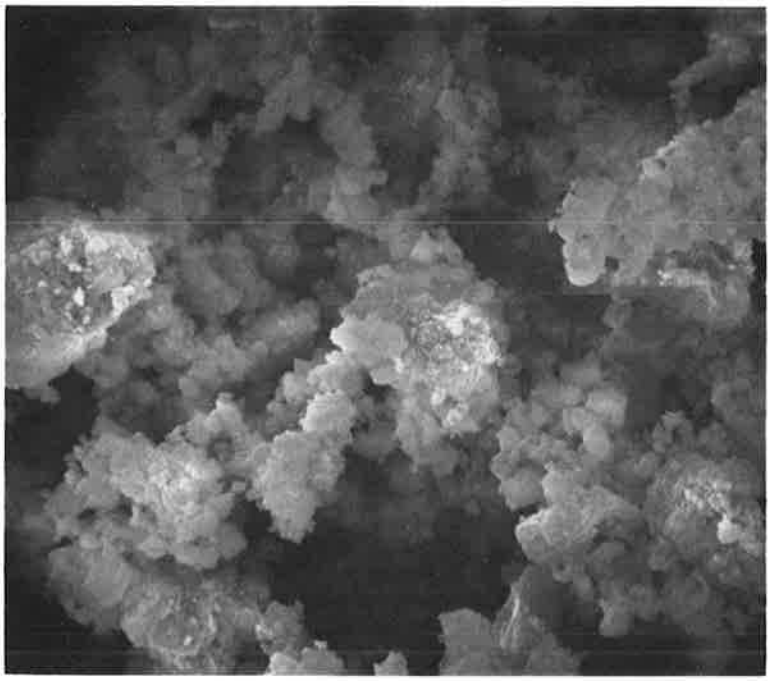

Figure 2-5. SEM of Raw Lurgi spent shale (800X).

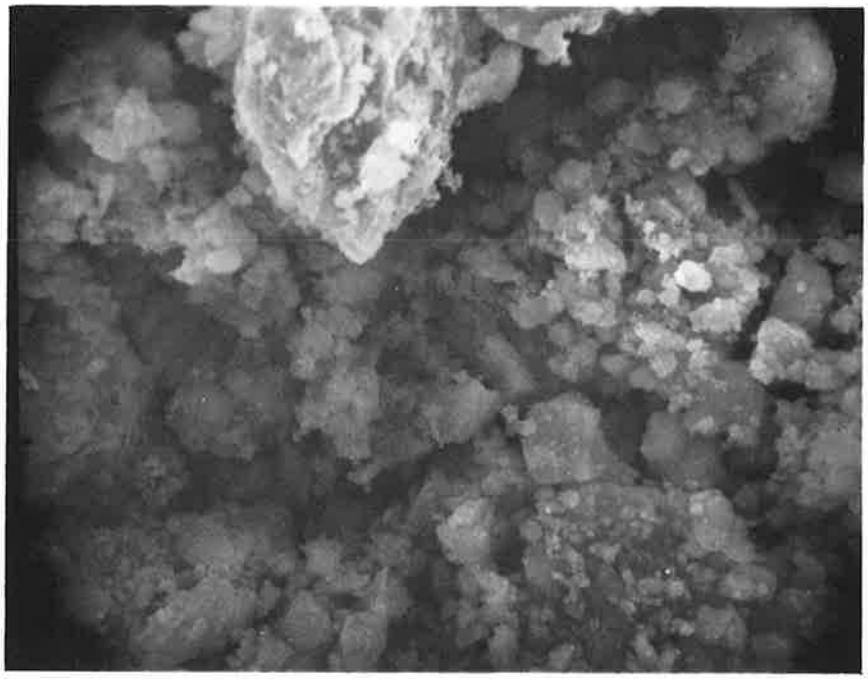

Figure 2-6. SEM of Hydrated Lurgi spent shale (800X).

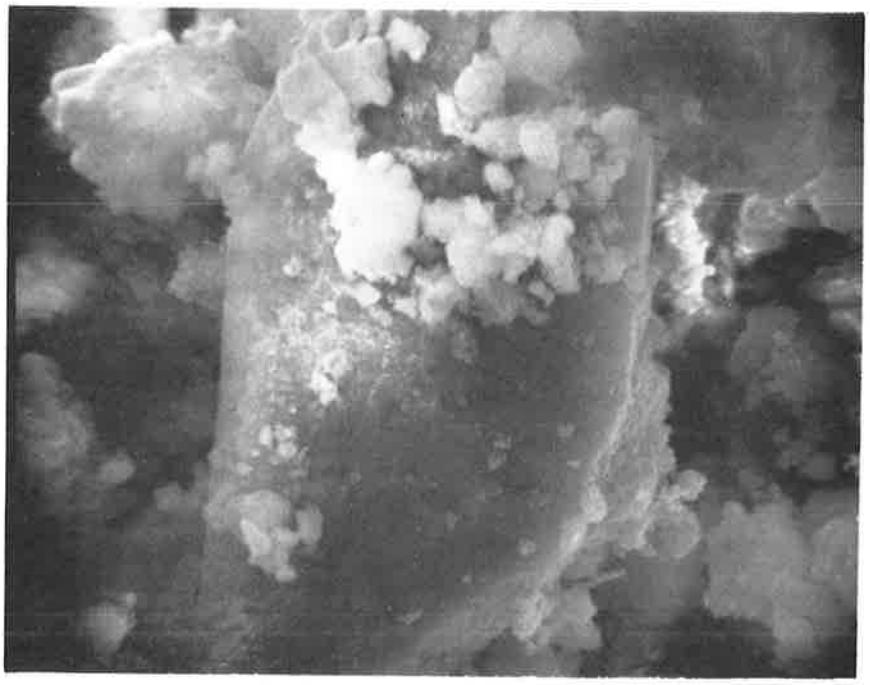

Figure 2-7. SEM of Quartz Particle (1600X).

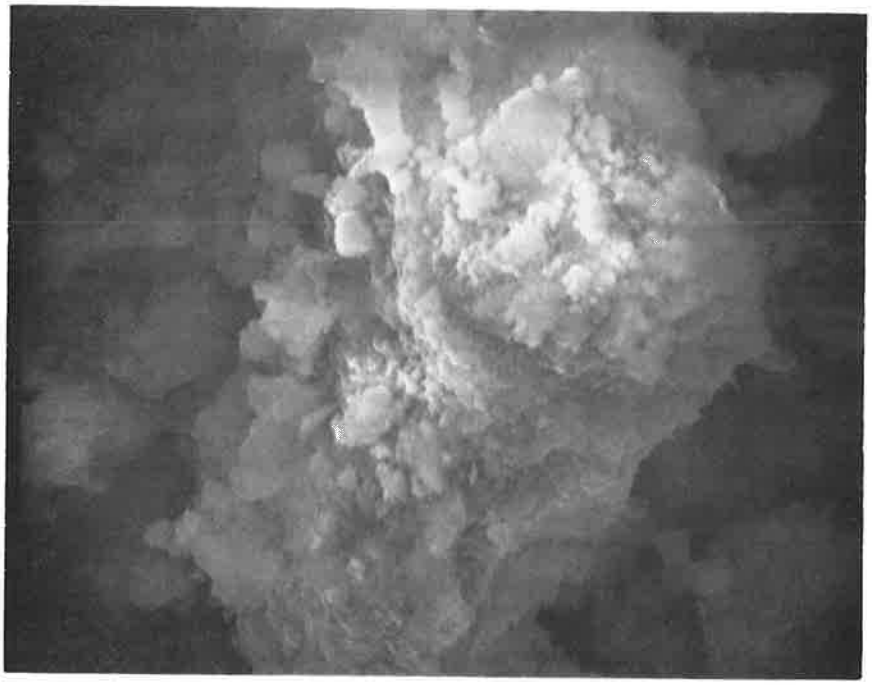

Figure 2-8. SEM of Rough Particle (1800X).

Figure 2-9. SEM of Probable Felspar Particle (9000X).

Conclusions from Cementing Tests

From the tests performed three conclusions about the cementing processes in Lurgi spent shale can be made. First, only a small portion of the material reacts during cementing. This is confirmed by the relatively small amount of hydrated water (3.6 percent vs 25 percent in a regular cement) and that XRD and SEM detected only minor changes between raw and hydrated samples. Second, the cementing minerals are almost all on the surface. This is indicated by the short, 28 day period needed to hydrate. This "surface only" effect is consistent with a short residence time in the retort (Fox, 1983). Third and finally, the cementing and hydration must be accounted for when testing Lurgi spent shale.

SAMPLE PREPARATION

The cementing properties of Lurgi spent shale caused considerable concern for the manner by which the material is prepared for hydraulic testing. There are no known similar cases in the literature. Therefore, the sample preparation method was designed to replicate, to the extent possible, the conditions in the field.

Since the principle area of concern was the long-term properties of the material, it was decided to test only hydrated samples. The disposal pile will probably have 10 to 20 percent water by weight added at placement and it is believed, based on the results of the wetting tests, that all the shale should hydrate within a month.

Packing columns with wetted material and allowing it to hydrate in place was considered as a means of creating a column of hydrated material. This was rejected due to the difficulty of drying the column and keeping cracks from forming. Likewise, it was considered impractical to drill a core of the material since its strength is relatively low. Therefore, it

was decided to grind the hydrated material to a particle size distribution which replicated the initial distribution. It is believed that this procedure results in packed columns with a pore structure reasonably similar to that expected in the field. Following is a description of the sample preparation.

A sample of Lurgi spent shale was wetted with distilled water to 30 percent by weight. The sample was allowed to hydrate in a closed container at 100 percent relative humidity and approximately 22°C. After 28 days the sample was removed and oven dried at 105°C. The entire sample was then ground by hand with an iron mortar and pestle. A portion of the sample was placed in a disk mill and ground to obtain the smaller size fractions needed. The sample was then dry sieved. The separate size fractions were weighed and remixed to obtain a size distribution which replicated the initial size distribution shown previously in Figure 2-1. Finally, the sample was redried at 105°C to remove any moisture it may have gained in processing. Sample processed in this manner was used in all subsequent tests.

WATER HOLDING CAPACITY

Vapor Sorption

Water vapor adsorption and desorption were used to determine the water holding capability at large values of apparent capillary tension. The equivalent capillary tension for a given water vapor density can be approximated by using the relation

$$h_c = - \frac{R^o T^o}{M\, g} \ln \frac{\rho_v}{\rho_{v_s}} \qquad (2\text{-}1)$$

where h_c = capillary water tension (L)

R^o = gas constant ($ML/T^{2o}K$ mole)

T^{o} = absolute temperature (^{o}K)

M = molecular weight of water (M/mole)

g = acceleration of gravity (L/T^2)

ρ_v = water vapor density, mass of vapor per unit volume of air (M/L^3)

ρ_{vs} = saturated water vapor density (M/L^3)

The ratio ρ_v/ρ_{v_s} is the relative humidity, RH. Using appropriate values for R^{o}, M, and g and assuming T^{o} equals $299^{o}K$ yields

$$h_c = -1.39 \times 10^6 \ln RH \qquad (2\text{-}2)$$

where h_c is in centimeters of water. The value of h_c calculated in this manner is only an approximation of the actual capillary tension because of dissolved salts which are not accounted for in eqn. 2-1.

In the vapor adsorption tests, approximately five grams of oven dried hydrated and processed Lurgi retorted shale were weighed into sample cans. Duplicate samples were then equilibrated in closed chambers over various saturated salt solutions. The chambers were kept at atmospheric pressure and were maintained at $22^{o}C \pm 1^{o}C$ by a constant temperature bath. Once a day the samples were weighed to an accuracy of 0.0001 gm. The sample cans were covered during weighing to minimize evaporation or condensation. The samples were considered to reach equilibrium if their weight did not change more than 0.001 gm over 24 hours. Table 2-5 lists the saturated solutions used.

For the vapor desorption test the samples were "wetted" by vapor adsorption over distilled water to water contents in excess of 20 percent by weight. To speed the desorption process the samples were placed in vacuum desiccators between weighings. The vacuum in the chambers was about

Table 2-5. Saturated salt solutions used in vapor sorption.[1]

Salt	Vapor Density gm/cm^3	RH 22°C	h_c[2] (cm)
NaOH	1.2×10^{-6}	0.061	3.89×10^{6}
$ZnCl_2$	1.90×10^{-6}	0.100	3.20×10^{6}
$MgCl_2$	6.31×10^{-6}	0.328	1.55×10^{6}
K_2CO_3	8.40×10^{-6}	0.436	1.15×10^{6}
$Mg(NO_3)_2$	1.04×10^{-5}	0.542	8.51×10^{5}
$NaNo_2$	1.25×10^{-5}	0.649	6.00×10^{5}
NaCl	1.46×10^{-5}	0.758	3.85×10^{5}
KCl	1.64×10^{-5}	0.850	2.26×10^{5}
KNO_3	1.79×10^{-5}	0.931	9.93×10^{4}
$Ca(H_2PO_4)_2$	1.84×10^{-5}	0.948	7.42×10^{4}
KH_2PO_4	1.85×10^{-5}	0.963	5.24×10^{4}
$K_2Cr_2O_7$	1.89×10^{-5}	0.980	2.82×10^{4}

[1]From: Ecology 41:233 (1960) Saturated Solutions for the Control of Humidity in Biological Research.

[2]Value of h_c is unadjusted for osmotic pressure.

20 in. of Hg. The chambers were kept in a constant temperature room at 23.5 ± 1°C.

Figure 2-10 presents the vapor adsorption and desorption isotherms for the Lurgi retorted shale where θ is the water content by volume and ϕ is the total porosity. The adsorption isotherm shows that the water content, θ, is strongly dependent upon the vapor pressure for $\theta < 0.12$.

Pressure Plate

The water holding capacities at capillary tension heads of 88 to 1.5×10^4 cm of H_2O attained by both drainage and wetting were measured using methods described by Klute (1984) and ASTM D 2325. Approximately 66 grams

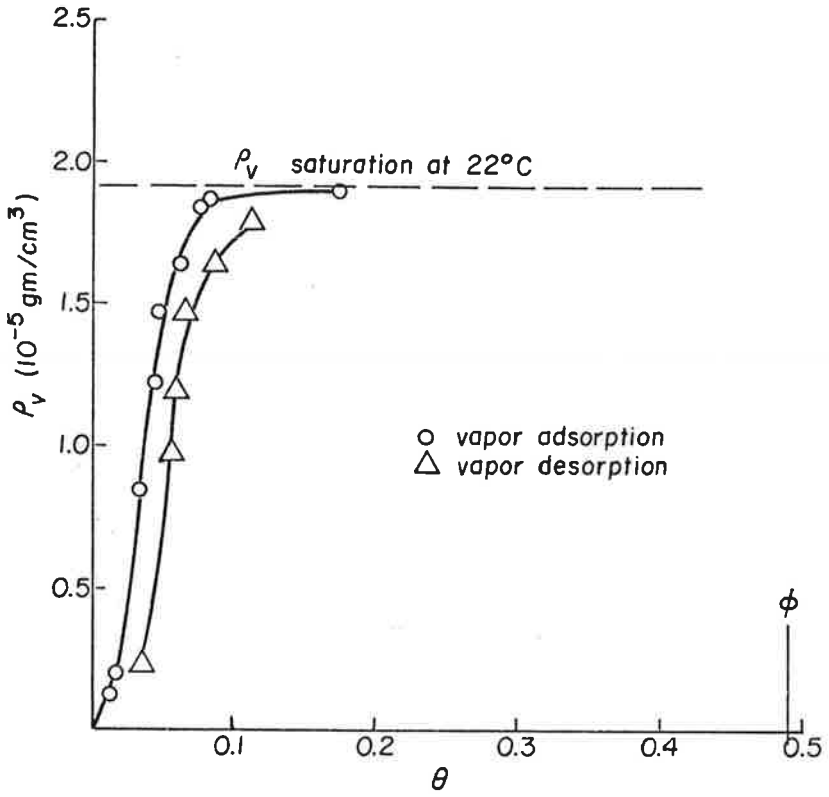

Figure 2-10. Vapor sorption isotherms for Lurgi retorted shale.

of oven dried hydrated and processed material were packed in sample rings at a bulk density of 1.4 gm/cm^3. Samples for the drainage curve were wetted over night to "natural" saturation. Triplicate samples were then placed in pressure cells at various constant pressures for 3 to 5 days, removed, weighed and oven dried to determine their water content. If the triplicate samples were not in agreement the test was rerun. Figure 2-11 presents the retention relations for both drainage and wetting.

The vapor sorption data is also plotted on Figure 2.11. The values of h_c on the vapor sorption have been reduced by 2.5 x 10^4 cm to account for the osmotic potential. The value of 2.5 x 10^4 cm was arrived at by matching the 98 percent RH adsorption water content to the pressure plate data. In any event, the curves shown in Figure 2-11 are insensitive to the

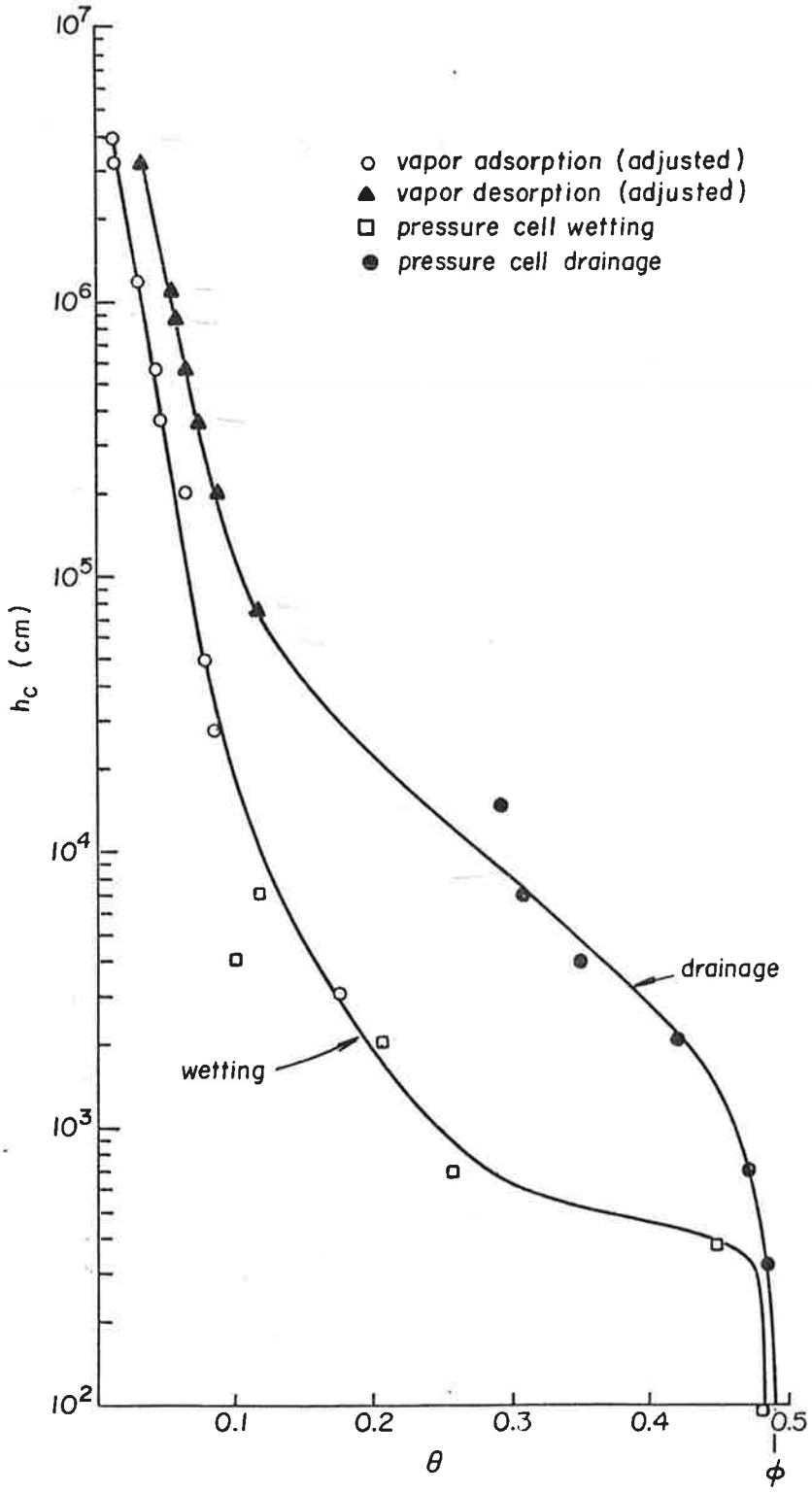

Figure 2-11. Water retention relations for Lurgi spent shale.

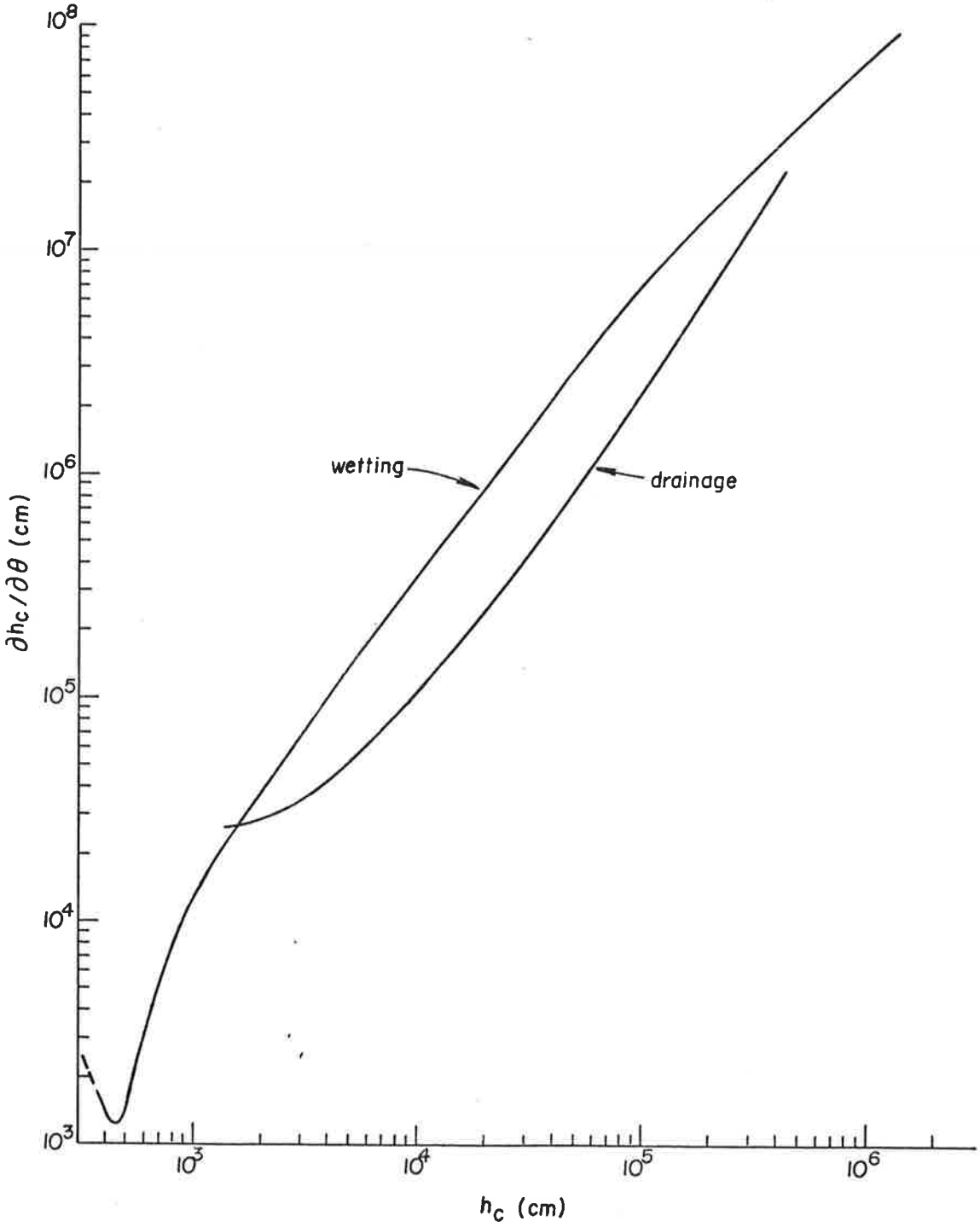

Figure 2-12. Water retention slopes versus capillary head.

estimated osmotic potential.

In later calculations the slope of the water retention curve as a function of h_c will be used. Figure 2-12 presents that relationship.

SPECIFIC SURFACE

Using the vapor adsorption data and B.E.T. theory (Brunauer, Emmett and Teller, 1938) it is possible to calculate the specific surface of the Lurgi retorted shale. Brunauer, Emmett and Teller showed that, for many materials, the volume of a vapor absorbed by a porous media could be related to the vapor pressure and specfic surface of the media. The B.E.T. equation for low vapor densities can be stated as:

$$\frac{\rho_v}{\theta(\rho_{vs}-\rho_v)} = \frac{1}{\theta_m C} + \frac{(C-1)\rho_v}{\theta_m C \rho_{vs}} \qquad (2\text{-}3)$$

where θ_m = volume of gas adsorbed for one monolayer per volume of media (L^3/L^3)

C = constant

Using the vapor adsorption data for the four lowest vapor densities and a least squares linear regression yields a value for θ_m of .0175, with a regression coefficient of 1.0000. Thus, at a water content of .0175 there is enough water in the retorted shale to, on the average, cover all exterior and interior surfaces with one molecular layer of water. Using an area of 9.6×10^{-16} cm^2 for a water molecule yields a specific surface of 5.6×10^5 cm^2/cm^3, ($40 m^2/gm$) at a bulk density of 1.4. This is a relatively large value for a non-clay material.

SATURATED HYDRAULIC CONDUCTIVITY

The saturated hydraulic conductivity of the processed Lurgi retorted shale was determined by a falling head permeameter. A single column 6.95 cm in diameter with a test section of 33 cm was packed to a dry bulk density of 1.37 gm/cm^3. The column was allowed to saturate overnight by filling with solution from the bottom. A one-third saturated $CaSO_4$ solution was used to minimize any claylike swelling. During the test the hyraulic gradient varied from 3.5 to 6.6.

A total of eight measurements were made over a three day period. The conductivity ranged from 9.69 to 9.13×10^{-6} cm/s.

Chapter 3

HYDRAULIC SORPTION AND REDISTRIBUTION TEST

THEORETICAL

Chemical water as part of the bulk solution is known to move through less than saturated porous media by 1) convection in the solution due to hydraulic gradients, 2) diffusion in the solution phase affected by gradients of chemical potential, 3) vapor convection in the gas phase due to bulk gas flow, and 4) vapor diffusion in the gas phase due to gradients of the vapor density. Grismer (1984) has shown that liquid phase convection and vapor phase diffusion are the only significant processes in a soil similar to Lurgi retorted shale.

The volume flux of the solution phase (both water and solute) is given by Darcy's Law

$$q = -K \nabla (h + z) \qquad (3\text{-}1)$$

where q = volume flux of solution (L^3/L^2-T)

K = hydraulic conductivity (permeability) (L/T)

h = water pressure head, negative in unsaturated conditions; note that $h_c = -h$, (L)

z = vertical coordinate (L)

The permeability K in Darcy's law is a strong function of the degree of wetness (water content), decreasing by orders of magnitude as the water content decreases. The validity of Eq. 3-1 and of the entire concept of permeability depends upon continuity of the liquid phase within the porous medium. There exists a water content, different for different porous media, below which the liquid phase is discontinuous and bulk flow of liquid is no longer possible (Rose, 1963; Jackson, 1964; Philip and De Vries, 1957).

For horizontal flow, the convective mass flux of the component water in the solution phase is given by:

$$F_l = C_\omega \, q = - C_w \, K \, \partial h/\partial x \qquad (3\text{-}2)$$

where F_l = liquid water mass flux (M/L^2-T)

C_ω = water concentration in solution phase (M/L^3)

x = horizontal coordinate (L)

It is necessary to consider the component water concentration in the solution phase because solute concentrations can become quite large in sorption tests.

In unsaturated flow tests usual methods of measuring pressure head such as tensiometers and thermocouple psychrometers, fail in the very dry range, and the gradient of pressure head cannot be measured. This difficulty is circumvented by assuming a unique, equilibrium relation between water pressure head and the water content such that:

$$D_l = K \frac{dh}{d\theta} = -K \frac{dh_c}{d\theta} \qquad (3\text{-}3)$$

where D_l = the liquid phase diffusivity (L^3/L-T)

θ = the volumetric solution content (L^3/L^3)

Placing Eq. 3-3 into 3-2 yields

$$F_l = -C_\omega \, D_l \frac{\partial \theta}{\partial x} \qquad (3\text{-}4)$$

Equations 3-3 and 3-4 suggest an especially simple method of determining the permeability K as a function of water content. All that is required is to establish a known mass flux of liquid water and measure the corresponding water content gradient $\partial\theta/\partial x$. The liquid diffusivity D_l is calculated as the ratio of liquid flux to water content gradient. In turn K is calculated from Eq. 3-3 and a measured relationship $h_c = h_c(\theta)$ (Figures 2-11 and 2-12). This method is relatively simple and has been widely

used in both steady state and transient flow situations.

Implicit in the above described procedure is the assumption that the mass flux of liquid is known. At low water contents, the water content changes in both space and time as the result of combined vapor and liquid flux and it is not possible to interpret measured gradients of water content as being affected by liquid flow only. It is possible, however, to include the influence of vapor flux by writing Fick's law for vapor diffusion:

$$F_v = -D_v \frac{\partial \rho_v}{\partial x} \tag{3-5}$$

where F_v = vapor mass flux (M/L^2-T)

D_v = vapor diffusion coefficient (L^2/T)

ρ_v = vapor density (M/L^3)

Again it is extremely difficult to measure the vapor density gradient in a porous media at low water contents. Thus, it is assumed that a unique, equilibrium relationship between vapor density and water content exists such that:

$$F_v = -D_v \frac{d\rho_v}{d\theta} \frac{\partial \theta}{\partial x} \tag{3-6}$$

Combining Eqs. 3-4 and 3-6 yields the total mass flux of water, F_w in both liquid and vapor phases:

$$F_w = F_l + F_v = -\left(C_\omega D_l + D_v \frac{d\rho_v}{d\theta}\right) \frac{\partial \theta}{\partial x} \tag{3-7}$$

Performing a mass balance on a control volume of porous media will yield the equation of flow for the component water:

$$\frac{\partial(\theta C_\omega)}{\partial t} = -\frac{\partial F_w}{\partial x} = \frac{\partial}{\partial x}\left[\left(C_\omega D_l + D_v \frac{d\rho_v}{d\theta}\right) \frac{\partial \theta}{\partial x}\right] \tag{3-8}$$

This result suggests that a transport coefficient be defined that combines the contributions of both vapor and liquid.

$$C_\omega D_{lv} = C_\omega D_l + D_v \frac{d\rho_v}{d\theta} \tag{3-9}$$

Substituting Eq. 3-9 into 3-19 yields:

$$\frac{\partial(\theta C_\omega)}{\partial t} = \frac{\partial}{\partial x}\left(C_\omega D_l \frac{\partial \theta}{\partial x}\right) \tag{3-10}$$

Experimenters have found it possible to measure F_w and $\partial\theta/\partial x$ at the dry end of the water content range and, therefore, to determine the combined transport coefficient shown in Eq. 3-9 (e.g., Jackson, 1964a, b, and c, 1965; Rose, 1963a and b, 1968a and b). It has not been possible to measure the separate phase fluxes and thus to directly determine the individual diffusivities for both phases.

Integrating Eq. 3-10 with respect to x, from x=0 to x=x' and using a known total mass influx, Q at x=0 yields an equation for the combined liquid-vapor diffusivity:

$$D_{lv}(\theta_{x'}) = \frac{1}{C_{\omega_{x'}} \frac{\partial \theta_{x'}}{\partial x}}\left[\left(\int_0^{x'} \frac{\partial(\theta C_\omega)}{\partial t} dx\right) - Q\right] \tag{3-11}$$

where the variable x' indicates an arbitrary value of x. To evaluate Eq. 3-11 would require an instantaneous measurement of $\partial\theta/\partial t$ which is not possible. Instead the change in θ over a finite time period t_1 to t_2 is measured. Using a central finite different approximation yields:

$$D_{lv}\left(\frac{\theta_{x't_1} + \theta_{x't_2}}{2}\right) = \frac{2\left[\left(\sum_0^{x'} \Delta(\theta C_\omega)\Delta x\right) - Q\right]}{\left(C_{\omega_{x't_1}} \frac{\Delta\theta}{\Delta x_{t_1}} + C_{\omega_{x't_2}} \frac{\Delta\theta}{\Delta x_{t2}}\right)\Delta t} \tag{3-12}$$

Equation 3-12 is based on the assumption that $D_{lv}(\theta)$ is linear over the range θ_{t_2} to θ_{tt_2}. This is an accurate approximation provided that a small increment of θ is used in the computations.

As stated previously it is not possible to directly separate the liquid and vapor fluxes. Jackson (1964c) estimates the vapor contribution to the combined coefficient by an independent method and then subtracts to determine the liquid diffusivity. His independent estimate of the vapor contribution is made from

$$D_v = D_a \frac{(\phi-\theta)}{T} \qquad (3\text{-}13)$$

where D_a = vapor diffusivity in air (L^2/T)

ϕ = porosity (L^3/L^3)

T = tortuosity (L/L)

Also required is a measurement of the equilibrium adsorption isotherm $\rho_v=\rho_v(\theta)$ from which $d\rho_v/d\theta$ is calculated.

By this means, Jackson was able to estimate the water content at which the permeability to liquid is zero. We will refer to this water content as the critical water content. For the two soils used in his investigation, the critical water contents ranged from 0.03 to 0.06 on a volume basis. These corresponded to relative humidities of 0.5-0.7. Very similar results were reported by Rose (1963). Philip and De Vries (1957) speculated on theoretical grounds that K should be zero at a relative humidity of about 0.6.

Grismer (1984) has shown that the critical water content can be directly measured by using a tracer salt NaI which is detectable by dual source gamma ray attenuation. In Grismer's method, a NaI solution is injected into a dry column and traced as it advances. At some point, pure water is observed moving ahead of a salt front. The only reasonable

explanation of this observation is that pure water has moved ahead of the continuous liquid phase by vapor diffusion. Using gamma ray attentuation has the advantage that the water contents can be measured without destroying the test column. Thus, it is possible to collect much more data from fewer columns.

EXPERIMENTAL

Two separate tests were performed. In each test a lucite column with an internal diameter of 3.8 cm and 15 cm length was packed with the Lurgi retorted shale. Care was taken during packing to insure the material did not separate by sizes or into layers. The compacted bulk density obtained in the columns was 1.4 gm/cm^3 (87 lb/ft^3). The total column porosity was 49 percent. The columns packed with oven dry material were placed horizontally between a gamma-ray detector and two different energy gamma ray sources (^{241}Am, 60 KEV and ^{137}Cs, 600 KEV). A 0.10 molar sodium iodine solution was injected by syringe pump into one end and traced by the attenuation of the two energy gamma rays as measured by the detector. Figure 3-1 shows the system.

Since the attentuation coefficients for the water and the salt are different for each energy source, it is possible to calculate both the water content and the salt concentration along the column as the water moved through it. At intervals ranging from 12 to 48 hours over a seven day period, the column was scanned and the water content and salt concentration was determined at several positions. Between scans the injection rate was held constant but was adjusted at the end of scans if necessary to produce adequate profiles. The flows used varied from 1.7×10^{-5} to 3.7×10^{-4} gm/s.

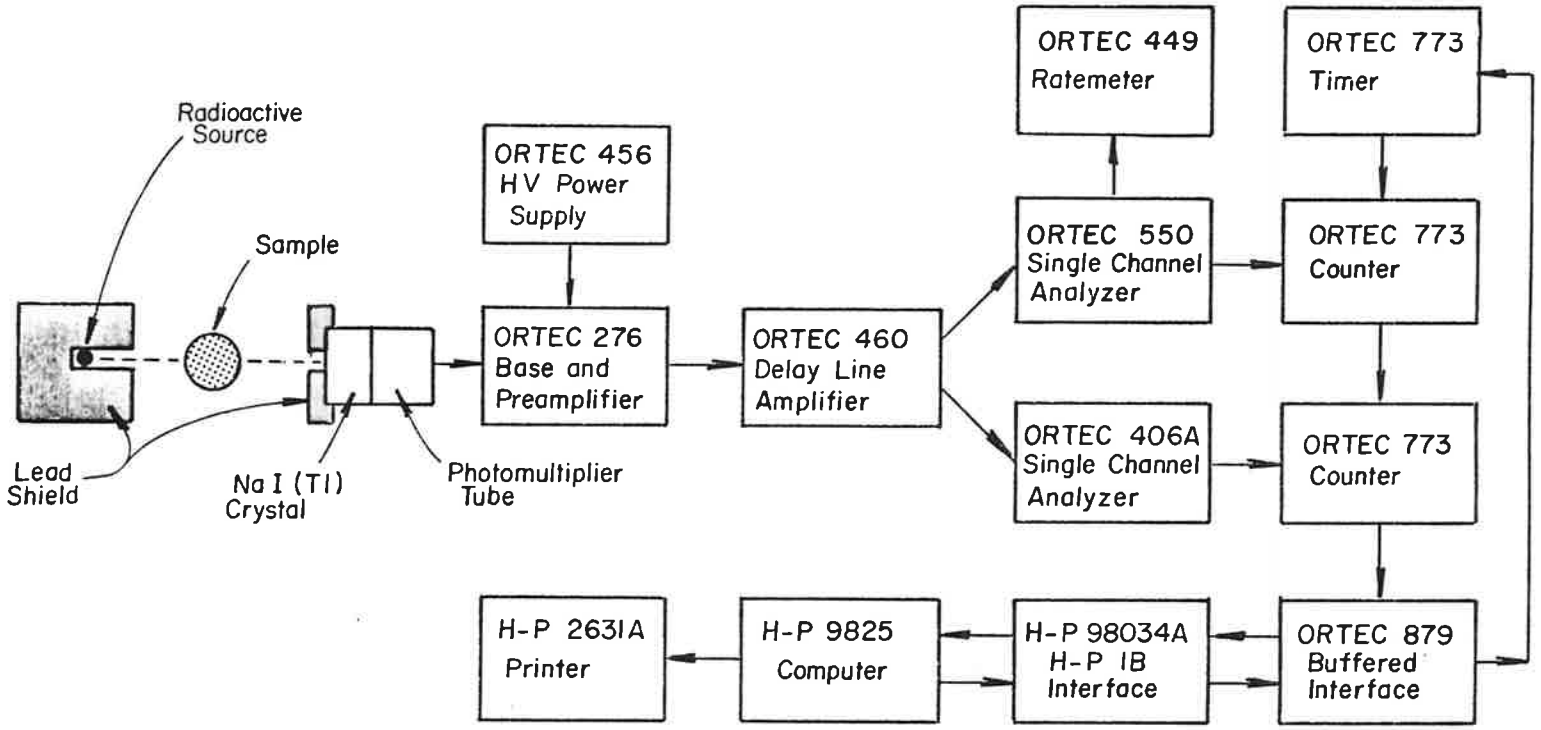

Figure 3.1. Dual source gamma system.

Data were read from the gamma system into a HP-9825 computer where it was stored and reduced. After the second scan, the combined liquid-vapor diffusivity at the various positions was calculated by Eq. 3-12. The appendix presents the experiment results.

Chapter 4

RESULTS

INTERPRETATION

Before the test data are detailed it will be instructive to describe in general terms the expected results. Figure 4.1a, b, and c presents an idealized depiction of a soil's properties and a single scan on an initially dry column. Figure 4-1a shows a typical vapor adsorption isotherm similar to Figure 2.10. Notice that the slope $d\rho_v/d\theta$ is large at small water contents and decreases to zero well before saturation. Figure 4.1b shows a typical graph of combined liquid-vapor diffusivity for a fine grained material. This shape was first proposed by Phillip (1957) and later confirmed by Jackson (1964a, b and c) and Rose (1963a and b). Notice the local maximum that occurs at low water contents. In Figure 4.1c the horizontal axis is the column position (length) from the inlet. The vertical axis is both the volumetric water content, θ and the solution salt concentration. The profiles shown would be typical of conditions after injecting solution for a day or more. When examining the water content profile it is necessary to remember that the flow is unsteady and that the profile is only valid for an instant of time. At a later moment the profile would lie above the one shown.

The water content profile shows that, at the injection end, the water content has been raised to a relatively large, but less than saturated value. Since the material's diffusivity increases with increasing water content (Figure 4-1b) the gradient $\partial\theta/\partial x$ needed to drive the flow is relatively small near the inflow end. Also at the large water contents the slope of the vapor adsorption isotherm, $d\rho_v/d\theta$, is practically zero, and therefore, vapor transport is practically zero (Figure 4-1a). All flow is by liquid convection.

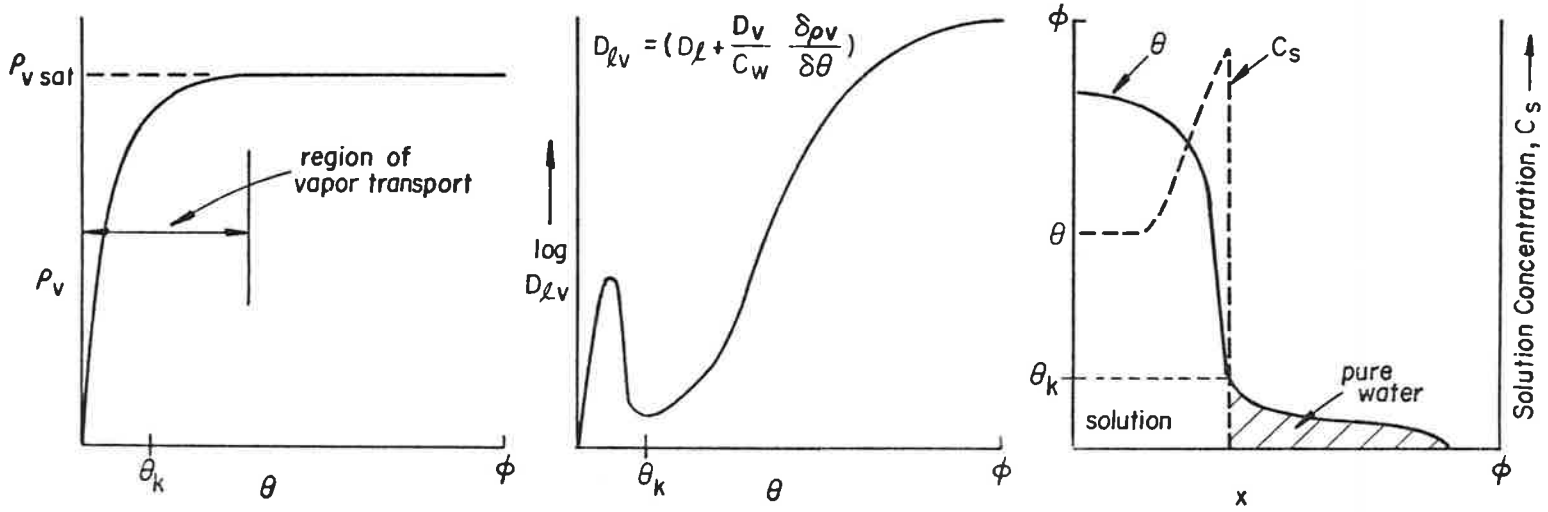

a) Vapor adsorption isotherm

b) Diffusivity

c) Water and salt profiles after injection

Figure 4-1. Idealized depiction of dry column behavior.

Further into the column the water content decreases rapidly. In this region, the diffusivity becomes small (Figure 4-1b), and the gradient $\partial\theta/\partial x$ increases in order to maintain the flow. At these intermediate water contents vapor transport becomes significant relative to liquid convection (see Figure 4-1a).

Still further into the column, the water contents reach very small values. At these values of water content the liquid phase may be discontinuous but the slope of the vapor adsorption isotherm ($d\rho_v/d\theta$) is quite large (Figure 4-1a). Thus, vapor transport is responsible for the increased D_{lv} (Figure 4-1b). Notice in Figure 4-1c that, due to the larger value of D_{lv} the water content gradient ($\partial\theta/\partial x$) can be reduced to almost zero and is still adequate to drive the small mass flux that occurs in the vapor phase.

The salt concentration in Figure 4-1c is equal to the injection concentration at x=0. Further into the column, the salt concentration increases significantly. The increase is due to the initiation of vapor transport. As water evaporates from the solution phase the remaining solution must contain the same mass of salt in less solution volume. As the salt concentration increases, back diffusion toward the inlet of the column occurs. At some point in the column the concentration decreases to zero in a sharp front. In an ideal case the solution content just beyond the salt front will be the critical content, θ_k as shown. At that content the liquid phase becomes discontinuous and the salt cannot advance.

In most instances the limited spatial resolution of the expertmental data, coupled with the steep gradients of salt concentration and water content, make it impossible to identify the critical water content from a single measurement of the profiles. Instead, a series of measurements provide a range of water contents within which the critical value lies.

The range is progressively narrowed by measuring several salt and solution-content profiles.

RUN NUMBER 1

In the first test a total of 6.05 gm of 0.1 molar NaI solution was injected over a 7 day period. Due to an equipment failure no solution was injected during a period from hours 48 to 96. This failure did not affect results from the latter part of the test. The injection rate was held constant at about 1.5×10^{-5} gm/s. The inlet mass flux of NaI was 1.3×10^{-6} gm/cm^2-s. Seven scans were performed. Figures 4-2 and 4-3 show three of the water content and NaI concentration profiles during the wetting period. The profiles are quite similar to the ideal profiles in Figure 4-1. Notice that a significant zone of salt free water developed ahead of the salt front.

After the injection was terminated the solution redistribution was measured. The redistribution was monitored for a total of 97 days. Fourteen redistribution scans were performed. Figure 4-4 and 4-5 show typical redistribution profiles for NaI concentration and solution content. The graphs show that while the water content profile adjusted toward a more uniform distribution, the salt concentration profile continued to exhibit a sharp front and the concentration behind the front continued to increase as water moved forward in the column by vapor diffusion.

RUN NUMBER 2

In the second run the column was injected with 34.75 gm of solution at varying rates of 2.9×10^{-5} to 3.7×10^{-4} gm/s. The mass flux of NaI was 2.6×10^{-6} to 3.4×10^{-5} gm/cm^{2}s. Injection was stopped after 8 days. No redistribution was measured since the final water contents were well above the critical value. A total of 17 scans were performed. Figures 4-6 and 4-7 shows typical salt concentration and water content profiles

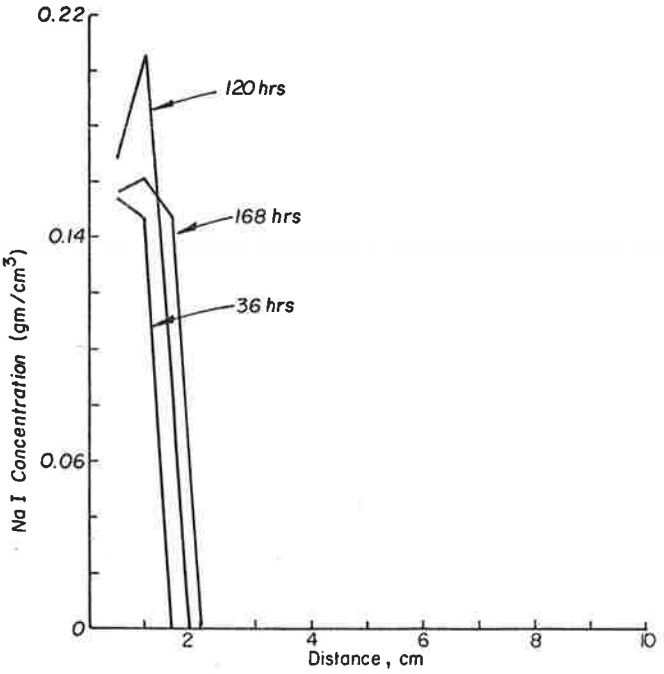

Figure 4-2. Concentration profiles for wetting in Run 1.

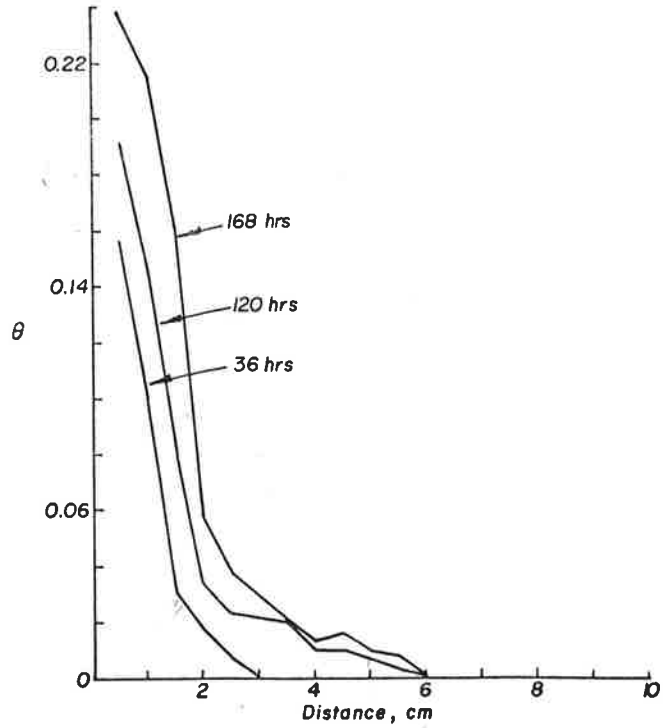

Figure 4-3. Solution content profiles for wetting in Run 1.

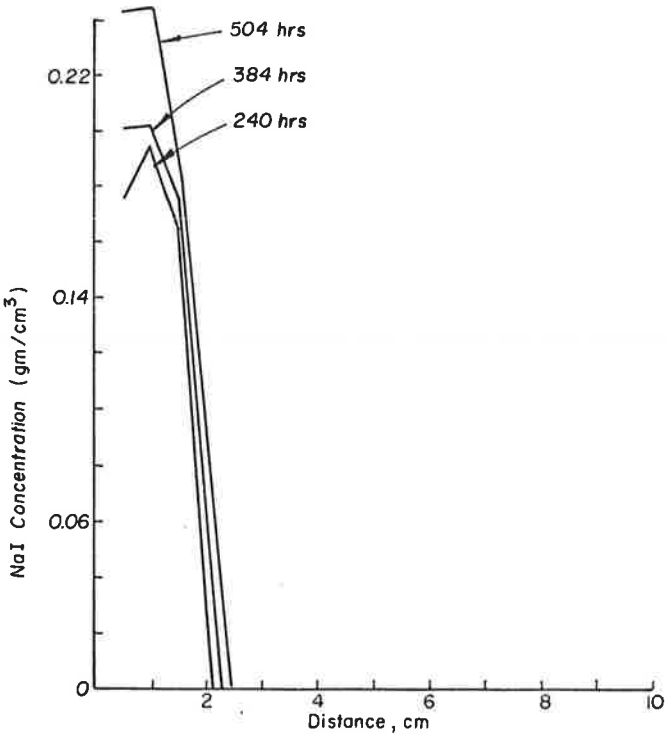

Figure 4-4. Concentration profiles for redistribution in Run 1.

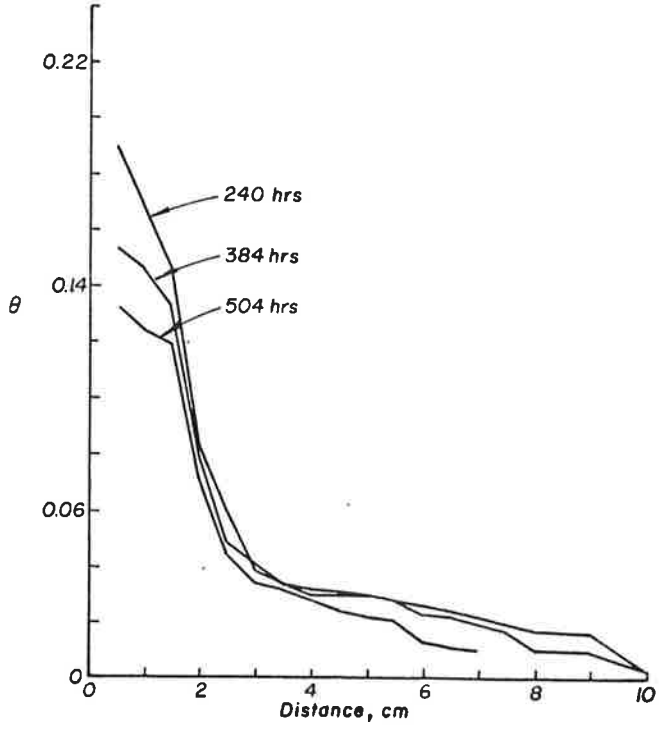

Figure 4-5. Solution content profiles for redistribution in Run 1.

for the run. The early profile at 120.5 hrs, which corresponds to the lower injection rates, is similar to Run 1 but the profiles resulting from high injection rates show a much steeper water content front. This could be expected since the diffusivity increases greatly with water content. The sharpness of the salt front is reduced due to the piston displacement of the salt free water and subsequent NaI diffusion.

CRITICAL WATER CONTENT

Figure 4-8 presents the range of water contents at the salt front in Run 1 for each scan. Scans 13 to 21 are unsuitable due to the redistribution to water content below previous values. The top of each bar represents the lowest water content at which salt was observed while the bottom of the bars represents the highest water content with pure water. The shaded water content range 0.063 to 0.083, is common to all but one observation.

Figure 4-9 shows the range of water contents at the salt front in Run 2. Scans 15, 16 and 17 are unsuitable due to piston displacement. Due to the steep water content profiles caused by the high injection rates, the ranges tend to be much larger than in Run 1. Two scans, Number 1 and 13 show dashed regions. In these scans the position of the salt front was uncertain. The shaded common area from 0.053 to 0.066 water content is common to 12 of the 14 scans.

Comparison of Figures 4-8 and 4-9 indicates a common overlap of water contents between 0.063 and 0.066 by volume. Examination of the detailed data in the appendix would indicate the critical water content is at the upper end of this range and possibly somewhat greater. This is due to the upper limit being set by the readings at high flow rates which are subject to greater error. It is concluded that a value of 0.066 for the critical water content is conservative.

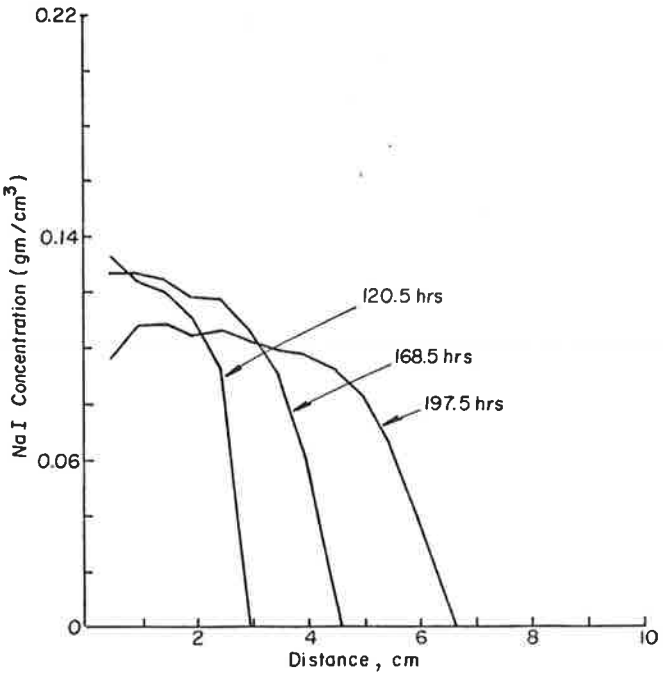

Figure 4-6. Concentration profiles for Run 2.

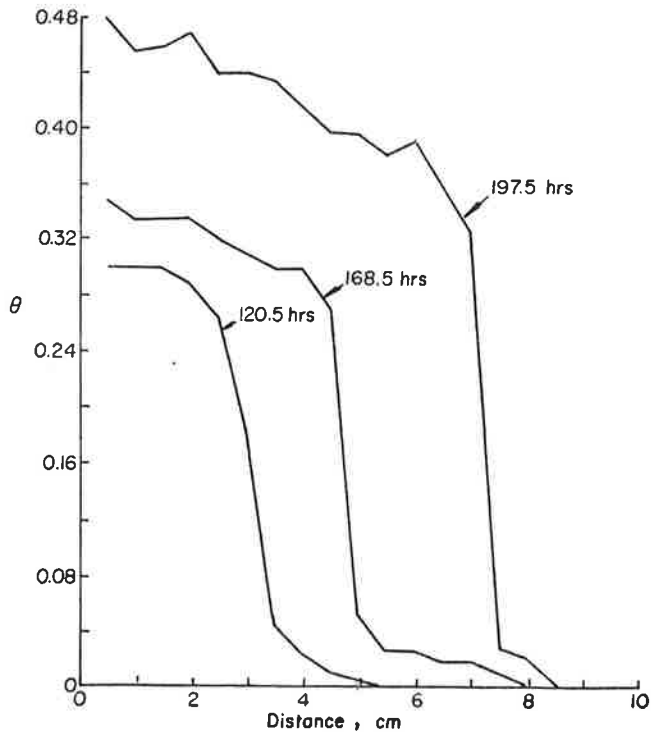

Figure 4-7. Solution content profiles for Run 2.

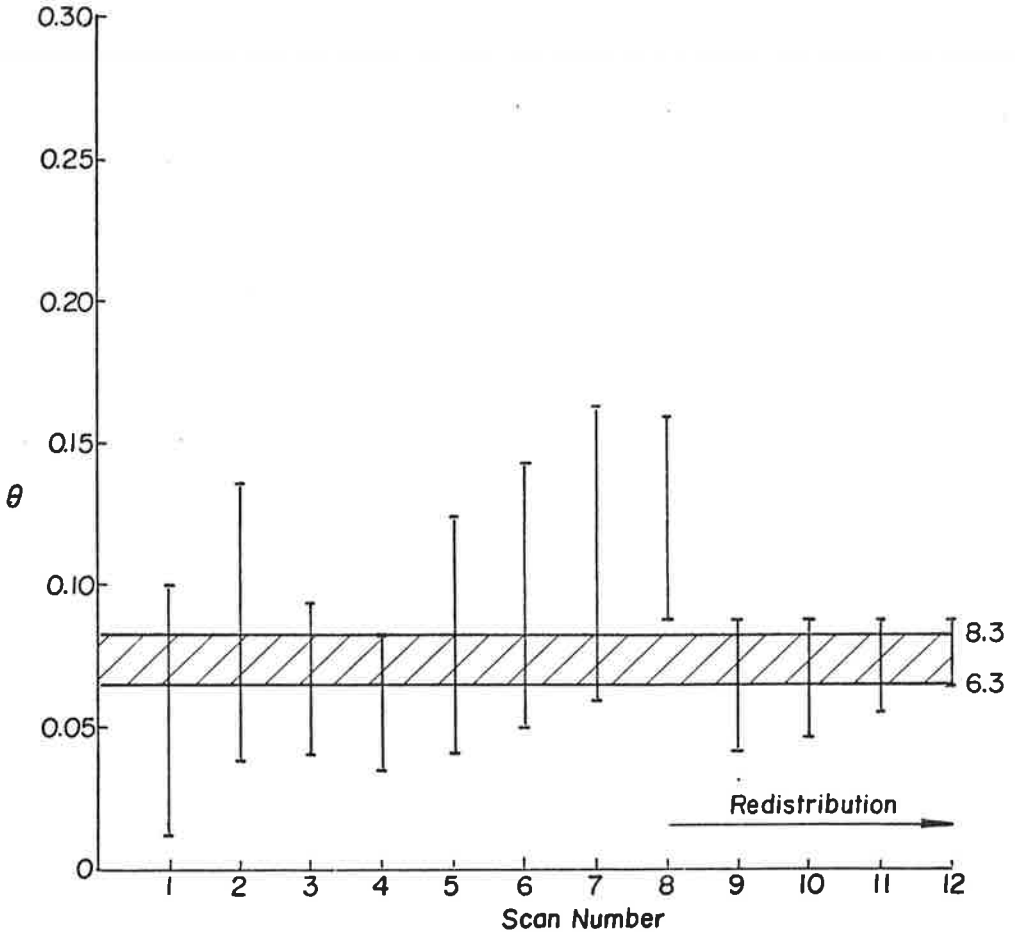

Figure 4-8. Range of water contents at salt front for Run 1.

While the foregoing is strong evidence that the liquid becomes discontinuous at 0.066, it does not rule out the possibility that diffusion of NaI at very slow rates is occurring at the low water contents. While it is very difficult to prove that no diffusion is occurring it is possible to estimate the maximum value that the diffusion coefficient could be using the data from Run 1 scans 20 and 21. Between the scans the salt front was stationary at 2.0 cm from the inlet. Even though the salt concentrations were quite large (.081 to .125 gm/cm^3) at that position no salt was observed to move forward into the column during the 700 hours between the scans.

Fick's law for diffusion is:

$$F_s = -D_s \frac{\partial C_s}{\partial X} \qquad (4\text{-}1)$$

where F_s = mass flux of solute (M/L^2T)

D_s = diffusion coefficient of solute (L^2/T)

C_s = solute concentration (m/L^3)

Rearranging the equation, converting to finite difference and supplying the appropriate inequality yields the relationship for D_s:

$$D_s \leq -F_s \frac{\Delta x}{\Delta C_s}$$

For this case Δx = .5 cm, and ΔC_s has an average value of .103 gm/cm^3. The maximum concentration of NaI that would go undetected at 2.5 cm is 4.3×10^{-4} gm/cm^3, which would correspond to a flux of 1.7×10^{-10} gm/cm^2-sec. Using these values yield $D_s \leq 8 \times 10^{-11}$ cm^2/sec. The smallest known diffusion coefficient in the literature (Kemper, Maasland and Porter, 1964) is an order of magnitude greater. Thus it can be concluded that no diffusion is occurring and no continuous liquid phase is present.

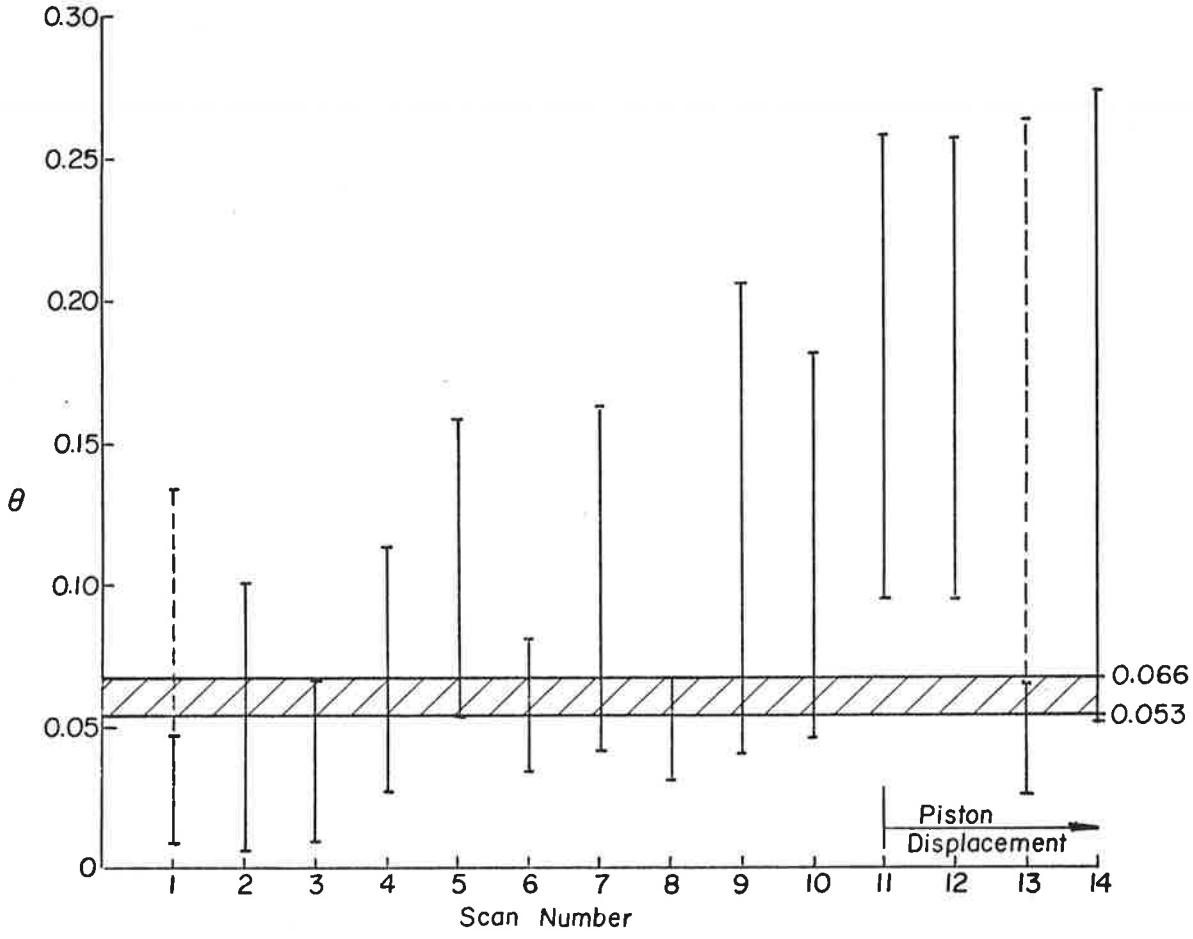

Figure 4-9. Range of water contents at salt front for Run 2 (dashed lines indicate probable range).

HYDRAULIC PROPERTIES

Using Eq. 3-12 the diffusivity for each position and between each scan was calculated using the HP9825 computer. Figure 4-10 presents a graph of D_{lv} versus θ for the results of both runs. As can be seen the function exhibits the expected local maximum in the region where vapor transport dominates. The minimum value of D_{lv} occurs at the critical water content of 0.066. This is interesting but not of great importance. Grismer (1984) found in the materials he tested that the minimum diffusivity occurred at water contents less than the critical.

Using Eq. 3-3 and the data from the water retention curve (Figures 2-11 and 2-12), the hydraulic conductivity, K as a function of water content can be calculated. Figure 4-11 presents this relationship. As the figure shows the conductivity varies over nine orders of magnitude from 10^{-5} cm/s at saturation to 10^{-13} cm/s at the critical water content. This is a very large range, but similar results has been obtained by Rose (1968). Insofar as the critical water content of 0.066 represents the value at which the liquid phase become discontinuous, the hydraulic conductivity curve ends at the position shown (i.e. for $\theta < 0.066$, K=0).

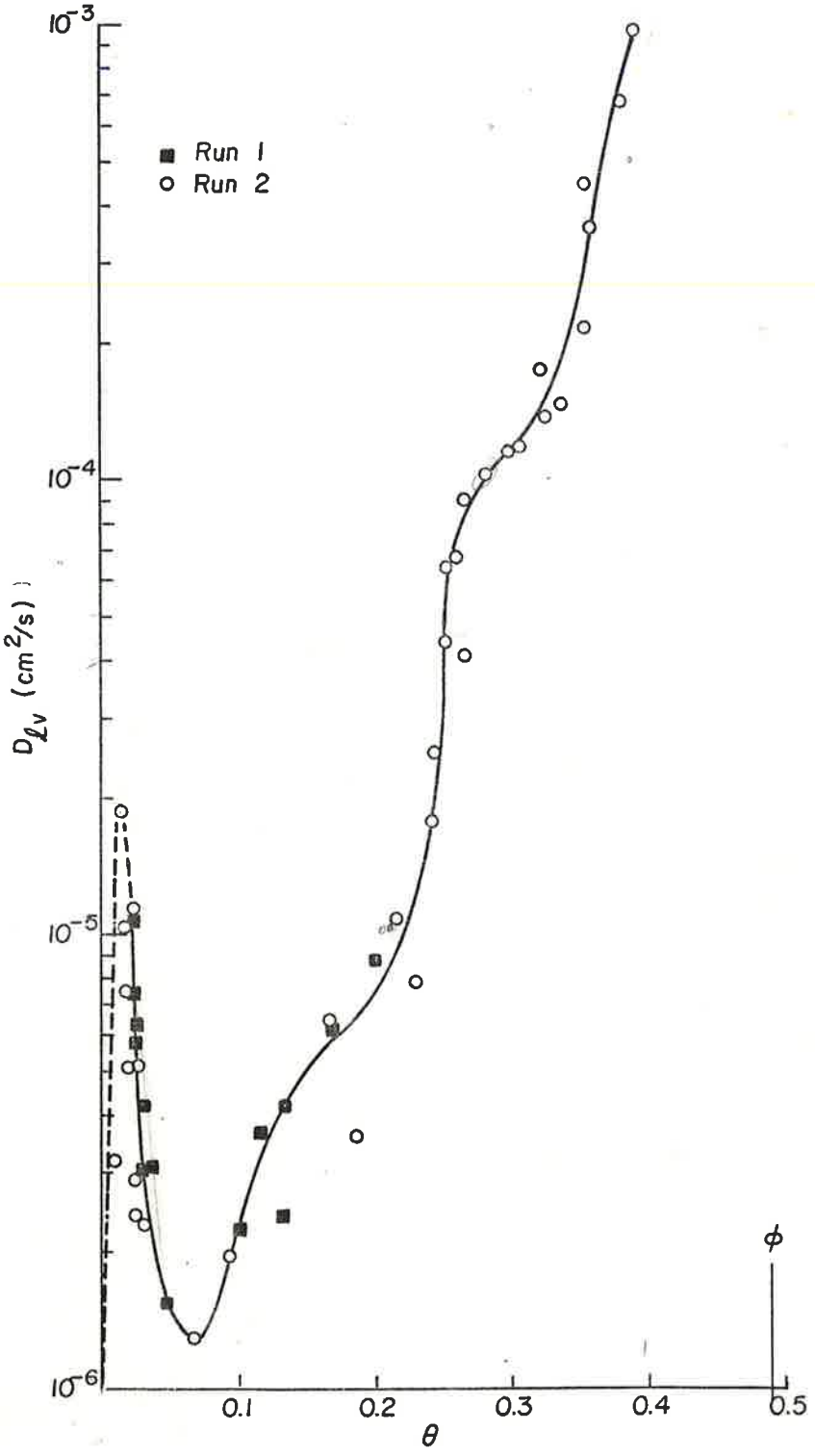

Figure 4-10. Diffusivity for Lurgi retorted shale.

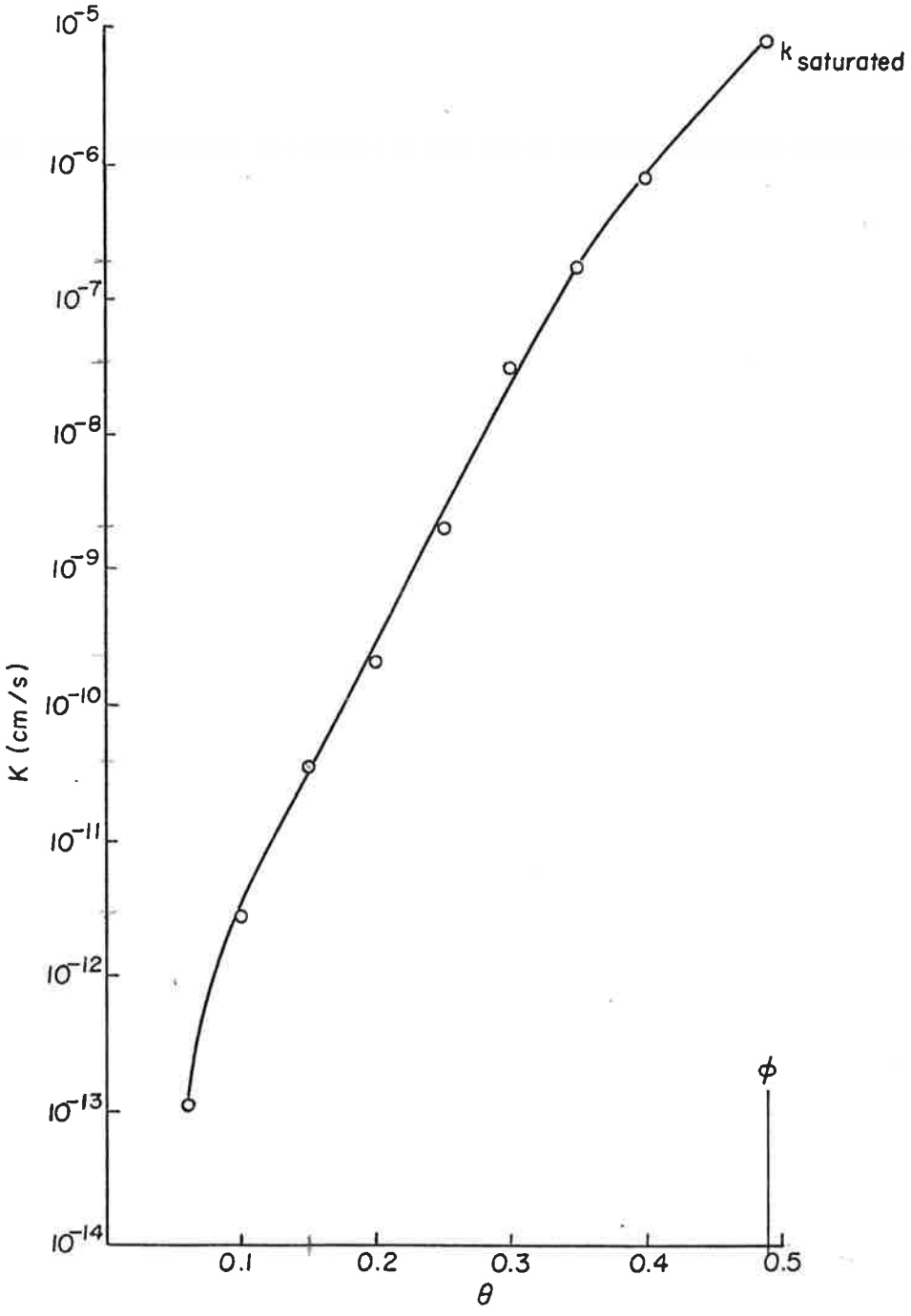

Figure 4-11. Effective hydraulic conductivity (permeability) for Lurgi retorted shale.

Chapter 5

IMPLICATIONS FOR PILE DESIGN

DRAINAGE OF EMPLACED LIQUIDS

This section describes a simple analysis of the role of permeability of Lurgi retorted shale in the control of liquid movement in a disposal pile. There are two issues addressed: 1) the potential for and rate of drainage of liquids emplaced with the solids at the time of disposal, and 2) the rate of penetration of net infiltration.

The investigation has shown, in agreement with others, that some water is chemically bound by hydration when liquid water is added to the Lurgi material. Our data indicate that hydrated water ranges from 3.5 to 3.7 percent by weight. This water is not available to participate in flow of either liquid or vapor and may be considered as part of the solid for purposes of flow computations. Water added in excess of about 3.6 percent by weight is regarded as capillary water. Although the capillary water may exist under the influence of strong adsorptive forces and possibly as a cement gel, it is not chemically bound. It can be removed by oven drying at 105^{o}C.

The sorption and redistribution experiments of the simultaneous movement of NaI, liquid, and vapor have shown that dissolved NaI is not transported by convection with the liquid phase nor by diffusion in the liquid phase at capillary liquid contents below 4.6 percent by weight. We interpret these measurements to mean that liquid water existing in the retorted shale at water contents at or below 4.6 percent by weight is discontinuous. At capillary liquid contents at or below 4.6 percent by weight, water moves principally in the vapor phase according to these measurements. This means that capillary liquid in the weight percent range of 0 to 4.6 is immobile and will not drain in response to gradients of

mechanical potential (i.e. gravity or pressure differences).

The significance of the above is that a total quantity of water equal to 8.2 percent by weight can be added to dry Lurgi retorted shale without incurring the potential for liquid flow. We believe this value to be relatively insensitive to the dry bulk density of the material, but this was not thoroughly investigated. The measurements were made on material compacted to a dry bulk density of 1.4 g/cm^3 (87 lb/ft^3).

In the event that more than 8.2 percent water must be emplaced with the solids, there will exist the potential for drainage. The measurements made permit the estimation of the rate at which such drainage will occur. Unavoidable variations in water content are expected to result from variations in water volumes added, variations in density of the fill, and climatic factors such as precipitation and evaporation during emplacement. The result will be local gradients of pore water pressure. However, if the water content variations are small and the average water content does not vary from the top to bottom gravity will be the dominant driving force influencing the overall movement of liquid in the embankment. Liquid flow is described by the Darcy equation

$$q = -K \nabla (h + z) \qquad (5\text{-}1)$$

wherein q is the volume flux of liquid, K is the effective permeability (hydraulic conductivity), h is the pressure head of the pore water and z is the vertical coordinate of the point in question. In gravity dominated flow, the driving forces due to gradients of pore water pressure are zero and the Darcy equation reduces to

$$q = K (\theta). \qquad (5\text{-}2)$$

The fact that the gradient of pore water pressure is zero does not imply, of course, that the pressure is zero. In fact the pressure may be very highly negative, depending upon the flux, q.

The effective permeability is a very strong function of water content and can range over 8 orders of magnitude while the water content ranges from saturation to practically dry. Figure 4-11 shows K as a function of volumetric water content for the Lurgi retorted shale. The water content in this figure is the capillary water content and is in addition to the chemically bound liquid.

Equation 5-2 is interpreted in two different ways depending upon the boundary conditions relevant to the problem. If the boundary conditions are such that the flux, q is specified (controlled), then the effective permeability will adjust by changing the water content so Eq. 5-2 is satisfied after a transient period. This is, in fact, the expected situation when net infiltration available for penetration of the pile will be controlled by precipitation, infiltration, runoff, and evapotranspiration in the surface and near surface zone. For the drainage situation, on the other hand, the effective permeability corrsponding to the emplacement water content will control the rate of drainage so that Eq. 5-2 is satisfied, at least during the early stages.

The emplacement water content in the commercial pile is unknown. Therefore the estimation of the maximum drainage flux will be made for an arbitrary value of water content. First of all, if the emplaced water content is less than 8.2 percent by weight, no drainage is anticipated. Suppose that the emplaced water content is 12 percent by weight. Chemically bound water will account for 3.6 percent, leaving 8.4 percent for the capillary water. At a dry bulk density of 1.4 g/cm^3 (87 lb/ft^3)

this translates to a volumetric water content of 0.084x1.4 = 0.118. The effective permeability corresponding to θ = 0.118 is read from Figure 4-11 and is found to be about 10^{-11} cm/s. Because of Eq. 5-2, we estimate the initial drainage flux to be 10^{-11} cm/s, also.

The question of how the permeability at saturation affects the drainage flux can be answered as follows. The effective permeability K is expressable as the product of the permeability at saturation, K_s, and the relative permeability, K_r, which remains a function of water content;

$$K = K_s K_r \ . \qquad (5\text{-}3)$$

It is expected that the functional dependence of K_r on water content is quite insensitive to changes in bulk density over the range of practical importance. That is, at a particular value of water content, K_r is expected to have about the same value regardless of the bulk density. The value of K_s is, however, expected to be strongly dependent upon bulk density. Thus, the drainage flux is expected to be directly related to the saturated permeability. Our measurements indicate a value of K_s equal to 10^{-5} cm/s (see Figure 4.11). The relative permeability at θ = 0.118 is $10^{-11}/10^{-5} = 10^{-6}$. If the value of saturated permeability in the field turns out to be 10^{-4} cm/s, then the drainage flux would be

$$q = K_s K_r = (10^{-4})(10^{-6}) = 10^{-10} \text{cm/s} \ .$$

Thus, the maximum drainage flux is expected to be directly proportional to K_s, other factors being equal.

RATE OF PENETRATION OF NET INFILTRATION

As mentioned previously, when the conditions are such that the flux, q, is controlled, the equality indicated in Eq. 5-2 is achieved by an

adjustment in water content until K becomes equal to q. In this case, the flux rate is independent of the saturated permeability. The same flux would occur in a material with $K_s = 10^{-4}$ cm/s as in one for which $K_s = 10^{-5}$ cm/s. The water contents at which Eq. 5-2 is satisfied would be different, however, and would result in a different rate of penetration of the "wetting front". The following is an example of the effect.

Suppose that the net infiltration rate is 2 cm/yr or 6.3×10^{-8} cm/s. According to Figure 4-11, Eq. 5-2 will be satisfied at $\theta \sim 0.32$. Assuming that the emplacement water content is $\theta_i = 0.12$, as before, the rate of penetration of the "wetting front" will be

$$R = q/(\theta - \theta_i) = \frac{2 \text{ cm/yr}}{0.32 - 0.12} = 10 \text{ cm/yr} .$$

We now assume all the same conditions except the saturated permeability is 10^{-4} cm/s. In this case, the relative permeability corresponding to a flux of 6.3×10^{-8} cm/s is

$$K_r = \frac{6.3 \times 10^{-8}}{10^{-4}} = 6.3 \times 10^{-4}$$

while in the first case it was 6.2×10^{-3}. Assuming that the relative permeability function is the same in both cases, a relative permeability of 6.3×10^{-4} corresponds to a water content of $\theta \sim 0.28$. The rate of penetration of the "wetting front" in this case is

$$R = \frac{2 \text{ cm/yr}}{0.28 - 0.12} = 12.5 \text{ cm/yr} .$$

From the above calculations it is observed that the "wetting front" moves more rapidly in the more permeable case, even though the liquid flux is the same in both cases. The difference in water content that will prevail in the two cases is responsible for the different rates of wetting

front penetration. Notice that increasing the saturated permeability by a factor of 10 increased the penetration rate by only 25 percent. Thus, the rate of penetration is quite insensitive to the value of saturated permeability when the flux is controlled.

The above conclusions are valid so long as the flux imposed remains less than the value of saturated permeability. Even if the system is composed of random layers, the rate of penetration is largely controlled by the value of the imposed flux, just as demonstrated above. These conclusions change only if the tightest layer in the sequence has a saturated permeability less than the imposed flux.

WATER CONTENT PROFILE ABOVE A DRY FOUNDATION

Golder Associates (1983) have proposed that excess infiltration in a pile of disposed Lurgi retorted shale might be removed by vapor transport if the pile foundation were kept "dry". A dry foundation would be any material which could be maintained at a relative humidity less than the pile. Golder Associates have proposed that the disposal pile have a foundation several meters thick comprised of highly permeable rock which would outcrop or exhaust at the pile center like a chimney. Dry outside air would enter the foundation at the pile base and then exhaust out the top carrying with it water vapor absorbed from the pile. It is not the purpose of this report to discuss the feasibility or mechanics of such a leachate control system. However, it is possible using the data obtained here to calculate the details of liquid flow and vapor diffusion adjacent to a dry foundation, regardless of how this foundation may be maintained at a low relation humidity.

As the draining water approaches the dry pile bottom the water content will depart from the essentially constant value dictated by gravity flow as

described in the last section. Near the bottom of the pile, the water content will decrease to the water content in equilibrium with the relative humidity in the foundation. The volume flux of water is given by

$$q = -D_{lv}(\theta) \frac{\partial \theta}{\partial z} + K(\theta) \qquad (5\text{-}4)$$

where z is measured positive downward. In the interior of the pile, the water content is practically constant and Eq. 5-4 reduces to Eq. 5-2. The first term on the right contains the combined liquid-vapor diffusivity as defined previously while the second term, K is the hydraulic conductivity at the prevailing water contents and represents the contribution to flow caused by gravity. While gravity is the dominant driving force in the interior of the pile, the gradient of pore water pressure, as manifest by a gradient of water content, becomes the dominant driving force for liquid near the dry foundation. Therefore, we neglect the effects of gravity near the dry foundation and write Eq. 5-4 as

$$q = -D_{lv}(\theta) \frac{\partial \theta}{\partial z} \qquad (5\text{-}5)$$

which is equivalent to Eq. 3-7.

We now assume steady flow so that the total water flux, q, is a constant, independent of both time and space. Even though the total water flux is constant, the relative contributions of liquid and vapor are not constant in space. In the interior of the pile, the flux q is comprised entirely of liquid flow. As the dry foundaion if approached, an increasingly larger fraction of q is contributed by vapor diffusion. Provided that the water content at the bottom of the disposed shale is less than the critieal water content of 0.066, all water will exit the pile as vapor. This condition can be acheived only by maintaining the relative

humidity in the foundation to values less than about 0.8

The thickness of the transition zone near the bottom of the pile in which liquid flow is converted to vapor diffusion can be estimated from Eq. 5-5. For this illustrative calculaion, it is assumed that the relative humidity in the dry foundation is maintained at zero. Equation 5-5 is then integrated to yield

$$Z' = \frac{1}{q} \int_0^{\theta'} D_{lv}(\theta) d\theta \qquad (5\text{-}6)$$

wherein Z' is the distance above the foundation at which the water content is θ'.

Again, for purposes of illustration, we take q = 2 cm/yr. In the interior of the pile where gravity driven liquid flow prevails, the corresponding water content is $\theta = 0.32$ in agreement with previous discussion. An estimate at what point above the foundation the water content will be 0.32 is made by putting $\theta' = 0.32$ in Eq. 5-6 and graphically carrying out the indicated integration using Fig. 4-10 for the $D_{lv}(\theta)$ function. This calculation indicates that the transtion zone will extend 137 cm upward from the base of the disposed shale.

The same calculation using various values of θ' between 0 and 0.32 results in the distribution of water content within the transition zone. The results are shown in Fig. 5-1. Also indicated on Fig. 5-1 are the zones in which the flow is comprised of vapor only, liquid and vapor, and liquid only. It is in the zone of combined liquid and vapor that essentially all evaporation takes place. The present calculation shows this zone to extend over 9 cm. Dissovle solutes will be contentrated in this zone and eventually precipitate. The thickness of this evaporative zone is maximized by maintaining the water content at the bottom of the

disposed shale equal to or less than 0.066. This, in turn, requires that the relative humidity in the foundation be maintained at less than about 0.8.

If the drainage or evaporation do not occur at uniform rates, the transition zone will act to store water for a period of time. The volume of potential storage between any two elevations can be estimated by:

$$S = \int_{\theta'}^{\theta=.32} (.32-\theta')dz$$

where S is the volume of storage and $\theta = .32$ is again the equilibrium water content for q = 2 cm/yr. Graphically evaluating the integral yields a storage at 4.23 cm^3 between 137 and 16 cm, (the liquid transition zone), 1.53 cm^3 between 16 and 6 cm, (the evaporation zone) and 1.79 cm^3 from 6 to 0 cm, (the vapor transport zone). The total storage is 7.55 cm^3 which is almost four times the assumed annual drainage. Thus, there is adequate storage in the transition zone to moderate any variation in the drainage or evaporation rates.

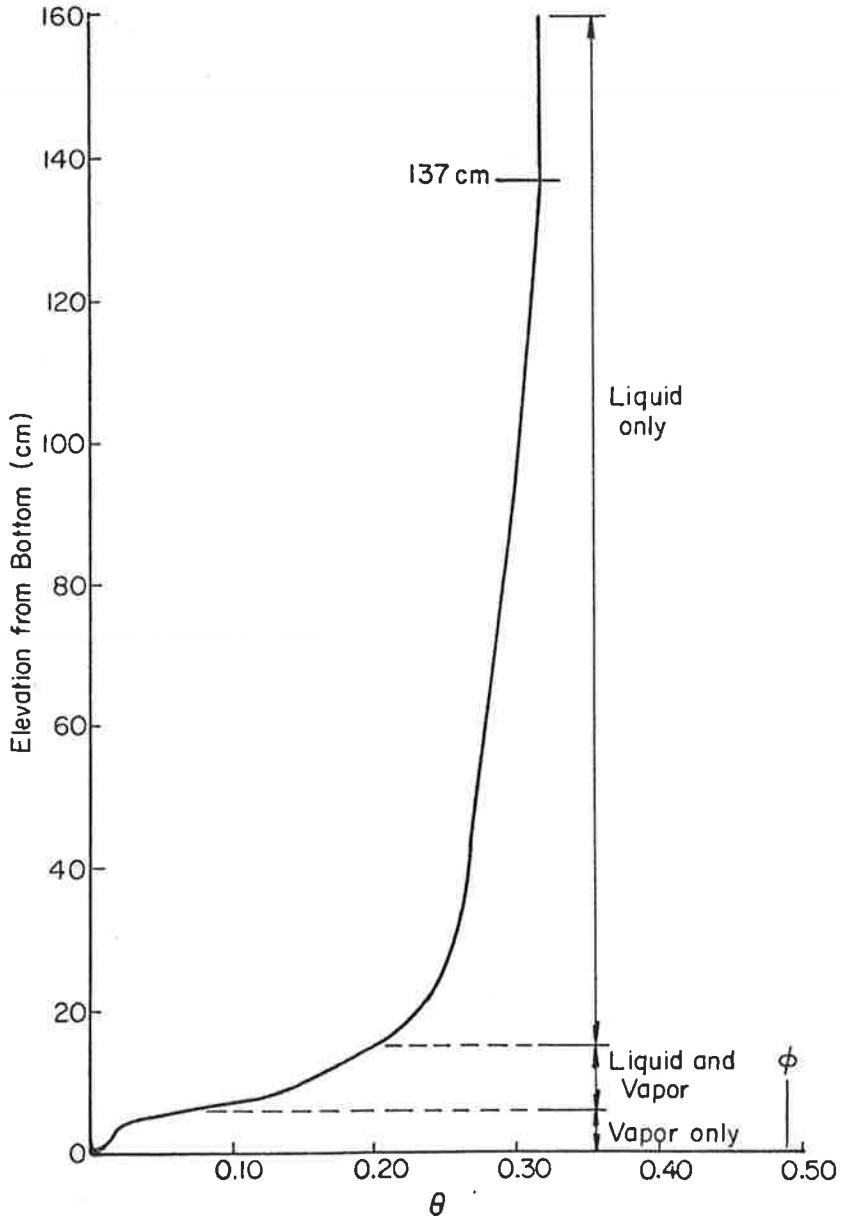

Figure 5-1. Water content profile above dry foundation.

Chapter 6

CONCLUSIONS AND RECOMMENDATIONS

Water is retained in the Lurgi retorted shale used in this study in two primary states: water of hydration associated with cementing reactions and as capillary water. We include as capillary water, all waters not chemically bound. Thus, waters under the influence of adsorptive forces near solid surfaces are regared as capillary waters.

The weight of water used in hydration is estimated to be 3.6 percent of the dry weight of solids. This water is not available to participate in flow of either liquid or vapor and may be considered as part of the solid for purposes of flow computations. Water added in excess of this amount is regared as capillary water.

Sorption and redistribution experiments involving the simultaneous movement of NaI, liquid, and vapor indicate that bulk liquid flow does not occur for capillary water contents less than 4.6 percent by weight. This is interpreted to mean that capillary liquid in the weight percent range of 0 to 4.6 is immobile. The significance of these observations is that a total quantity of water equal to 8.2 percent by weight can be added to dry Lurgi retorted shale without incurring the potential for liquid flow.

In the event that more than 8.2 percent water is emplaced with the solids, there will exist the potential for internal drainage. The combined liquid-vapor diffusivity, water retention, and hydraulic conductivity were measured as functions of water content in order to enable the estimation of potential rates of internal drainage. The measurements were carried out over the range of water contents from saturation down to about 1 percent capillary water on a weight basis. The hydraulic conductivity was 9×10^{-6} cm/s at saturation and ranged downward to 1×10^{-13} cm/s at a water content of 4.6 percent by weight (0.066 volumetric water content).

A calculation illustrating the use of the hydraulic conductivity data for estimating the rate of internal drainage is provided. A water content of 12 percent by weight will result in 3.6 percent by weight of chemically bound water and 8.4 percent capillary water. With a dry bulk density of 1.4 g/cm^3, the capillary water translates to a volumetric water content of 12 percent. The rate of internal drainage corresponding to this water content is estimated to be about $1x10^{-11}$ cm/s or $1x10^{-5}$ ft/yr. The rate of internal drainage is expected to be closely approximated by the hydraulic conductivity corresponding to the capillary water content at which the materials are placed. The more permeable the disposal pile, the greater will be the rate of internal drainage. The above estimated rate is exceedingly small. If collected on an impervious surface external to the pile, 10,000 yrs would be required to develop a depth of 1 foot.

The permeability of the disposed shale will have no effect on the quantity of net infiltration that penetrates the pile. The quantity of net infiltration will be controlled by phenomena in the active zone extending over perhaps the first 2 or 3 meters at the top of the pile. In the interior of the pile, the water content will adjust until the hydraulic conductivity equals the net infiltration rate. While the rate at which net infiltration enters the disposal pile will be independent of the permeability of the retorted shale, the rate of penetration of the net infiltration is weakly dependent upon the permeability. For a net infiltration rate of 2 cm/yr, the rates of penetration are estimated to be about 10 cm/yr and 12.5 cm/yr for saturated hydraulic conductivities of $1x10^{-5}$ cm/s and $1x10^{-4}$ cm/s, respectively. A ten fold increase in saturated permeability results in only a 25 percent increase in the rate of penetration.

The measured liquid-vapor diffusivity was used to illustrate the calculation of the conversion of liquid leachate to vapor near a foundation material with low relative humidity. It was found that 2 cm/yr of liquid leachate can be evaporated into the foundation provided the relative humidity of the foundation is maintained below about 0.8. A energy source adequate to drive the evaporation process would be required, also. This report does not address the mechanisms by which the relative humidity might be maintained nor the possible sources of the energy required.

REFERENCES

Brunauer, S., Emmett, P. H., and Teller, E., 1938. Adsorption of Gases in Multimolecular Layers, J. Am. Chem. Soc. 60:309-319.

Cooper, J. E., and Evans, W. S., 1983. Ammonium-Nitrogen in Green River Formation Oil Shale, Science 219:492-493.

Fox, J. P., 1983. Leaching of Oil Shale Solid Wastes: A Critical Review, prepared for Center for Environmental Sciences, University of Colorado at Denver, supported by U.S. Department of Energy.

Grismer, M. E., 1984. Water and salt movement in relatively dry soils, Ph.D. dissertation, Department of Agricultural and Chemical Engineering, Colorado State University, Fort Collins, Colorado.

Golder Associates, 1983. Movement of Water through a Processed Oil Shale Pile, Report to Amoco/Rio Blanco Oil Shale Co., March.

Jackson, R. D., 1964a. Water Vapor Diffusion in Relatively Dry Soil: I. Theoretical Considerations and Sorption Experiments. Soil Sci. Soc. Am. Proc. 28:172-176.

Jackson, R. D., 1964b. Water Vapor Diffusion in Relatively Dry Soil: II. Desorption Experiments, Soil Sci. Soc. Am. Proc. 28:464-466.

Jackson, R. D., 1964c. Water Vapor Diffusion in Relatively Dry Soil: III. Steady-State Experiments, Soil Sci. Soc. Am. Proc. 28:467-470.

Jackson, R. D., 1965. Water Vapor Diffusion in Relatively Dry Soil: IV. Temperature and Pressure Effects on Sorption Diffusion Coefficients, Soil Sci. Soc. Am. Proc. 29:144-148.

Kemper, W. D., 1960. Water and Ion Movement in Thin Films as Influenced by the Electrostatic Charge and Diffuse Layer of Cations Associated with Clay Mineral Surfaces, Soil Sci. Soc. Am. Proc. 24:10-16

Kemper, W. D., Maasland, E. L. and Porter, L. K., 1964. Mobility of Water Adjacent to Mineral Surfaces, Soil Sci. Soc. Am. Proc. 28:164-167.

Klute, A., 1984, Personal communication, Department of Agronomy, Colorado State University.

Lea, M. M., 1970. The Chemistry of Cement and Concrete, 3rd Ed., Edward Arnold, London, United Kingdom.

Marcus, D., Sangrey, D. A. and Miller, S. A., 1984. Environmental Effects of Cementation Process on Spent Shale Leachates. Presented at the SME-AIME Annual Meeting, Los Angeles, California, February 26-March 1.

Nazareth, V. A., 1984. A Laboratory Column Leach Test for Oil Shale Solid Wastes. Ph.D. dissertation, Department of Agricultural and Chemical Engineering, Colorado State University, Fort Collins, Colorado.

Pilz, J., 1982, The saturated and unsaturated shear strength of spent oil shale, Ph.D. dissertation, Department of Civil Engineering, Colorado State University, Fort Collins, Colorado.

Philip, J. R., 1957, Evaporation and moisture and heat fields in the soil, J. Meteorology 14(4):354-366.

Philip and De Vries, 1957, Moisture Movement in Porous Materials under Temperature Gradients, A.G.U. Trans., 38(2):222-231.

Rio Blanco Oil Shale Project, 1976, Detailed development plan, tract C-a, Vol. 3, Mining, Processing and Support Facilities.

Rio Blanco Oil Shale Project, 1977, Revised detailed development plan, tract C-a, Vol. 2, Mining, Processing and Support Facilities.

Rio Blanco Oil Shale Company, 1981, Tract C-a, modification to the detailed development plan, Lurgi Demonstration Project.

Rose, D. A., 1963a. Water Movement in Porous Materials: I. Isothermal Vapor Transfer. Brit. J. App. Phys. 14:256-262.

Rose, D. A., 1963b. Water Movement in Porous Materials: II. The Separation of the Components of Water Movement, Brit. J. App. Phys. 14:491-496.

Rose, D. A., 1968a. Water Movement in Porous Materials: III. Evaporation of Water from Soil. Brit. J. App. Phys., 2(1):1779-1791.

Rose, D. A., 1968b. Water Movement in Dry Soils: I. Physical Factors Affecting Sorption of Water by Soil. J. of Soil Sci. 19(1):81-93.

APPENDIX

Detail Test Results and Calculations

DISPERSION COLUMN TEST ON LURGI SPENT SHALE

Run 1 Scan 1
time 35.0 hr
solution influx 2.21 gm

LENGTH cm	Am	Cs	Theta %	t Sol. gm	Slope cm-1	NaI gm/cm3	t NaI gm
0.00	8490.5	28718					
0.50	1737.6	10719	0.157	0.98	-0.0573	0.148	0.132
1.00	2317.4	10978	0.100	1.79	-0.1359	0.141	0.238
1.50	3471.3	11308	0.022	2.16	-0.0894	0.000	0.278
2.00	3424.4	11274	0.011	2.25	-0.0151	0.000	0.278
2.50	3474.5	11379	0.006	2.30	-0.0103	0.000	0.278
3.00	3438.9	11375	0.000	2.32	-0.0064	0.000	0.278
3.50	3473.8	11391	0.000	2.32	-0.0005	0.000	0.278

DISPERSION COLUMN TEST ON LURGI SPENT SHALE

Run 1 Scan 2
time 47.0 hr
solution influx 0.70 gm

LENGTH cm	Am	Cs	Theta %	t Sol. gm	Slope cm-1	NaI gm/cm3	t NaI gm
0.00	8489.8	28272					
0.50	1564.1	10459	0.184	1.15	-0.0478	0.146	0.152
1.00	2000.2	10677	0.136	2.15	-0.1464	0.141	0.283
1.50	3430.6	11048	0.038	2.68	-0.1167	0.000	0.337
2.00	3402.1	11033	0.020	2.84	-0.0172	0.000	0.337
2.50	3438.9	11157	0.021	2.96	-0.0134	0.000	0.337
3.00	3423.9	11150	0.006	3.03	-0.0202	0.000	0.337
3.50	3472.6	11156	0.000	3.05	-0.0064	0.000	0.337
4.00	3456.8	11179	0.000	3.05	-0.0005	0.000	0.337

DISPERSION COLUMN TEST ON LURGI SPENT SHALE

Run 1 Scan 3
time 119.0 hr
solution influx 0.64 gm

LENGTH cm	Am	Cs	Theta %	t Sol. gm	Slope cm-1	NaI gm/cm3	t NaI gm
0.00	8447.5	28410					
0.50	1648.6	10634	0.147	0.94	-0.0205	0.175	0.145
1.00	1776.9	10753	0.127	1.81	-0.0545	0.193	0.286
1.50	2781.2	10959	0.093	2.49	-0.0868	0.075	0.374
2.00	3336.7	11065	0.040	2.88	-0.0662	0.000	0.394
2.50	3407.5	11157	0.026	3.07	-0.0302	0.000	0.394
3.00	3399.2	11150	0.010	3.17	-0.0072	0.000	0.394
3.50	3409.0	11155	0.019	3.25	0.0081	0.000	0.394
4.00	3389.5	11185	0.018	3.35	-0.0124	0.000	0.394
4.50	3499.6	0	0.007	3.42	-0.0088	0.000	0.394
5.00	3438.3	0	0.009	3.47	-0.0068	0.000	0.394

DISPERSION COLUMN TEST ON LURGI SPENT SHALE

Run 1 Scan 4
time 130.0 hr
solution influx 0.54 gm

LENGTH cm	Am	Cs	Theta %	t Sol. gm	Slope cm-1	NaI gm/cm3	t NaI gm
0.00	8439.0	28389					
0.50	1377.3	10459	0.195	1.23	-0.0485	0.163	0.179
1.00	1565.6	10671	0.146	2.32	-0.1118	0.199	0.351
1.50	2838.2	10985	0.083	3.04	-0.1116	0.077	0.451
2.00	3345.9	11039	0.035	3.38	-0.0596	0.000	0.469
2.50	3411.9	11124	0.023	3.54	-0.0172	0.000	0.469
3.00	3376.5	11125	0.017	3.66	-0.0029	0.000	0.469
3.50	3402.8	11172	0.020	3.76	-0.0055	0.000	0.469
4.00	3400.0	11180	0.012	3.85	-0.0094	0.000	0.469
4.50	3485.7	0	0.011	3.92	-0.0065	0.000	0.469
5.00	3443.1	0	0.005	3.96	-0.0075	0.000	0.469
5.50	3506.9	0	0.003	3.99	-0.0054	0.000	0.469

DISPERSION COLUMN TEST ON LURGI SPENT SHALE

Run 1 Scan 5
time 147.0 hr
solution influx 0.97 gm

LENGTH cm	Am	Cs	Theta %	t Sol. gm	Slope cm-1	NaI gm/cm3	t NaI gm
0.00	8431.6	28372					
0.50	1270.5	10374	0.218	1.37	-0.0245	0.158	0.194
1.00	1437.7	10506	0.193	2.66	-0.0941	0.162	0.379
1.50	2283.9	10826	0.124	3.65	-0.1523	0.116	0.508
2.00	3327.6	11038	0.041	4.14	-0.0954	0.000	0.548
2.50	3396.9	11130	0.028	4.34	-0.0200	0.000	0.548
3.00	3365.0	11127	0.021	4.48	-0.0088	0.000	0.548
3.50	3402.2	0	0.019	4.59	-0.0050	0.000	0.548
4.00	3387.2	0	0.016	4.69	-0.0058	0.000	0.548
4.50	3476.1	0	0.014	4.77	-0.0084	0.000	0.548
5.00	3434.8	0	0.008	4.83	-0.0012	0.000	0.548
5.50	3481.3	0	0.012	4.89	-0.0067	0.000	0.548
6.00	3438.4	0	0.001	4.93	-0.0124	0.000	0.548

DISPERSION COLUMN TEST ON LURGI SPENT SHALE

Run 1 Scan 6
time 155.0 hr
solution influx 0.44 gm

LENGTH cm	Am	Cs	Theta %	t Sol. gm	Slope cm-1	NaI gm/cm3	t NaI gm
0.00	8459.6	28351					
0.50	1241.4	10333	0.227	1.43	-0.0271	0.155	0.199
1.00	1383.4	10472	0.200	2.78	-0.0843	0.164	0.391
1.50	2009.7	10743	0.143	3.85	-0.1511	0.134	0.537
2.00	3318.6	11018	0.049	4.43	-0.1123	0.000	0.592
2.50	3401.5	11122	0.031	4.66	-0.0262	0.000	0.592
3.00	3370.9	11132	0.023	4.81	-0.0092	0.000	0.592
3.50	3407.7	0	0.022	4.94	-0.0046	0.000	0.592
4.00	3392.3	0	0.018	5.05	-0.0072	0.000	0.592
4.50	3485.3	0	0.014	5.14	-0.0111	0.000	0.592
5.00	3446.7	0	0.007	5.20	-0.0046	0.000	0.592
5.50	3499.1	0	0.010	5.25	-0.0074	0.000	0.592
6.00	3452.2	0	0.000	5.28	-0.0099	0.000	0.592

DISPERSION COLUMN TEST ON LURGI SPENT SHALE

Run 1 Scan 7
time 167.0 hr
solution influx 0.55 gm

LENGTH cm	Am	Cs	Theta %	t Sol. gm	Slope cm-1	NaI gm/cm3	t NaI gm
0.00	8452.6	28375					
0.50	1206.9	10297	0.241	1.51	-0.0231	0.149	0.203
1.00	1334.6	10422	0.218	2.95	-0.0786	0.155	0.400
1.50	1816.6	10681	0.163	4.14	-0.1604	0.141	0.559
2.00	3296.1	10993	0.058	4.80	-0.1267	0.000	0.624
2.50	3386.5	11094	0.036	5.07	-0.0357	0.000	0.624
3.00	3371.0	11117	0.022	5.23	-0.0157	0.000	0.624
3.50	3408.6	0	0.020	5.35	-0.0062	0.000	0.624
4.00	3396.2	0	0.016	5.45	-0.0053	0.000	0.624
4.50	3481.5	0	0.015	5.54	-0.0067	0.000	0.624
5.00	3439.7	0	0.009	5.60	-0.0067	0.000	0.624
5.50	3500.7	0	0.008	5.65	-0.0075	0.000	0.624
6.00	3445.4	0	0.002	5.68	-0.0081	0.000	0.624

DISPERSION COLUMN TEST ON LURGI SPENT SHALE

Run 1 Scan 8
time 191.0 hr
solution influx 0.00 gm

LENGTH cm	Am	Cs	Theta %	t Sol. gm	Slope cm-1	NaI gm/cm3	t NaI gm
0.00	8443.7	28419					
0.50	1303.6	10422	0.208	1.31	-0.0184	0.162	0.190
1.00	1396.4	10532	0.190	2.57	-0.0489	0.172	0.377
1.50	1807.5	10707	0.159	3.67	-0.1014	0.145	0.534
2.00	3220.1	10966	0.088	4.42	-0.1219	0.000	0.599
2.50	3378.7	11113	0.038	4.78	-0.0541	0.000	0.599
3.00	3337.2	11138	0.034	4.98	-0.0100	0.000	0.599
3.50	3386.8	0	0.028	5.15	-0.0151	0.000	0.599
4.00	3383.9	0	0.019	5.29	-0.0070	0.000	0.599
4.50	3463.3	0	0.021	5.40	-0.0056	0.000	0.599
5.00	3424.5	0	0.014	5.49	-0.0037	0.000	0.599
5.50	3474.7	0	0.017	5.58	-0.0043	0.000	0.599
6.00	3422.2	0	0.009	5.66	-0.0069	0.000	0.599
6.50	3401.3	0	0.010	5.71	-0.0095	0.000	0.599

DISPERSION COLUMN TEST ON LURGI SPENT SHALE

Run 1 Scan 9
time 216.0 hr
solution influx 0.00 gm

LENGTH cm	Am	Cs	Theta %	t Sol. gm	Slope cm-1	NaI gm/cm3	t NaI gm
0.00	8411.5	28381					
0.50	1336.4	10453	0.195	1.24	-0.0157	0.169	0.186
1.00	1403.3	10553	0.179	2.43	-0.0272	0.182	0.370
1.50	1811.0	10666	0.168	3.52	-0.0927	0.135	0.526
2.00	3105.4	10921	0.087	4.28	-0.1271	0.016	0.594
2.50	3358.6	11089	0.041	4.65	-0.0526	0.000	0.598
3.00	3325.6	11090	0.034	4.86	-0.0140	0.000	0.598
3.50	3376.4	11142	0.027	5.03	-0.0102	0.000	0.598
4.00	3360.2	0	0.024	5.17	-0.0021	0.000	0.598
4.50	3440.6	0	0.025	5.30	-0.0088	0.000	0.598
5.00	3408.4	0	0.015	5.41	-0.0076	0.000	0.598
5.50	3461.6	0	0.017	5.50	-0.0045	0.000	0.598
6.00	3406.7	0	0.010	5.58	-0.0080	0.000	0.598
6.50	3391.2	0	0.009	5.64	-0.0105	0.000	0.598

DISPERSION COLUMN TEST ON LURGI SPENT SHALE

Run 1 Scan 10
time 244.0 hr
solution influx 0.00 gm

LENGTH cm	Am	Cs	Theta %	t Sol. gm	Slope cm-1	NaI gm/cm3	t NaI gm
0.00	8437.8	28358					
0.50	1360.3	10449	0.194	1.23	-0.0221	0.166	0.182
1.00	1429.6	10569	0.172	2.40	-0.0461	0.187	0.364
1.50	1800.2	10721	0.148	3.41	-0.0909	0.159	0.521
2.00	3030.1	10929	0.081	4.11	-0.1025	0.034	0.595
2.50	3357.0	11041	0.046	4.48	-0.0402	0.000	0.603
3.00	3319.1	11040	0.041	4.72	-0.0133	0.000	0.603
3.50	3373.0	11106	0.032	4.93	-0.0188	0.000	0.603
4.00	3374.6	11108	0.022	5.08	-0.0077	0.000	0.603
4.50	3450.9	0	0.025	5.21	0.0002	0.000	0.603
5.00	3400.9	0	0.022	5.34	-0.0034	0.000	0.603
5.50	3461.7	0	0.021	5.47	-0.0083	0.000	0.603
6.00	3408.4	0	0.014	5.57	-0.0098	0.000	0.603
6.50	3395.5	0	0.011	5.64	-0.0038	0.000	0.603
7.00	3434.3	0	0.010	5.70	-0.0115	0.000	0.603

DISPERSION COLUMN TEST ON LURGI SPENT SHALE

Run 1 Scan 11
time 287.0 hr
solution influx 0.00 gm

LENGTH cm	Am	Cs	Theta %	t Sol. gm	Slope cm-1	NaI gm/cm3	t NaI gm
0.00	8426.1	28374					
0.50	1387.7	10548	0.166	1.07	-0.0130	0.195	0.182
1.00	1440.8	10639	0.153	2.10	-0.0289	0.212	0.364
1.50	1825.3	10766	0.137	3.03	-0.0730	0.171	0.521
2.00	2946.3	10938	0.079	3.69	-0.0815	0.050	0.598
2.50	3329.3	11090	0.055	4.08	-0.0375	0.000	0.609
3.00	3312.2	11077	0.042	4.36	-0.0228	0.000	0.609
3.50	3368.3	11104	0.032	4.56	-0.0138	0.000	0.609
4.00	3355.4	11125	0.028	4.73	-0.0025	0.000	0.609
4.50	3433.3	0	0.030	4.90	-0.0075	0.000	0.609
5.00	3400.4	0	0.021	5.04	-0.0052	0.000	0.609
5.50	3448.4	0	0.025	5.17	-0.0020	0.000	0.609
6.00	3392.6	0	0.019	5.29	-0.0099	0.000	0.609
6.50	3382.7	0	0.015	5.38	-0.0037	0.000	0.609
7.00	3418.3	0	0.015	5.47	-0.0148	0.000	0.609

DISPERSION COLUMN TEST ON LURGI SPENT SHALE

Run 1 Scan 12
time 337.0 hr
solution influx 0.00 gm

LENGTH cm	Am	Cs	Theta %	t Sol. gm	Slope cm-1	NaI gm/cm3	t NaI gm
0.00	8427.5	28364					
0.50	1410.9	10567	0.159	1.03	-0.0048	0.200	0.179
1.00	1459.0	10631	0.154	2.04	-0.0272	0.206	0.359
1.50	1820.3	10778	0.132	2.96	-0.0755	0.179	0.515
2.00	2889.0	10936	0.079	3.61	-0.0684	0.061	0.595
2.50	3310.5	11050	0.063	4.02	-0.0354	0.000	0.608
3.00	3310.0	11066	0.043	4.32	-0.0341	0.000	0.608
3.50	3376.6	11078	0.029	4.53	-0.0127	0.000	0.608
4.00	3350.5	11104	0.030	4.69	0.0023	0.000	0.608
4.50	3429.9	0	0.031	4.87	-0.0053	0.000	0.608
5.00	3390.0	0	0.025	5.03	0.0088	0.000	0.608
5.50	3410.4	0	0.040	5.21	-0.0076	0.000	0.608
6.00	3395.8	0	0.018	5.37	-0.0192	0.000	0.608
6.50	3368.0	0	0.021	5.48	0.0001	0.000	0.608
7.00	3412.1	0	0.018	5.59	-0.0061	0.000	0.608
7.50	3430.3	0	0.015	5.68	-0.0177	0.000	0.608

DISPERSION COLUMN TEST ON LURGI SPENT SHALE

Run 1 Scan 13
time 384.0 hr
solution influx 0.00 gm

LENGTH cm	Am	Cs	Theta %	t Sol. gm	Slope cm-1	NaI gm/cm3	t NaI gm
0.00	8450.8	28381					
0.50	1417.7	10584	0.156	1.01	-0.0064	0.204	0.179
1.00	1469.0	10653	0.149	2.00	-0.0209	0.213	0.359
1.50	1854.6	10776	0.135	2.92	-0.0673	0.169	0.512
2.00	2907.9	10932	0.082	3.58	-0.0749	0.055	0.590
2.50	3327.7	11052	0.060	3.99	-0.0356	0.000	0.602
3.00	3311.6	11025	0.046	4.29	-0.0255	0.000	0.602
3.50	3373.4	0	0.034	4.52	-0.0162	0.000	0.602
4.00	3360.4	0	0.030	4.70	-0.0011	0.000	0.602
4.50	3435.0	0	0.033	4.88	0.0004	0.000	0.602
5.00	3386.2	0	0.031	5.05	-0.0058	0.000	0.602
5.50	3451.7	0	0.027	5.22	-0.0072	0.000	0.602
6.00	3391.2	0	0.023	5.36	-0.0050	0.000	0.602
6.50	3374.1	0	0.022	5.49	0.0040	0.000	0.602
7.00	3397.8	0	0.027	5.63	-0.0054	0.000	0.602
7.50	3434.7	0	0.017	5.75	-0.0175	0.000	0.602
8.00	3432.5	0	0.010	5.83	-0.0043	0.000	0.602
9.00	3474.5	0	0.011	5.94	-0.0033	0.000	0.602
10.00	3609.0	0	0.003	6.02	0.0012	0.000	0.602

DISPERSION COLUMN TEST ON LURGI SPENT SHALE

Run 1 Scan 14
time 503.0 hr
solution influx 0.00 gm

LENGTH cm	Am	Cs	Theta %	t Sol. gm	Slope cm-1	NaI gm/cm3	t NaI gm
0.00	8452.8	28390					
0.50	1453.9	10657	0.135	0.89	-0.0095	0.233	0.177
1.00	1486.7	10736	0.125	1.76	-0.0136	0.255	0.356
1.50	1902.1	10826	0.121	2.56	-0.0541	0.183	0.508
2.00	2828.1	10968	0.071	3.17	-0.0720	0.085	0.588
2.50	3354.1	11030	0.049	3.52	-0.0341	0.000	0.605
3.00	3334.1	11031	0.037	3.76	-0.0165	0.000	0.605
3.50	3378.1	11084	0.033	3.96	-0.0055	0.000	0.605
4.00	3357.3	11097	0.032	4.14	-0.0016	0.000	0.605
4.50	3441.0	0	0.031	4.32	-0.0058	0.000	0.605
5.00	3398.2	0	0.026	4.48	-0.0033	0.000	0.605
5.50	3451.4	0	0.028	4.63	-0.0039	0.000	0.605
6.00	3395.0	0	0.022	4.77	-0.0038	0.000	0.605
6.50	3370.8	0	0.024	4.90	-0.0002	0.000	0.605
7.00	3412.0	0	0.022	5.03	-0.0011	0.000	0.605
7.50	3420.8	0	0.023	5.15	-0.0133	0.000	0.605
8.00	3436.4	0	0.009	5.24	-0.0039	0.000	0.605
9.00	3458.9	0	0.017	5.39	-0.0035	0.000	0.605
10.00	3613.6	0	0.002	5.49	0.0019	0.000	0.605

DISPERSION COLUMN TEST ON LURGI SPENT SHALE

Run 1 Scan 15
time 624.0 hr
solution influx 0.00 gm

LENGTH cm	Am	Cs	Theta %	t Sol. gm	Slope cm-1	NaI gm/cm3	t NaI gm
0.00	8471.7	28479					
0.50	1476.6	10750	0.117	0.79	-0.0032	0.268	0.177
1.00	1518.5	10808	0.114	1.57	-0.0089	0.276	0.354
1.50	1926.7	10904	0.108	2.31	-0.0419	0.204	0.505
2.00	2848.7	11000	0.072	2.88	-0.0517	0.081	0.584
2.50	3343.8	11094	0.057	3.25	-0.0205	0.000	0.601
3.00	3306.8	11086	0.052	3.56	-0.0196	0.000	0.601
3.50	3375.1	11120	0.037	3.81	-0.0194	0.000	0.601
4.00	3363.5	11136	0.032	4.00	-0.0075	0.000	0.601
4.50	3452.7	0	0.030	4.18	-0.0040	0.000	0.601
5.00	3400.1	0	0.028	4.34	-0.0007	0.000	0.601
5.50	3456.6	0	0.029	4.50	-0.0021	0.000	0.601
6.00	3392.5	0	0.026	4.66	-0.0053	0.000	0.601
6.50	3379.7	0	0.023	4.79	0.0024	0.000	0.601
7.00	3403.3	0	0.029	4.94	-0.0050	0.000	0.601
7.50	3439.5	0	0.018	5.07	-0.0151	0.000	0.601
8.00	3432.1	0	0.013	5.16	-0.0005	0.000	0.601
9.00	3464.9	0	0.018	5.34	-0.0031	0.000	0.601
10.00	3607.4	0	0.007	5.48	0.0020	0.000	0.601

DISPERSION COLUMN TEST ON LURGI SPENT SHALE

Run 1 Scan 16
time 720.0 hr
solution influx 0.00 gm

LENGTH cm	Am	Cs	Theta %	t Sol. gm	Slope cm-1	NaI gm/cm3	t NaI gm
0.00	8476.7	28427					
0.50	1486.2	10772	0.105	0.72	-0.0039	0.301	0.178
1.00	1529.9	10834	0.101	1.43	-0.0023	0.314	0.356
1.50	1989.6	10906	0.102	2.11	-0.0322	0.205	0.504
2.00	2843.2	10992	0.068	2.65	-0.0521	0.088	0.580
2.50	3361.2	11142	0.050	3.00	-0.0264	0.000	0.597
3.00	3332.0	11079	0.042	3.26	-0.0188	0.000	0.597
3.50	3390.8	11140	0.031	3.46	-0.0100	0.000	0.597
4.00	3366.2	11147	0.032	3.64	0.0033	0.000	0.597
4.50	3441.7	0	0.035	3.83	-0.0030	0.000	0.597
5.00	3400.3	0	0.029	4.01	-0.0037	0.000	0.597
5.50	3453.2	0	0.031	4.18	-0.0023	0.000	0.597
6.00	3393.1	0	0.027	4.34	-0.0055	0.000	0.597
6.50	3376.7	0	0.026	4.49	-0.0003	0.000	0.597
7.00	3410.3	0	0.026	4.63	-0.0074	0.000	0.597
7.50	3442.4	0	0.018	4.76	-0.0094	0.000	0.597
8.00	3425.1	0	0.017	4.86	0.0042	0.000	0.597
9.00	3450.3	0	0.024	5.09	-0.0038	0.000	0.597
10.00	3603.4	0	0.009	5.28	0.0027	0.000	0.597

DISPERSION COLUMN TEST ON LURGI SPENT SHALE

Run 1 Scan 17
time 864.0 hr
solution influx 0.00 gm

LENGTH cm	Am	Cs	Theta %	t Sol. gm	Slope cm-1	NaI gm/cm3	t NaI gm
0.00	8464.5	28406					
0.50	1482.9	10808	0.091	0.65	-0.0017	0.350	0.180
1.00	1539.6	10863	0.090	1.29	-0.0003	0.353	0.359
1.50	1972.6	10935	0.091	1.91	-0.0218	0.238	0.510
2.00	2870.7	10987	0.068	2.42	-0.0378	0.082	0.586
2.50	3349.3	11060	0.053	2.77	-0.0212	0.000	0.602
3.00	3316.1	11120	0.047	3.05	-0.0216	0.000	0.602
3.50	3385.6	0	0.032	3.27	-0.0144	0.000	0.602
4.00	3360.6	0	0.032	3.45	-0.0012	0.000	0.602
4.50	3447.7	0	0.030	3.62	-0.0094	0.000	0.602
5.00	3410.4	0	0.023	3.77	0.0077	0.000	0.602
5.50	3430.8	0	0.038	3.94	0.0062	0.000	0.602
6.00	3382.5	0	0.029	4.13	-0.0118	0.000	0.602
6.50	3370.2	0	0.026	4.29	-0.0017	0.000	0.602
7.00	3403.2	0	0.027	4.44	-0.0075	0.000	0.602
7.50	3436.0	0	0.019	4.57	-0.0104	0.000	0.602
8.00	3420.4	0	0.017	4.67	0.0065	0.000	0.602
9.00	3435.3	0	0.028	4.93	-0.0014	0.000	0.602
10.00	3586.3	0	0.014	5.17	0.0032	0.000	0.602

DISPERSION COLUMN TEST ON LURGI SPENT SHALE

Run 1 Scan 18
time 1008.0 hr
solution influx 0.00 gm

LENGTH cm	Am	Cs	Theta %	t Sol. gm	Slope cm-1	NaI gm/cm3	t NaI gm
0.00	8455.2	28352					
0.50	1491.9	10820	0.082	0.59	0.0074	0.391	0.180
1.00	1543.5	10844	0.089	1.21	0.0049	0.353	0.359
1.50	2009.1	10931	0.087	1.81	-0.0289	0.242	0.507
2.00	2805.1	10990	0.060	2.28	-0.0364	0.112	0.585
2.50	3352.7	11087	0.050	2.61	-0.0152	0.000	0.604
3.00	3316.5	11096	0.045	2.88	-0.0210	0.000	0.604
3.50	3387.6	0	0.029	3.08	-0.0142	0.000	0.604
4.00	3360.8	0	0.031	3.25	0.0045	0.000	0.604
4.50	3435.6	0	0.034	3.43	-0.0012	0.000	0.604
5.00	3390.5	0	0.029	3.61	0.0002	0.000	0.604
5.50	3437.3	0	0.034	3.79	0.0003	0.000	0.604
6.00	3377.0	0	0.030	3.97	-0.0072	0.000	0.604
6.50	3365.4	0	0.027	4.13	-0.0051	0.000	0.604
7.00	3406.0	0	0.025	4.27	-0.0027	0.000	0.604
7.50	3419.0	0	0.024	4.41	-0.0048	0.000	0.604
8.00	3409.4	0	0.020	4.53	0.0017	0.000	0.604
9.00	3436.2	0	0.027	4.80	-0.0021	0.000	0.604
10.00	3578.3	0	0.016	5.03	0.0030	0.000	0.604

DISPERSION COLUMN TEST ON LURGI SPENT SHALE

Run 1 Scan 19
time 1331.0 hr
solution influx 0.00 gm

LENGTH cm	Am	Cs	Theta %	t Sol. gm	Slope cm-1	NaI gm/cm3	t NaI gm
0.00	8449.4	28324					
0.50	1491.4	10797	0.085	0.61	-0.0046	0.373	0.179
1.00	1566.4	10863	0.081	1.21	-0.0049	0.386	0.357
1.50	2051.4	10943	0.080	1.77	-0.0200	0.252	0.502
2.00	2878.6	10980	0.061	2.22	-0.0305	0.093	0.574
2.50	3351.1	11062	0.050	2.55	-0.0138	0.000	0.590
3.00	3309.8	11027	0.047	2.82	-0.0267	0.000	0.590
3.50	3400.0	11074	0.023	3.02	-0.0214	0.000	0.590
4.00	3371.4	11090	0.025	3.15	0.0059	0.000	0.590
4.50	3444.6	0	0.029	3.31	-0.0020	0.000	0.590
5.00	3403.3	0	0.023	3.45	0.0046	0.000	0.590
5.50	3435.3	0	0.034	3.61	0.0027	0.000	0.590
6.00	3383.8	0	0.026	3.78	-0.0064	0.000	0.590
6.50	3361.4	0	0.027	3.93	-0.0006	0.000	0.590
7.00	3401.7	0	0.025	4.08	-0.0070	0.000	0.590
7.50	3425.7	0	0.020	4.21	-0.0093	0.000	0.590
8.00	3416.1	0	0.016	4.31	0.0032	0.000	0.590
9.00	3437.5	0	0.025	4.55	-0.0009	0.000	0.590
10.00	3579.4	0	0.014	4.77	0.0028	0.000	0.590

DISPERSION COLUMN TEST ON LURGI SPENT SHALE

Run 1 Scan 20
time 1800.0 hr
solution influx 0.00 gm

LENGTH cm	Am	Cs	Theta %	t Sol. gm	Slope cm-1	NaI gm/cm3	t NaI gm
0.00	8441.9	28383					
0.50	1501.3	10870	0.070	0.53	0.0147	0.455	0.180
1.00	1570.5	10871	0.085	1.10	0.0126	0.363	0.357
1.50	2063.8	10957	0.083	1.68	-0.0177	0.239	0.500
2.00	2872.7	10980	0.067	2.15	-0.0343	0.081	0.571
2.50	3351.2	11055	0.049	2.49	-0.0217	0.000	0.587
3.00	3309.9	11065	0.046	2.76	-0.0244	0.000	0.587
3.50	3394.4	11091	0.024	2.95	-0.0204	0.000	0.587
4.00	3369.1	11101	0.025	3.09	0.0017	0.000	0.587
4.50	3449.3	0	0.026	3.23	0.0006	0.000	0.587
5.00	3394.4	0	0.026	3.38	0.0074	0.000	0.587
5.50	3433.2	0	0.033	3.55	0.0034	0.000	0.587
6.00	3373.3	0	0.029	3.72	-0.0022	0.000	0.587
6.50	3349.3	0	0.031	3.89	-0.0041	0.000	0.587
7.00	3399.9	0	0.025	4.05	-0.0131	0.000	0.587
7.50	3428.4	0	0.018	4.17	-0.0062	0.000	0.587
8.00	3406.6	0	0.019	4.27	0.0073	0.000	0.587
9.00	3424.7	0	0.029	4.54	-0.0039	0.000	0.587
10.00	3584.9	0	0.011	4.77	0.0032	0.000	0.587

DISPERSION COLUMN TEST ON LURGI SPENT SHALE

Run 1 Scan 21
time 2500.0 hr
solution influx 0.00 am

LENGTH cm	Am	Cs	Theta %	t Sol. am	Slope cm-1	NaI am/cm3	t NaI am
0.00	8180.1	28338					
0.50	1466.1	10845	0.073	0.54	0.0039	0.433	0.178
1.00	1530.6	10882	0.077	1.10	0.0090	0.401	0.354
1.50	1951.5	10942	0.082	1.65	-0.0248	0.255	0.500
2.00	2746.0	11013	0.052	2.09	-0.0453	0.125	0.577
2.50	3275.7	11104	0.037	2.35	-0.0258	0.000	0.595
3.00	3252.1	11078	0.026	2.53	-0.0162	0.000	0.595
3.50	3298.5	11120	0.020	2.66	-0.0052	0.000	0.595
4.00	3274.0	11101	0.021	2.77	0.0059	0.000	0.595
4.50	3341.7	0	0.026	2.91	-0.0029	0.000	0.595
5.00	3306.9	0	0.018	3.03	0.0002	0.000	0.595
5.50	3343.4	0	0.026	3.16	-0.0017	0.000	0.595
6.00	3298.5	0	0.017	3.28	-0.0030	0.000	0.595
6.50	3263.6	0	0.023	3.39	0.0070	0.000	0.595
7.00	3297.9	0	0.024	3.52	-0.0059	0.000	0.595
7.50	3323.5	0	0.017	3.64	-0.0172	0.000	0.595
8.00	3330.9	0	0.006	3.70	0.0030	0.000	0.595
9.00	3335.6	0	0.022	3.86	0.0046	0.000	0.595
10.00	3462.2	0	0.016	4.07	0.0024	0.000	0.595

DIFFUSIVITY CALCULATIONS ON LURGI SPENT SHALE

Run 1 Scans 1 and 2
Mass Correction Factor 0.95

Pt #	Slope 1 cm-1	Theta 1	Slope 2 cm-1	Theta 2	2 I 10-6	2 eI 10-6	Theata Mean	D cm2/s	
2	-0.1359	0.100	-0.1464	0.136	-0.9937	0.1323	0.118	3.66	*
3	-0.0894	0.022	-0.1167	0.038	-0.6372	0.1042	0.030	3.10	*
4	-0.0151	0.011	-0.0172	0.020	-0.4409	0.0902	0.015	13.65	
5	-0.0103	0.006	-0.0134	0.021	-0.1306	0.0807	0.014	5.52	
6	-0.0064	0.000	-0.0202	0.006	-0.0006	0.0737	0.003	0.02	
7	-0.0005	0.000	-0.0064	0.000	0.0072	0.0682	0.000	-1.05	

DIFFUSIVITY CALCULATIONS ON LURGI SPENT SHALE

Run 1 Scans 2 and 3
Mass Correction Factor 1.61

Pt #	Slope 1 cm-1	Theta 1	Slope 2 cm-1	Theta 2	2 I 10-6	2 eI 10-6	Theata Mean	D cm2/s	
2	-0.1464	0.136	-0.0545	0.127	-0.8098	0.0224	0.132	4.21	*
3	-0.1167	0.038	-0.0868	0.093	-0.4813	0.0177	0.065	2.39	
4	-0.0172	0.020	-0.0662	0.040	-0.3574	0.0150	0.030	4.29	
5	-0.0134	0.021	-0.0302	0.026	-0.3212	0.0134	0.024	7.38	*
6	-0.0202	0.006	-0.0072	0.010	-0.3018	0.0123	0.008	11.04	
7	-0.0064	0.000	0.0081	0.019	-0.1856	0.0114	0.010	-108.05	
8	-0.0005	0.000	-0.0124	0.018	-0.0764	0.0106	0.009	5.95	

DIFFUSIVITY CALCULATIONS ON LURGI SPENT SHALE

Run 1 Scans 3 and 4
Mass Correction Factor 1.09

Pt #	Slope 1 cm-1	Theta 1	Slope 2 cm-1	Theta 2	2 I 10-6	2 eI 10-6	Theata Mean	D cm2/s	
2	-0.0545	0.127	-0.1118	0.146	0.2024	0.1466	0.136	-1.28	
3	-0.0868	0.093	-0.1116	0.083	-0.0619	0.1159	0.088	0.32	
4	-0.0662	0.040	-0.0596	0.035	-0.2048	0.0984	0.037	1.63	
5	-0.0302	0.026	-0.0172	0.023	-0.2923	0.0880	0.025	6.18	*
6	-0.0072	0.010	-0.0029	0.017	-0.0761	0.0803	0.013	7.49	
7	0.0081	0.019	-0.0055	0.020	-0.0453	0.0744	0.020	-17.40	
8	-0.0124	0.018	-0.0094	0.012	-0.2022	0.0696	0.015	9.30	
9	-0.0088	0.007	-0.0065	0.011	-0.0886	0.0656	0.009	5.81	
10	-0.0068	0.009	-0.0075	0.005	-0.1806	0.0622	0.007	12.63	

DIFFUSIVITY CALCULATIONS ON LURGI SPENT SHALE

Run 1 Scans 4 and 5
Mass Correction Factor 1.02

Pt #	Slope 1 cm-1	Theta 1	Slope 2 cm-1	Theta 2	2 I 10-6	2 eI 10-6	Theata Mean	D cm2/s	
2	-0.1118	0.146	-0.0941	0.193	-1.2239	0.0939	0.170	6.25	*
3	-0.1116	0.083	-0.1523	0.124	-0.5808	0.0758	0.103	2.26	*
4	-0.0596	0.035	-0.0954	0.041	-0.4747	0.0637	0.038	3.07	*
5	-0.0172	0.023	-0.0200	0.028	-0.3932	0.0570	0.026	10.61	*
6	-0.0029	0.017	-0.0088	0.021	-0.3345	0.0520	0.019	28.50	
7	-0.0055	0.020	-0.0050	0.019	-0.3510	0.0481	0.020	33.60	
8	-0.0094	0.012	-0.0058	0.016	-0.2838	0.0450	0.014	18.74	
9	-0.0065	0.011	-0.0084	0.014	-0.2404	0.0424	0.012	16.25	*
10	-0.0075	0.005	-0.0012	0.008	-0.2049	0.0403	0.007	23.62	
11	-0.0054	0.003	-0.0067	0.012	-0.0563	0.0384	0.008	4.66	

DIFFUSIVITY CALCULATIONS ON LURGI SPENT SHALE

Run 1 Scans 5 and 6
Mass Correction Factor 1.29

Pt #	Slope 1 cm-1	Theta 1	Slope 2 cm-1	Theta 2	2 I 10-6	2 eI 10-6	Theata Mean	D cm2/s	
2	-0.0941	0.193	-0.0843	0.200	-1.5157	0.1997	0.197	8.88	*
3	-0.1523	0.124	-0.1511	0.143	-0.6944	0.1618	0.133	2.37	*
4	-0.0954	0.041	-0.1123	0.049	-0.3212	0.1353	0.045	1.55	*
5	-0.0200	0.028	-0.0262	0.031	-0.1998	0.1210	0.030	4.33	*
6	-0.0088	0.021	-0.0092	0.023	-0.1037	0.1105	0.022	5.77	*
7	-0.0050	0.019	-0.0046	0.022	0.0015	0.1023	0.021	-0.15	
8	-0.0058	0.016	-0.0072	0.018	0.1131	0.0957	0.017	-8.73	
9	-0.0084	0.014	-0.0111	0.014	0.1546	0.0902	0.014	-7.98	
10	-0.0012	0.008	-0.0046	0.007	0.1462	0.0856	0.007	-25.34	
11	-0.0067	0.012	-0.0074	0.010	0.0351	0.0816	0.011	-2.50	
12	-0.0124	0.001	-0.0099	0.000	-0.0061	0.0781	0.000	0.27	

DISPERSION COLUMN TEST ON LURGI SPENT SHALE

Run 2 Scan 1
time 12.0 hr
solution influx 1.26 gm

LENGTH cm	Am	Cs	Theta %	t Sol. gm	Slope cm-1	NaI gm/cm3	t NaI gm
0.00	8230.4	28350					
0.50	2130.4	10788	0.134	0.83	-0.0870	0.115	0.087
1.00	2862.4	11022	0.047	1.38	-0.1244	0.098	0.144
1.50	3425.6	11260	0.009	1.55	-0.0468	0.000	0.157
2.00	3479.1	11347	0.000	1.58	-0.0095	0.000	0.157
2.50	3319.5	0	0.000	1.58	0.0000	0.000	0.157

DISPERSION COLUMN TEST ON LURGI SPENT SHALE

Run 2 Scan 2
time 23.5 hr
solution influx 1.04 gm

LENGTH cm	Am	Cs	Theta %	t Sol. gm	Slope cm-1	NaI gm/cm3	t NaI gm
0.00	8259.8	28380					
0.50	1781.3	10626	0.181	1.12	-0.0861	0.119	0.123
1.00	2197.3	10846	0.095	1.98	-0.1717	0.150	0.224
1.50	3401.5	11287	0.010	2.31	-0.0887	0.046	0.266
2.00	3471.9	11341	0.006	2.36	-0.0027	0.000	0.268
2.50	3312.1	11230	0.007	2.40	-0.0063	0.000	0.268
3.00	3486.8	0	0.000	2.42	-0.0068	0.000	0.268

DISPERSION COLUMN TEST ON LURGI SPENT SHALE

Run 2 Scan 3
time 36.0 hr
solution influx 1.15 gm

LENGTH cm	Am	Cs	Theta %	t Sol. gm	Slope cm-1	NaI gm/cm3	t NaI gm
0.00	8259.9	28086					
0.50	1553.3	10522	0.176	1.12	-0.0393	0.156	0.156
1.00	1887.4	10583	0.137	2.10	-0.1098	0.142	0.289
1.50	3173.0	10969	0.066	2.72	-0.1177	0.024	0.349
2.00	3440.1	11083	0.019	2.97	-0.0524	0.000	0.353
2.50	3295.5	10982	0.014	3.06	-0.0139	0.000	0.353
3.00	3470.2	11089	0.005	3.11	-0.0090	0.000	0.353
3.50	3446.8	0	0.005	3.14	-0.0049	0.000	0.353

DISPERSION COLUMN TEST ON LURGI SPENT SHALE

Run 2 Scan 4
time 48.5 hr
solution influx 1.39 gm

LENGTH cm	Am	Cs	Theta %	t Sol. gm	Slope cm-1	NaI gm/cm3	t NaI gm
0.00	8244.1	28428					
0.50	1359.5	10411	0.245	1.53	-0.0526	0.125	0.175
1.00	1561.8	10510	0.193	2.89	-0.1317	0.132	0.335
1.50	2311.5	10912	0.114	3.84	-0.1654	0.117	0.445
2.00	3412.0	11288	0.027	4.27	-0.0972	0.000	0.483
2.50	3282.4	11183	0.016	4.40	-0.0153	0.000	0.483
3.00	3445.3	11333	0.012	4.48	-0.0132	0.000	0.483
3.50	3443.7	0	0.003	4.52	-0.0120	0.000	0.483
4.00	3386.7	0	0.000	4.53	0.0055	0.000	0.483
4.50	3346.4	0	0.009	4.56	0.0000	0.000	0.483

DISPERSION COLUMN TEST ON LURGI SPENT SHALE

Run 2 Scan 5
time 59.0 hr
solution influx 0.93 gm

LENGTH cm	Am	Cs	Theta %	t Sol. gm	Slope cm-1	NaI gm/cm3	t NaI gm
0.00	8226.1	28338					
0.50	1285.8	10321	0.262	1.63	-0.0303	0.124	0.185
1.00	1412.5	10343	0.232	3.16	-0.1040	0.122	0.358
1.50	1920.3	10712	0.158	4.37	-0.1790	0.124	0.494
2.00	3341.6	11191	0.053	5.01	-0.1307	0.000	0.550
2.50	3249.4	11150	0.027	5.23	-0.0370	0.000	0.550
3.00	3429.1	0	0.015	5.36	-0.0147	0.000	0.550
3.50	3412.9	0	0.012	5.44	-0.0044	0.000	0.550
4.00	3345.1	0	0.011	5.50	0.0046	0.000	0.550
4.50	3318.6	0	0.017	5.58	-0.0111	0.000	0.550

DISPERSION COLUMN TEST ON LURGI SPENT SHALE

Run 2 Scan 6
time 72.5 hr
solution influx 1.14 gm

LENGTH cm	Am	Cs	Theta %	t Sol. gm	Slope cm-1	NaI gm/cm3	t NaI gm
0.00	8253.5	28332					
0.50	1221.1	10281	0.272	1.69	-0.0232	0.126	0.196
1.00	1307.8	10278	0.249	3.32	-0.0625	0.125	0.383
1.50	1625.0	10524	0.210	4.74	-0.1690	0.119	0.543
2.00	2933.5	11059	0.080	5.63	-0.1768	0.059	0.628
2.50	3246.5	11107	0.033	5.96	-0.0589	0.000	0.641
3.00	3426.4	11278	0.021	6.11	-0.0188	0.000	0.641
3.50	3420.1	0	0.014	6.21	-0.0115	0.000	0.641
4.00	3360.1	0	0.010	6.28	-0.0063	0.000	0.641
4.50	3352.6	0	0.008	6.32	-0.0072	0.000	0.641
5.00	3463.7	0	0.002	6.35	-0.0077	0.000	0.641
5.50	3536.1	0	0.000	6.36	-0.0023	0.000	0.641

DISPERSION COLUMN TEST ON LURGI SPENT SHALE

Run 2 Scan 7
time 83.5 hr
solution influx 0.96 gm

LENGTH cm	Am	Cs	Theta %	t Sol. gm	Slope cm-1	NaI gm/cm3	t NaI gm
0.00	8241.7	28330					
0.50	1182.9	10291	0.268	1.68	-0.0122	0.134	0.204
1.00	1245.7	10252	0.256	3.31	-0.0285	0.129	0.400
1.50	1446.8	10417	0.239	4.85	-0.0940	0.121	0.576
2.00	2244.1	10757	0.162	6.08	-0.1977	0.082	0.696
2.50	3221.0	11047	0.041	6.68	-0.1405	0.000	0.734
3.00	3421.3	11240	0.021	6.86	-0.0194	0.000	0.734
3.50	3394.8	0	0.022	6.99	-0.0037	0.000	0.734
4.00	3335.8	0	0.017	7.10	-0.0009	0.000	0.734
4.50	3314.4	0	0.021	7.21	-0.0116	0.000	0.734
5.00	3449.8	0	0.006	7.28	-0.0189	0.000	0.734
5.50	3522.8	0	0.002	7.31	-0.0051	0.000	0.734
6.00	3527.1	0	0.001	7.32	-0.0024	0.000	0.734
6.50	3225.1	0	0.000	7.32	-0.0006	0.000	0.734

DISPERSION COLUMN TEST ON LURGI SPENT SHALE

Run 2 Scan 8
time 96.0 hr
solution influx 1.18 gm

LENGTH cm	Am	Cs	Theta %	t Sol. gm	Slope cm-1	NaI gm/cm3	t NaI gm
0.00	8241.3	28396					
0.50	1144.4	10295	0.273	1.71	-0.0091	0.135	0.211
1.00	1179.7	10244	0.264	3.39	-0.0261	0.132	0.416
1.50	1337.3	10409	0.247	4.99	-0.0432	0.129	0.606
2.00	1719.6	10562	0.221	6.44	-0.1813	0.102	0.762
2.50	3032.0	11006	0.066	7.31	-0.1898	0.027	0.831
3.00	3395.7	11229	0.031	7.58	-0.0410	0.000	0.836
3.50	3387.9	0	0.025	7.74	-0.0188	0.000	0.836
4.00	3348.0	0	0.012	7.85	-0.0053	0.000	0.836
4.50	3318.6	0	0.019	7.94	-0.0112	0.000	0.836
5.00	3461.3	0	0.001	8.00	-0.0192	0.000	0.836
5.50	3528.2	0	0.000	8.00	0.0040	0.000	0.836
6.00	3514.9	0	0.005	8.02	-0.0003	0.000	0.836
6.50	3227.6	0	0.000	8.03	-0.0046	0.000	0.836
7.00	3363.2	0	0.001	8.04	0.0000	0.000	0.836

DISPERSION COLUMN TEST ON LURGI SPENT SHALE

Run 2 Scan 9
time 107.5 hr
solution influx 1.29 gm

LENGTH cm	Am	Cs	Theta %	t Sol. gm	Slope cm-1	NaI gm/cm3	t NaI gm
0.00	8257.6	28365					
0.50	1111.4	10239	0.287	1.79	-0.0162	0.132	0.216
1.00	1137.8	10210	0.270	3.53	-0.0247	0.134	0.427
1.50	1252.2	10345	0.262	5.20	-0.0223	0.131	0.629
2.00	1501.4	10451	0.248	6.78	-0.0561	0.111	0.805
2.50	2192.4	10497	0.206	8.15	-0.2081	0.054	0.914
3.00	3380.4	11195	0.040	8.87	-0.1845	0.000	0.946
3.50	3403.5	11254	0.021	9.05	-0.0206	0.000	0.946
4.00	3337.3	0	0.019	9.16	-0.0106	0.000	0.946
4.50	3346.8	0	0.011	9.25	-0.0127	0.000	0.946
5.00	3454.2	0	0.007	9.30	-0.0071	0.000	0.946
5.50	3526.3	0	0.004	9.33	0.0023	0.000	0.946
6.00	3512.2	0	0.009	9.36	-0.0037	0.000	0.946
6.50	3232.7	0	0.000	9.39	-0.0055	0.000	0.946
7.00	3362.9	0	0.003	9.40	0.0019	0.000	0.946
7.50	3519.6	0	0.002	9.41	-0.0034	0.000	0.946

DISPERSION COLUMN TEST ON LURGI SPENT SHALE

Run 2 Scan 10
time 120.5 hr
solution influx 1.94 gm

LENGTH cm	Am	Cs	Theta %	t Sol. gm	Slope cm-1	NaI gm/cm3	t NaI gm
0.00	8260.8	28403					
0.50	1029.4	10181	0.307	1.92	0.0032	0.132	0.231
1.00	1052.9	10091	0.310	3.84	-0.0034	0.123	0.455
1.50	1152.5	10217	0.304	5.75	-0.0237	0.120	0.668
2.00	1323.0	10329	0.287	7.57	-0.0389	0.110	0.862
2.50	1518.2	10289	0.265	9.26	-0.1051	0.093	1.022
3.00	2817.7	10711	0.182	10.59	-0.2203	0.018	1.101
3.50	3346.3	11200	0.045	11.24	-0.1588	0.000	1.111
4.00	3329.9	0	0.023	11.44	-0.0345	0.000	1.111
4.50	3349.4	0	0.010	11.53	-0.0181	0.000	1.111
5.00	3460.4	0	0.005	11.57	-0.0102	0.000	1.111
5.50	3537.4	0	0.000	11.59	-0.0037	0.000	1.111
6.00	3534.2	0	0.001	11.59	0.0000	0.000	1.111
6.50	3238.1	0	0.000	11.59	0.0012	0.000	1.111
7.00	3367.1	0	0.002	11.60	0.0000	0.000	1.111
7.50	3526.8	0	0.000	11.60	-0.0022	0.000	1.111
8.00	3529.0	0	0.000	11.60	0.0000	0.000	1.111
9.00	3483.3	0	0.000	11.60	0.0000	0.000	1.111

DISPERSION COLUMN TEST ON LURGI SPENT SHALE

Run 2 Scan 14
time 168.5 hr
solution influx 2.23 gm

LENGTH cm	Am	Cs	Theta %	t Sol. gm	Slope cm-1	NaI gm/cm3	t NaI gm
0.00	8296.2	28373					
0.50	923.4	10036	0.347	2.16	-0.0123	0.127	0.251
1.00	931.6	9995	0.334	4.28	-0.0077	0.128	0.498
1.50	975.8	10082	0.339	6.38	0.0039	0.125	0.741
2.00	1047.0	10134	0.338	8.48	-0.0179	0.118	0.976
2.50	1072.7	10072	0.321	10.52	-0.0264	0.117	1.197
3.00	1246.1	10208	0.312	12.47	-0.0199	0.107	1.399
3.50	1444.1	10238	0.301	14.34	-0.0107	0.091	1.572
4.00	1759.7	10220	0.301	16.15	-0.0277	0.060	1.701
4.50	2540.9	10321	0.273	17.83	-0.2514	0.013	1.763
5.00	3361.4	11067	0.050	18.76	-0.2483	0.000	1.773
5.50	3486.9	11262	0.025	18.97	-0.0263	0.000	1.773
6.00	3491.1	0	0.023	19.11	-0.0066	0.000	1.773
6.50	3199.4	0	0.019	19.23	-0.0034	0.000	1.773
7.00	3337.4	0	0.020	19.34	-0.0066	0.000	1.773
7.50	3509.6	0	0.012	19.43	-0.0167	0.000	1.773
8.00	3517.6	0	0.003	19.47	-0.0080	0.000	1.773
9.00	3478.2	0	0.000	19.49	-0.0017	0.000	1.773
10.00	3213.2	0	0.000	19.49	0.0000	0.000	1.773

DISPERSION COLUMN TEST ON LURGI SPENT SHALE

Run 2 Scan 11
time 131.0 hr
solution influx 1.40 gm

LENGTH cm	Am	Cs	Theta %	t Sol. gm	Slope cm-1	NaI gm/cm3	t NaI gm
0.00	8264.0	28330					
0.50	1025.2	10150	0.309	1.93	-0.0164	0.132	0.231
1.00	1042.7	10121	0.292	3.81	-0.0164	0.135	0.459
1.50	1118.5	10226	0.292	5.63	-0.0078	0.130	0.680
2.00	1255.0	10306	0.284	7.43	-0.0046	0.119	0.885
2.50	1342.9	10180	0.288	9.19	-0.0260	0.101	1.064
3.00	2027.3	10404	0.258	10.83	-0.1931	0.057	1.188
3.50	3226.4	11000	0.095	11.87	-0.2227	0.000	1.230
4.00	3299.9	11162	0.036	12.24	-0.0627	0.000	1.230
4.50	3297.5	0	0.032	12.43	-0.0219	0.000	1.230
5.00	3438.9	0	0.014	12.56	-0.0190	0.000	1.230
5.50	3505.0	0	0.013	12.63	0.0005	0.000	1.230
6.00	3501.3	0	0.014	12.71	-0.0041	0.000	1.230
6.50	3210.0	0	0.009	12.78	-0.0043	0.000	1.230
7.00	3349.3	0	0.010	12.83	-0.0067	0.000	1.230
7.50	3521.6	0	0.002	12.87	-0.0100	0.000	1.230
8.00	3523.8	0	0.000	12.87	-0.0014	0.000	1.230

DISPERSION COLUMN TEST ON LURGI SPENT SHALE

Run 2 Scan 12
time 144.5 hr
solution influx 2.24 gm

LENGTH cm	Am	Cs	Theta %	t Sol. gm	Slope cm-1	NaI gm/cm3	t NaI gm
0.00	8264.7	28354					
0.50	963.7	10070	0.335	2.08	-0.0226	0.127	0.242
1.00	987.4	10062	0.312	4.10	-0.0209	0.131	0.479
1.50	1054.2	10160	0.314	6.06	-0.0027	0.127	0.709
2.00	1172.0	10228	0.310	7.99	-0.0123	0.116	0.926
2.50	1209.3	10136	0.302	9.88	-0.0335	0.109	1.122
3.00	1543.9	10333	0.276	11.64	-0.0444	0.092	1.288
3.50	2269.0	10410	0.257	13.23	-0.1799	0.038	1.388
4.00	3155.5	10977	0.096	14.26	-0.2241	0.000	1.416
4.50	3294.9	0	0.033	14.63	-0.0771	0.000	1.416
5.00	3425.6	0	0.019	14.77	-0.0162	0.000	1.416
5.50	3495.2	0	0.017	14.88	-0.0012	0.000	1.416
6.00	3492.1	0	0.018	14.98	-0.0057	0.000	1.416
6.50	3204.8	0	0.011	15.06	-0.0105	0.000	1.416
7.00	3355.9	0	0.007	15.11	-0.0041	0.000	1.416
7.50	3509.1	0	0.007	15.15	-0.0028	0.000	1.416
8.00	3501.1	0	0.005	15.18	-0.0047	0.000	1.416

DISPERSION COLUMN TEST ON LURGI SPENT SHALE

Run 2 Scan 13
time 156.5 hr
solution influx 2.00 gm

LENGTH cm	Am	Cs	Theta %	t Sol. gm	Slope cm-1	NaI gm/cm3	t NaI gm
0.00	8322.7	28360					
0.50	951.5	10128	0.317	1.99	-0.0059	0.138	0.249
1.00	965.6	10067	0.311	3.96	-0.0058	0.136	0.494
1.50	1022.3	10169	0.311	5.90	-0.0037	0.134	0.733
2.00	1115.3	10233	0.307	7.83	-0.0184	0.125	0.961
2.50	1136.0	10161	0.293	9.69	-0.0226	0.123	1.173
3.00	1361.1	10297	0.284	11.48	-0.0265	0.108	1.364
3.50	1712.3	10360	0.266	13.15	-0.0222	0.080	1.512
4.00	2406.7	10365	0.262	14.72	-0.2022	0.025	1.592
4.50	3200.4	11033	0.064	15.66	-0.2372	0.009	1.612
5.00	3434.2	11241	0.025	15.91	-0.0415	0.000	1.613
5.50	3505.3	0	0.022	16.05	-0.0055	0.000	1.613
6.00	3512.1	0	0.020	16.17	-0.0128	0.000	1.613
6.50	3231.2	0	0.010	16.25	-0.0028	0.000	1.613
7.00	3356.0	0	0.017	16.32	0.0053	0.000	1.613
7.50	3513.5	0	0.015	16.41	-0.0128	0.000	1.613
8.00	3527.1	0	0.004	16.47	-0.0087	0.000	1.613
9.00	3483.6	0	0.002	16.50	-0.0020	0.000	1.613

DISPERSION COLUMN TEST ON LURGI SPENT SHALE

Run 2 Scan 15
time 179.5 hr
solution influx 2.75 gm

LENGTH cm	Am	Cs	Theta %	t Sol. gm	Slope cm-1	NaI gm/cm3	t NaI gm
0.00	8262.5	28304					
0.50	871.2	9885	0.386	2.39	-0.0171	0.117	0.256
1.00	884.4	9860	0.369	4.72	-0.0092	0.119	0.510
1.50	915.4	9934	0.377	7.03	0.0023	0.116	0.759
2.00	966.7	10000	0.371	9.34	-0.0215	0.113	1.004
2.50	980.7	9933	0.355	11.58	-0.0271	0.113	1.238
3.00	1137.6	10074	0.344	13.73	-0.0317	0.105	1.454
3.50	1254.5	10130	0.324	15.78	-0.0136	0.100	1.649
4.00	1377.6	10083	0.331	17.77	-0.0087	0.083	1.819
4.50	1938.3	10141	0.315	19.69	-0.0138	0.043	1.935
5.00	2747.5	10330	0.317	21.51	-0.2666	0.000	1.973
5.50	3413.4	11139	0.048	22.55	-0.2900	0.000	1.973
6.00	3468.5	11213	0.027	22.77	-0.0284	0.000	1.973
6.50	3183.0	0	0.020	22.90	-0.0079	0.000	1.973
7.00	3326.9	0	0.019	23.01	-0.0144	0.000	1.973
7.50	3512.0	0	0.006	23.08	-0.0123	0.000	1.973
8.00	3495.1	0	0.007	23.11	-0.0037	0.000	1.973
9.00	3467.5	0	0.000	23.15	-0.0033	0.000	1.973
10.00	3197.1	0	0.000	23.15	0.0000	0.000	1.973

DISPERSION COLUMN TEST ON LURGI SPENT SHALE

Run 2 Scan 16
time 193.0 hr
solution influx 5.90 gm

LENGTH cm	Am	Cs	Theta %	t Sol. gm	Slope cm-1	NaI gm/cm3	t NaI gm
0.00	8265.0	28292					
0.50	802.9	9931	0.368	2.30	-0.0084	0.133	0.279
1.00	821.0	9879	0.359	4.57	0.0101	0.131	0.553
1.50	834.5	9920	0.378	6.87	0.0349	0.126	0.824
2.00	866.5	9916	0.394	9.27	-0.0124	0.116	1.090
2.50	886.8	9890	0.366	11.62	-0.0293	0.120	1.346
3.00	994.8	9994	0.365	13.88	-0.0130	0.112	1.588
3.50	1046.6	10021	0.353	16.09	-0.0163	0.111	1.816
4.00	1083.2	10002	0.349	18.25	-0.0114	0.105	2.032
4.50	1264.6	10021	0.341	20.35	-0.0040	0.089	2.223
5.00	1631.3	10088	0.345	22.41	-0.0106	0.061	2.369
5.50	2241.2	10183	0.331	24.39	-0.0150	0.027	2.454
6.00	2772.3	10298	0.330	26.29	-0.2586	0.000	2.479
6.50	3063.8	0	0.072	27.43	-0.3100	0.000	2.479
7.00	3325.5	0	0.020	27.69	-0.0538	0.000	2.479
7.50	3480.3	0	0.018	27.80	-0.0147	0.000	2.479
8.00	3500.1	0	0.005	27.87	-0.0121	0.000	2.479
9.00	3465.1	0	0.000	27.90	-0.0025	0.000	2.479

DISPERSION COLUMN TEST ON LURGI SPENT SHALE

Run 2 Scan 17
time 197.5 hr
solution influx 5.95 gm

LENGTH cm	Am	Cs	Theta %	t Sol. gm	Slope cm-1	NaI gm/cm3	t NaI gm	
0.00	8256.0	28306						
0.50	802.9	9604	0.477	2.91	-0.0219	0.096	0.260	
1.00	729.7	9585	0.455	5.76	-0.0179	0.108	0.530	
1.50	740.6	9668	0.459	8.57	0.0136	0.109	0.812	
2.00	760.1	9684	0.469	11.42	-0.0216	0.105	1.095	
2.50	794.2	9667	0.437	14.20	-0.0306	0.106	1.366	
3.00	862.5	9763	0.438	16.88	-0.0048	0.102	1.625	
3.50	894.0	9767	0.433	19.54	-0.0217	0.099	1.875	
4.00	930.8	9787	0.416	22.13	-0.0391	0.098	2.114	
4.50	1045.9	9849	0.394	24.60	-0.0240	0.093	2.336	
5.00	1191.6	9920	0.392	26.98	-0.0139	0.083	2.533	
5.50	1467.7	10000	0.380	29.30	-0.0018	0.066	2.696	
6.00	1858.4	10005	0.390	31.58	0.0809	0.038	2.809	
6.50	2295.6	0	0.461	34.03	-0.0664	0.000	2.851	#
7.00	2652.0	0	0.324	36.26	-0.4328	0.000	2.851	
7.50	3452.2	0	0.028	37.26	-0.3029	0.000	2.851	
8.00	3454.9	0	0.021	37.40	-0.0166	0.000	2.851	
9.00	3453.0	0	0.003	37.53	-0.0105	0.000	2.851	
10.00	3192.0	0	0.000	37.55	-0.0009	0.000	2.851	
# NaI present; true values			.36	36.98		.01	2.87	

DIFFUSIVITY CALCULATIONS ON LURGI SPENT SHALE

Run 2 Scans 1 and 2
Mass Correction Factor 1.30

Pt #	Slope 1 cm-1	Theta 1	Slope 2 cm-1	Theta 2	2 I 10-6	2 eI 10-6	Theata Mean	D cm2/s	
2	-0.1244	0.047	-0.1717	0.095	-0.4193	0.1384	0.071	1.47	
3	-0.0468	0.009	-0.0887	0.010	-0.4209	0.1100	0.009	3.14	*
4	-0.0095	0.000	-0.0027	0.006	-0.2220	0.0941	0.003	18.27	
5	0.0000	0.000	-0.0063	0.007	-0.0092	0.0842	0.003	1.46	

DIFFUSIVITY CALCULATIONS ON LURGI SPENT SHALE

Run 2 Scans 2 and 3
Mass Correction Factor 1.66

Pt #	Slope 1 cm-1	Theta 1	Slope 2 cm-1	Theta 2	2 I 10-6	2 eI 10-6	Theata Mean	D cm2/s
2	-0.1717	0.095	-0.1098	0.137	-2.9782	0.1271	0.116	11.01
3	-0.0887	0.010	-0.1177	0.066	-0.9104	0.1006	0.038	4.46
4	-0.0027	0.006	-0.0524	0.019	-0.4517	0.0866	0.013	8.21
5	-0.0063	0.007	-0.0139	0.014	-0.2011	0.0775	0.010	9.95
6	-0.0068	0.000	-0.0090	0.005	-0.0209	0.0707	0.002	1.32

DIFFUSIVITY CALCULATIONS ON LURGI SPENT SHALE

Run 2 Scans 3 and 4
Mass Correction Factor 0.98

Pt #	Slope 1 cm-1	Theta 1	Slope 2 cm-1	Theta 2	2 I 10-6	2 eI 10-6	Theata Mean	D cm2/s	
2	-0.1098	0.137	-0.1317	0.193	-1.5099	0.1267	0.165	6.49	*
3	-0.1177	0.066	-0.1654	0.114	-0.5423	0.1031	0.090	1.96	*
4	-0.0524	0.019	-0.0972	0.027	-0.3578	0.0866	0.023	2.40	*
5	-0.0139	0.014	-0.0153	0.016	-0.2976	0.0775	0.015	10.21	*
6	-0.0090	0.005	-0.0132	0.012	-0.1433	0.0707	0.008	6.46	
7	-0.0049	0.005	-0.0120	0.003	-0.1730	0.0655	0.004	10.25	

DIFFUSIVITY CALCULATIONS ON LURGI SPENT SHALE

Run 2 Scans 4 and 5
Mass Correction Factor 0.89

Pt #	Slope 1 cm-1	Theta 1	Slope 2 cm-1	Theta 2	2 I 10-6	2 eI 10-6	Theata Mean	D cm2/s	
2	-0.1317	0.193	-0.1040	0.232	-2.4581	0.1505	0.212	10.80	*
3	-0.1654	0.114	-0.1790	0.158	-1.4518	0.1229	0.136	4.36	
4	-0.0972	0.027	-0.1307	0.053	-0.8571	0.1031	0.040	3.77	
5	-0.0153	0.016	-0.0370	0.027	-0.6037	0.0922	0.022	11.56	*
6	-0.0132	0.012	-0.0147	0.015	-0.5221	0.0842	0.014	18.75	*
7	-0.0120	0.003	-0.0044	0.012	-0.3049	0.0779	0.008	18.59	
8	0.0055	0.000	0.0046	0.011	-0.0440	0.0729	0.006	-4.37	
9	0.0000	0.009	-0.0111	0.017	0.1533	0.0687	0.013	-13.90	

DIFFUSIVITY CALCULATIONS ON LURGI SPENT SHALE

Run 2 Scans 5 and 6
Mass Correction Factor 1.51

Pt #	Slope 1 cm-1	Theta 1	Slope 2 cm-1	Theta 2	2 I 10-6	2 eI 10-6	Theata Mean	D cm2/s	
2	-0.1040	0.232	-0.0625	0.249	-2.7689	0.1171	0.240	17.21	*
3	-0.1790	0.158	-0.1690	0.210	-1.2070	0.0955	0.184	3.59	*
4	-0.1307	0.053	-0.1768	0.080	-0.3956	0.0814	0.066	1.30	*
5	-0.0370	0.027	-0.0589	0.033	-0.2196	0.0717	0.030	2.29	*
6	-0.0147	0.015	-0.0188	0.021	-0.0486	0.0655	0.018	1.45	
7	-0.0044	0.012	-0.0115	0.014	0.0014	0.0606	0.013	-0.09	
8	0.0046	0.011	-0.0063	0.010	-0.0467	0.0567	0.010	27.73	
9	-0.0111	0.017	-0.0072	0.008	-0.3353	0.0535	0.012	18.39	

DIFFUSIVITY CALCULATIONS ON LURGI SPENT SHALE

Run 2 Scans 6 and 7
Mass Correction Factor 1.00

Pt #	Slope 1 cm-1	Theta 1	Slope 2 cm-1	Theta 2	2 I 10-6	2 eI 10-6	Theata Mean	D cm2/s	
2	-0.0625	0.249	-0.0285	0.256	-3.8860	0.1439	0.252	44.19	*
3	-0.1690	0.210	-0.0940	0.239	-3.1644	0.1172	0.224	12.44	*
4	-0.1768	0.080	-0.1977	0.162	-1.1601	0.1005	0.121	3.16	
5	-0.0589	0.033	-0.1405	0.041	-0.9407	0.0880	0.037	4.73	
6	-0.0188	0.021	-0.0194	0.021	-0.9383	0.0803	0.021	24.64	
7	-0.0115	0.014	-0.0037	0.022	-0.7339	0.0744	0.018	48.38	
8	-0.0063	0.010	-0.0009	0.017	-0.5356	0.0696	0.013	74.92	
9	-0.0072	0.008	-0.0116	0.021	-0.1939	0.0656	0.014	10.33	
10	-0.0077	0.002	-0.0189	0.006	-0.1061	0.0622	0.004	4.00	
11	-0.0023	0.000	-0.0051	0.002	-0.0454	0.0593	0.001	6.13	

DIFFUSIVITY CALCULATIONS ON LURGI SPENT SHALE

Run 2 Scans 7 and 8
Mass Correction Factor 1.73

Pt #	Slope 1 cm-1	Theta 1	Slope 2 cm-1	Theta 2	2 I 10-6	2 eI 10-6	Theata Mean	D cm2/s	
2	-0.0285	0.256	-0.0261	0.264	-3.5684	0.1267	0.260	67.62	*
3	-0.0940	0.239	-0.0432	0.247	-3.2930	0.1034	0.243	24.84	*
4	-0.1977	0.162	-0.1813	0.221	-1.1049	0.0889	0.191	2.99	
5	-0.1405	0.041	-0.1898	0.066	-0.1888	0.0780	0.054	0.57	
6	-0.0194	0.021	-0.0410	0.031	0.1977	0.0707	0.026	-3.28	
7	-0.0037	0.022	-0.0188	0.025	0.3009	0.0655	0.023	-13.41	
8	-0.0009	0.017	-0.0053	0.012	0.1095	0.0612	0.015	-17.72	
9	-0.0116	0.021	-0.0112	0.019	0.0409	0.0577	0.020	-1.80	
10	-0.0189	0.006	-0.0192	0.001	-0.1338	0.0548	0.003	3.52	
11	-0.0051	0.002	0.0040	0.000	-0.2162	0.0522	0.001	197.25	
12	-0.0024	0.001	-0.0003	0.005	-0.0387	0.0500	0.003	14.56	
13	-0.0006	0.000	-0.0046	0.000	-0.0387	0.0480	0.000	7.36	

DIFFUSIVITY CALCULATIONS ON LURGI SPENT SHALE

Run 2 Scans 8 and 9
Mass Correction Factor 0.93

Pt #	Slope 1 cm-1	Theta 1	Slope 2 cm-1	Theta 2	2 I 10-6	2 eI 10-6	Theata Mean	D cm2/s	
2	-0.0261	0.264	-0.0247	0.270	-4.4019	0.1378	0.267	89.76	*
3	-0.0432	0.247	-0.0223	0.262	-4.0870	0.1124	0.254	64.65	*
4	-0.1813	0.221	-0.0561	0.248	-3.5080	0.0969	0.235	15.21	
5	-0.1898	0.066	-0.2081	0.206	-0.4241	0.0854	0.136	1.08	
6	-0.0410	0.031	-0.1845	0.040	-0.2274	0.0769	0.036	1.01	
7	-0.0188	0.025	-0.0206	0.021	-0.3067	0.0712	0.023	7.81	*
8	-0.0053	0.012	-0.0106	0.019	-0.1500	0.0666	0.016	9.46	
9	-0.0112	0.019	-0.0127	0.011	-0.3466	0.0628	0.015	14.55	
10	-0.0192	0.001	-0.0071	0.007	-0.2243	0.0595	0.004	8.56	
11	0.0040	0.000	0.0023	0.004	-0.1481	0.0568	0.002	-23.45	
12	-0.0003	0.005	-0.0037	0.009	-0.0652	0.0543	0.007	16.69	
13	-0.0046	0.000	-0.0055	0.000	-0.0652	0.0522	0.000	6.42	
14	0.0000	0.001	0.0019	0.003	-0.0025	0.0503	0.002	-1.32	

DIFFUSIVITY CALCULATIONS ON LURGI SPENT SHALE

Run 2 Scans 9 and 10
Mass Correction Factor 0.87

Pt #	Slope 1 cm-1	Theta 1	Slope 2 cm-1	Theta 2	2 I 10-6	2 eI 10-6	Theata Mean	D cm2/s	
2	-0.0247	0.270	-0.0034	0.310	-5.3196	0.1216	0.290	196.46	
3	-0.0223	0.262	-0.0237	0.304	-4.5501	0.0992	0.283	102.36	*
4	-0.0561	0.248	-0.0389	0.287	-3.8518	0.0857	0.267	41.81	*
5	-0.2081	0.206	-0.1051	0.265	-2.8172	0.0763	0.235	9.17	
6	-0.1845	0.040	-0.2203	0.182	-0.2030	0.0683	0.111	0.50	
7	-0.0206	0.021	-0.1588	0.045	0.2313	0.0629	0.033	-1.29	
8	-0.0106	0.019	-0.0345	0.023	0.2965	0.0589	0.021	-6.59	
9	-0.0127	0.011	-0.0181	0.010	0.2868	0.0555	0.010	-9.33	
10	-0.0071	0.007	-0.0102	0.005	0.2518	0.0527	0.006	-14.64	
11	0.0023	0.004	-0.0037	0.000	0.1840	0.0502	0.002	-128.36	
12	-0.0037	0.009	0.0000	0.001	0.0374	0.0481	0.005	-10.26	
13	-0.0055	0.000	0.0012	0.000	0.0374	0.0462	0.000	-8.63	
14	0.0019	0.003	0.0000	0.002	0.0156	0.0445	0.003	8.41	
15	-0.0034	0.002	-0.0022	0.000	-0.0189	0.0430	0.001	3.34	

DIFFUSIVITY CALCULATIONS ON LURGI SPENT SHALE

Run 2 Scans 10 and 11
Mass Correction Factor 1.10

Pt #	Slope 1 cm-1	Theta 1	Slope 2 cm-1	Theta 2	2 I 10-6	2 eI 10-6	Theata Mean	D cm2/s	
2	-0.0034	0.310	-0.0164	0.292	-6.3881	0.1510	0.301	335.80	
3	-0.0237	0.304	-0.0078	0.292	-6.7382	0.1231	0.298	221.50	
4	-0.0389	0.287	-0.0046	0.284	-6.8238	0.1063	0.286	161.87	
5	-0.1051	0.265	-0.0260	0.288	-6.1973	0.0946	0.276	48.53	
6	-0.2203	0.182	-0.1931	0.258	-4.0540	0.0854	0.220	9.92	
7	-0.1588	0.045	-0.2227	0.095	-2.6062	0.0779	0.070	6.84	
8	-0.0345	0.023	-0.0627	0.036	-2.2364	0.0729	0.029	23.06	*
9	-0.0181	0.010	-0.0219	0.032	-1.6075	0.0687	0.021	40.28	
10	-0.0102	0.005	-0.0190	0.014	-1.3477	0.0652	0.009	46.33	
11	-0.0037	0.000	0.0005	0.013	-0.9736	0.0622	0.006	302.77	
12	0.0000	0.001	-0.0041	0.014	-0.5910	0.0595	0.008	146.02	
13	0.0012	0.000	-0.0043	0.009	-0.3346	0.0572	0.004	108.63	
14	0.0000	0.002	-0.0067	0.010	-0.1107	0.0551	0.006	16.60	
15	-0.0022	0.000	-0.0100	0.002	-0.0486	0.0532	0.001	3.99	

DIFFUSIVITY CALCULATIONS ON LURGI SPENT SHALE

Run 2 Scans 11 and 12
Mass Correction Factor 0.96

Pt #	Slope 1 cm-1	Theta 1	Slope 2 cm-1	Theta 2	2 I 10-6	2 eI 10-6	Theata Mean	D cm2/s	
2	-0.0164	0.292	-0.0209	0.312	-6.1986	0.1173	0.302	172.39	
3	-0.0078	0.292	-0.0027	0.314	-5.7798	0.0957	0.303	574.93	
4	-0.0046	0.284	-0.0123	0.310	-5.2926	0.0826	0.297	323.55	
5	-0.0260	0.288	-0.0335	0.302	-5.0377	0.0738	0.295	87.10	
6	-0.1931	0.258	-0.0444	0.276	-4.7425	0.0670	0.267	20.33	
7	-0.2227	0.095	-0.1799	0.257	-1.5854	0.0612	0.176	3.96	
8	-0.0627	0.036	-0.2241	0.096	-0.3912	0.0567	0.066	1.37	
9	-0.0219	0.032	-0.0771	0.033	-0.3685	0.0535	0.032	3.73	
10	-0.0190	0.014	-0.0162	0.019	-0.2635	0.0507	0.016	7.50	*
11	0.0005	0.013	-0.0012	0.017	-0.1868	0.0484	0.015	274.02	
12	-0.0041	0.014	-0.0057	0.018	-0.1151	0.0463	0.016	11.88	
13	-0.0043	0.009	-0.0105	0.011	-0.0698	0.0445	0.010	4.74	
14	-0.0067	0.010	-0.0041	0.007	-0.1204	0.0429	0.009	11.19	
15	-0.0100	0.002	-0.0028	0.007	-0.0242	0.0414	0.005	1.89	

DIFFUSIVITY CALCULATIONS ON LURGI SPENT SHALE

Run 2 Scans 12 and 13
Mass Correction Factor 1.49

Pt #	Slope 1 cm-1	Theta 1	Slope 2 cm-1	Theta 2	2 I 10-6	2 eI 10-6	Theata Mean	D cm2/s
2	-0.0209	0.312	-0.0058	0.311	-8.3951	0.1321	0.312	325.41
3	-0.0027	0.314	-0.0037	0.311	-8.5117	0.1078	0.3121	383.43
4	-0.0123	0.310	-0.0184	0.307	-8.6196	0.0932	0.308	289.95
5	-0.0335	0.302	-0.0226	0.293	-8.9588	0.0833	0.297	164.69
6	-0.0444	0.276	-0.0265	0.284	-8.7157	0.0757	0.280	126.17
7	-0.1799	0.257	-0.0222	0.266	-8.5137	0.0696	0.262	42.68
8	-0.2241	0.096	-0.2022	0.262	-2.8513	0.0642	0.179	6.72
9	-0.0771	0.033	-0.2372	0.064	-1.7962	0.0603	0.048	5.73
10	-0.0162	0.019	-0.0415	0.025	-1.5876	0.0571	0.022	27.58
11	-0.0012	0.017	-0.0055	0.022	-1.3966	0.0544	0.020	209.26
12	-0.0057	0.018	-0.0128	0.020	-1.3364	0.0521	0.019	72.53
13	-0.0105	0.011	-0.0028	0.010	-1.3917	0.0500	0.010	104.88
14	-0.0041	0.007	0.0053	0.017	-1.0679	0.0482	0.012	-901.77
15	-0.0028	0.007	-0.0128	0.015	-0.8003	0.0466	0.011	51.47

DIFFUSIVITY CALCULATIONS ON LURGI SPENT SHALE

Run 2 Scans 13 and 14
Mass Correction Factor 0.72

Pt #	Slope 1 cm-1	Theta 1	Slope 2 cm-1	Theta 2	2 I 10-6	2 eI 10-6	Theata Mean	D cm2/s	
2	-0.0058	0.311	-0.0077	0.334	-7.1055	0.1319	0.323	544.80	
3	-0.0037	0.311	0.0039	0.339	-6.6460	0.1076	0.325	$$$$$$$	
4	-0.0184	0.307	-0.0179	0.338	-6.1373	0.0930	0.323	174.94	*
5	-0.0226	0.293	-0.0264	0.321	-5.6706	0.0832	0.307	119.68	*
6	-0.0265	0.284	-0.0199	0.312	-5.2288	0.0757	0.298	115.93	*
7	-0.0222	0.266	-0.0107	0.301	-4.6716	0.0698	0.284	145.78	
8	-0.2022	0.262	-0.0277	0.301	-4.0774	0.0648	0.282	17.90	
9	-0.2372	0.064	-0.2514	0.273	-0.6170	0.0603	0.169	1.27	
10	-0.0415	0.025	-0.2483	0.050	-0.2090	0.0571	0.037	0.72	
11	-0.0055	0.022	-0.0263	0.025	-0.1626	0.0544	0.024	5.12	*
12	-0.0128	0.020	-0.0066	0.023	-0.0996	0.0521	0.022	5.15	
13	-0.0028	0.010	-0.0034	0.019	0.0503	0.0500	0.014	-8.08	
14	0.0053	0.017	-0.0066	0.020	0.1034	0.0482	0.018	-81.63	
15	-0.0128	0.015	-0.0167	0.012	0.0572	0.0466	0.013	-1.95	

DIFFUSIVITY CALCULATIONS ON LURGI SPENT SHALE

Run 2 Scans 14 and 15
Mass Correction Factor 0.72

Pt #	Slope 1 cm-1	Theta 1	Slope 2 cm-1	Theta 2	2 I 10-6	2 eI 10-6	Theata Mean	D cm2/s	
2	-0.0077	0.334	-0.0092	0.369	-9.3794	0.1435	0.352	575.25	
3	0.0039	0.339	0.0023	0.377	-8.6944	0.1171	0.358	$$$$$$$	
4	-0.0179	0.338	-0.0215	0.371	-8.1040	0.1013	0.355	212.28	*
5	-0.0264	0.321	-0.0271	0.355	-7.4913	0.0906	0.338	144.70	*
6	-0.0199	0.312	-0.0317	0.344	-6.9162	0.0825	0.328	138.01	*
7	-0.0107	0.301	-0.0136	0.324	-6.5289	0.0763	0.312	276.45	
8	-0.0277	0.301	-0.0087	0.331	-6.0375	0.0711	0.316	169.25	
9	-0.2514	0.273	-0.0138	0.315	-5.3270	0.0663	0.294	20.20	
10	-0.2483	0.050	-0.2666	0.317	-0.4692	0.0622	0.183	0.91	
11	-0.0263	0.025	-0.2900	0.048	-0.0453	0.0593	0.037	0.14	
12	-0.0066	0.023	-0.0284	0.027	0.0143	0.0568	0.025	-0.41	
13	-0.0034	0.019	-0.0079	0.020	0.0403	0.0546	0.019	-3.56	
14	-0.0066	0.020	-0.0144	0.019	0.0180	0.0526	0.019	-0.86	
15	-0.0167	0.012	-0.0123	0.006	-0.0990	0.0508	0.009	3.43	

DIFFUSIVITY CALCULATIONS ON LURGI SPENT SHALE

Run 2 Scans 15 and 16
Mass Correction Factor 1.26

Pt #	Slope 1 cm-1	Theta 1	Slope 2 cm-1	Theta 2	2 I 10-6	2 eI 10-6	Theata Mean	D cm2/s	
2	-0.0092	0.369	0.0101	0.359	-20.3758	0.1173	0.364$$$$$$		
3	0.0023	0.377	0.0349	0.378	-20.3750	0.0957	0.377	-567.92	
4	-0.0215	0.371	-0.0124	0.394	-19.8025	0.0826	0.383	602.38	
5	-0.0271	0.355	-0.0293	0.366	-19.5651	0.0740	0.360	358.47	*
6	-0.0317	0.344	-0.0130	0.365	-19.0569	0.0674	0.355	439.34	*
7	-0.0136	0.324	-0.0163	0.353	-18.3547	0.0624	0.338	631.80	
8	-0.0087	0.331	-0.0114	0.349	-17.9466	0.0583	0.340	919.29	
9	-0.0138	0.315	-0.0040	0.341	-17.3820	0.0547	0.328	992.03	
10	-0.2666	0.317	-0.0106	0.345	-16.7952	0.0515	0.331	60.74	
11	-0.2900	0.048	-0.0150	0.331	-9.5538	0.0487	0.189	31.40	
12	-0.0284	0.027	-0.2586	0.330	-1.7120	0.0463	0.178	5.98	
13	-0.0079	0.020	-0.3100	0.072	-0.3667	0.0445	0.046	1.16	
14	-0.0144	0.019	-0.0538	0.020	-0.3417	0.0429	0.019	5.02	*
15	-0.0123	0.006	-0.0147	0.018	-0.0146	0.0414	0.012	0.54	

DIFFUSIVITY CALCULATIONS ON LURGI SPENT SHALE

Run 2 Scans 16 and 17
Mass Correction Factor 0.58

Pt #	Slope 1 cm-1	Theta 1	Slope 2 cm-1	Theta 2	2 I 10-6	2 eI 10-6	Theata Mean	D cm2/s	
2	0.0101	0.359	-0.0179	0.455	-49.2404	0.3498	0.407	6425.97	
3	0.0349	0.378	0.0136	0.459	-46.3524	0.2857	0.418	-989.40	
4	-0.0124	0.394	-0.0216	0.469	-43.7147	0.2471	0.431	1326.19	
5	-0.0293	0.366	-0.0306	0.437	-41.1563	0.2211	0.401	708.70	
6	-0.0130	0.365	-0.0048	0.438	-38.5716	0.2016	0.401	2237.81	
7	-0.0163	0.353	-0.0217	0.433	-35.7330	0.1866	0.393	967.48	*
8	-0.0114	0.349	-0.0391	0.416	-33.3467	0.1745	0.382	679.84	*
9	-0.0040	0.341	-0.0240	0.394	-31.5228	0.1643	0.367	1156.70	
10	-0.0106	0.345	-0.0139	0.392	-29.9215	0.1554	0.368	1246.51	
11	-0.0150	0.331	-0.0018	0.380	-28.3049	0.1475	0.355	1702.92	
12	-0.2586	0.330	0.0809	0.390	-26.2614	0.1402	0.360	147.43	
13	-0.3100	0.072	-0.0664	0.461	-12.3074	0.1334	0.266	32.76	
14	-0.0538	0.020	-0.4328	0.324	-1.3787	0.1286	0.172	2.84	
15	-0.0147	0.018	-0.3029	0.028	-1.0384	0.1242	0.023	3.28	